Modelling Varying Amplitudes

Dipl.-Math. Winfried Theis

November 2003,

Corrections 02.02.2004

Thesis
submitted in Fulfillment of the
Requirements for the Degree of
'Doktor der Naturwissenschaften'
at University of Dortmund

To Uschi, for all the help!

Contents

Acknowledgements

First of all I want to thank the German Research Council (Deutsche Forschungsgemeinschaft – DFG) for the financial support of my work within the Collaborative Research Centre 475 'Reduction of Complexity for Multivariate Data Structures' and in the Graduate College 'Applied Statistics'.
Next I would like to thank Claus Weihs for his support of my work and his trust in my abilities. Without his asking I would not have started the adventure of writing a thesis in applied statistics after graduating in pure mathematics.
Special thanks go to Antoinette Stevens who invested a lot of time and effort to improve my English and make this work readable. Any errors, strange constructions and not really English sentences are absolutely my fault. And of course many thanks for being a great friend!
Oliver Webber helped me to understand the deep-hole drilling process from a mechanical engineers point of view. I want to thank him for his patience explaining all the subtle details which were necessary to make it possible to interprete my findings in our data.
I would like to thank all my colleagues at the Department of Statistics at the University of Dortmund for the warm welcome and many interesting discussions. For discussions that contributed in one way or another to this work I like to thank:
Claudia Becker, Anja Maria Busse, Martina Erdbrügge, Uschi Garczarek, Katja Ickstadt, Jutta Jessenberger, Joachim Kunert, Uwe Ligges, Karsten Lübke, Michael Meyners, Olaf Schoffer, and Detlef Steuer.
Another thanks goes to the **R** development team and all folks at the r-help mailing list for helping me to solve the more difficult programming questions that arose during this work. My colleagues Detlef Steuer and Uwe Ligges helped me to resolve not just **R** problems but all kinds of other computer problems as well. Christian Röver programmed for me the functions for the surfaceplots, spectrogram and automatic graphics output from **R** to LaTeX.
All my friends have supported me during this work and I like to thank them all for nudging me on and giving support and friendship. For special and constant love, friendship and support I like to name (this list is in no way exhaustive!!!):
Gregor and Mechthild Meschede, Uschi Garczarek, Swen Gonsberg, Jan Akkermann and Dirk Becker, Rouven Turck, Ursula Enneking, Ralf Heiligenhaus and Barbara Giovanelli, Klemens Hägele and Maribel Gomez, and Sonja Schlangmann.
Finally I want to thank my family for their love, understanding and support.

Dortmund, November 2003 Winfried Theis

Introduction

This thesis is based on the project 'Analysis and Modelling of the Deephole-Drilling Process with Methods of Statistics and Neuronal Networks' in the Collaborative Research Centre 475 'Reduction of Complexity for Multivariate Data Structures' of the German Research Council (Deutsche Forschungsgemeinschaft – DFG). The goal of this project is to model the BTA deep-hole drilling with statistical methods and phenomenological models from physics to understand and possibly prevent the dynamic disturbances chatter vibration and spiralling.

One of the first tasks in this project was to choose an experimental design to construct a database for the investigations on the dynamics of the deep-hole drilling process. Whenever statistical experimental design is applied, the application should determine the proceeding completely. So usually the application defines the appropriate model(s) which enable(s) the researcher to answer the questions at hand. The model defines criteria an experimental design has to fulfill to make a proper and meaningful fit possible. Besides the criteria dictated by the chosen model each application has special requirements concerning the maximal number of experiments, changes of the input variables and the amount of possible response sampling. Since the nature of the dynamics in the deep-hole drilling were still completely unknown the experimental design could not be based on a model for the dynamics. Instead a central-composite design was chosen to model the influence of machine parameters on quality measurements. The results from this experimental design are described in detail in Chapter 2.

Furthermore, a general search for experimental designs for experiments with time series as response did not reveal appropriate methods for a situation similar to the problem of the BTA deep-hole drilling. All experimental designs discussed in connection with time series are concerned with correlated errors between experiments and not time series as output which are independent between experiments. Chapter 3 gives an overview of the literature and points out a solution for such experiments.

During the experiments of the first experimental design seven on-line measurements were sampled. These time series were investigated more closely because in all experiments some chatter vibrations were observed. We discovered that the drilling torque was the most meaningful of the on-line measurements. The drilling torque was found to be dominated by single frequencies which are close to the eigen-frequencies of the boring bar. Different kinds of chatter observed in the experiments can be described by the change in the amplitudes of those dominating frequencies. The latter observation led to the idea of modelling varying amplitudes.

The distribution of periodogram ordinates plays the key-role when the most important or relevant frequencies have to be determined, and of course it has to be known for the correct modelling of varying amplitudes. The distribution of the periodogram ordinates is derived in Chapter 4, and a transformation is described which leads to a normal approximation of this distribution and gives an estimate of the amplitude. All theoretical results gained on these models are tested for their practical relevance in two simulation studies in Chapter 5. These simulation studies are also designed using the concepts of statistical experimental design.
The models on varying amplitudes are used to fit a descriptive model on the relevant frequencies for the deep-hole drilling process in Chapter 6. The results from this descriptive model are connected to the machine parameters and features of the machine assembly. The highly dynamic nature of the chatter vibrations meant that a general model could not be used for all experiments for the developments of the relevant frequencies. This dynamic nature of the process can be described from a phenomenological point of view as a bifurcation of a stochastic differential equation. In Chapter 7 the stochastic differential equation proposed for the description of the bifurcation into chatter vibration for one frequency is given. It is proved that the descriptive model for the developments of the amplitudes at the relevant frequencies is a solution of the corresponding amplitude equation.
Finally Chapter 8 summarises the results for the different areas – experimental design for experiments with time series as response; models on varying amplitudes; the project on the deep-hole drilling process – and points out open questions giving hints on possible solutions.

1 The BTA Deep-Hole Drilling Process

This chapter describes the BTA deep-hole drilling process and introduces more terminology from the area of metal cutting technology. First the machine tool and its special properties is described, then two quality measures and their measurement processes are introduced, and finally the dynamic process-disturbances chatter vibration and spiralling are described.

1.1 Deep-Hole Drilling

In metal cutting one speaks of deep-hole drilling, when for the proportion of length l to diameter D of the hole to be machined, $l/D \geq 3$ holds. When the diameter D exceeds 20mm typically the BTA deep-hole drilling process is applied. **BTA** stands for 'Boring and Trepaning Association'. This refers to the design of the tool which is explained in subsection 1.1.2 and shown in Figures 1.2 and 1.3. The special construction of this tool leads to long holes with very smooth walls and a high degree of straightness. In many cases the BTA deep-hole drilling process is the final step in the production of expensive workpieces. For example axial bores in turbines or compressor shafts are made with this process. It is extremely important to avoid dynamic disturbances in the process because such disturbances can mean high financial losses.
The machine tool used in the experiments, its components, and the process parameters are described in the next subsections. In the following subsection the tool and the general principal of BTA deep-hole drilling are described.

1.1.1 The Machine Tool

The machine tool has six main components: two drive units for the rotary motion of the workpiece and the rotary and translation motion of the tool, the machine bed, the oil supply device containing the starting bush, the damper, and the tool – boring bar assembly. Figure 1.1 gives a good impression of the machine.
A peculiarity of the BTA deep-hole drilling process is that the the tool and the workpiece may be driven. This means that drilling can be performed in three different ways:

(1) Turning tool and standing workpiece,

(2) Standing tool and turning workpiece,

(3) Turning tool and workpiece in opposite directions.

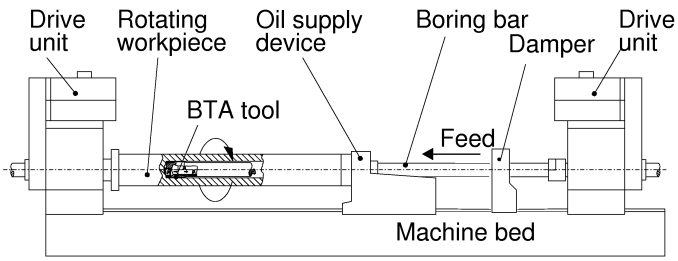

Figure 1.1: BTA-deep-hole-drilling machine

The following parameters can be influenced on the machine:

- The axial feed f in mm/rev
- The cutting velocity (cutting speed) v_c in m/min
- The flow rate of the oil $\dot{V}$ in l/min
- The position of the damper
- The operating-pressure of the damper

The *cutting velocity* is automatically controlled and therefore not exactly on target in the process. This is taken into account by measuring the true number of revolutions per second which then allows the effect of the variation in this parameter to be inferred.
The *axial feed* influences the speed of the boring substantially, since it determines the thickness of the chips which are removed by the cutting edge. The *flow rate of the oil* determines the speed of transportation of the chips from the cutting edge and the cooling and lubrication of the process. It also influences the damping properties of the whole assembly.
The *damper* serves to prevent dynamic disturbances (see section 1.3) and to this aim it can be positioned along the boring bar. Its position can be fixed on the machine bed or relative to the drive unit of the tool. The pressure, with which the damper is clamped to the boring bar, is determined by the machine operator. If the operator detects a disturbance (by sound or vibrations felt on the boring bar) he/she can vary the position and the pressure until the disturbance disappears.

1.1.2 Boring Tool and Principle of the BTA Deep-Hole Drilling

The BTA tool has only one cutting edge and two or three guiding pads. This is illustrated in Figure 1.2. The chips are transported away by the cutting fluid via

the chip mouth and through the boring bar. The asymmetrical geometry of the tool leads to forces pushing outwards against the walls of the hole. These forces are counteracted by reactive forces at the guiding pads. The tool is thereby guided in the machined hole and at the same time the bored hole walls are smoothened. Since the chips are transported within the boring bar they cannot damage the hole surface, and hence a high quality of the holes can be achieved.

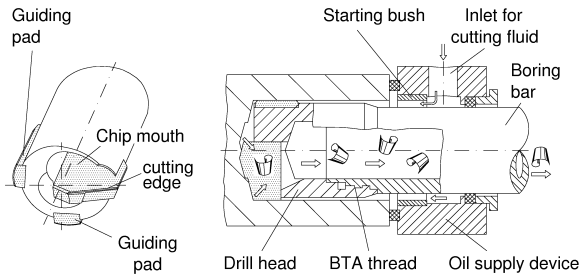

Figure 1.2: Boring tool and detail of working principle

In Figure 1.3 the tool used in the experiments of the project is shown. In contrast to the above description it has a parted cutting edge. The partition into two cutting edges has the advantage that they can be placed so that the forces pushing outwards which are counteracted by the guiding pads are substantially reduced (Latinovic and Osman, 1989).

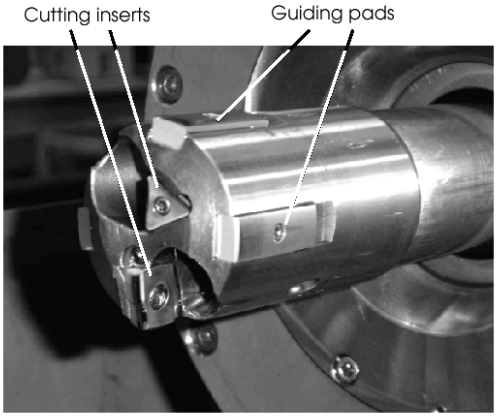

Figure 1.3: Boring tool as used in the experiments

1.2 Quality Measures

In mechanical engineering there are several possible quality measures to evaluate a hole. Roughness and roundness are obviously related to chatter and spiralling because chatter may lead to increased roughness and spiralling is a roundness error (cf. Section 1.3).

1.2.1 Roughness

Roughness measurements are defined to describe the deviation of the surface from the ideal totally smooth surface. They are generally determined by tracing a needle along a line segment and measuring its relative vertical movements. These measurements are then aggregated in several ways. Two of these aggregates are used in this work and therefore described here.
The simplest aggregate is the *single roughness depth* which is the difference between the minimum and the maximum of the measurements.

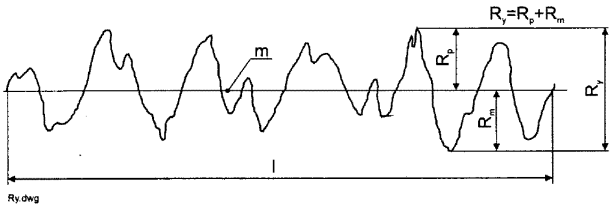

Figure 1.4: Determination of a single roughness depth

The *mean roughness depth* is defined as the mean of five single roughness depths on parts of a line segment.

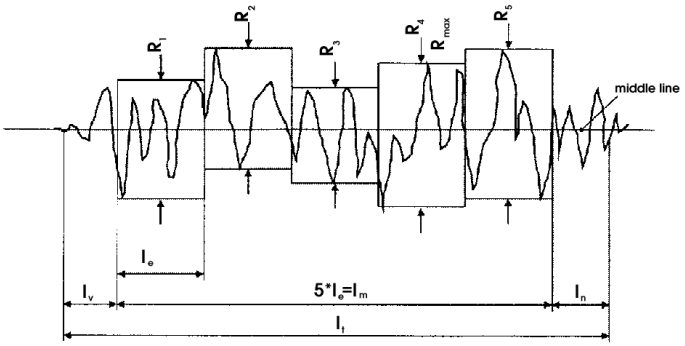

Figure 1.5: Determination of the mean roughness depth R_z

The drawback of these simple measurements is that they are highly influenced by extreme values observed in the measured line segment. If such extreme occurrences

are important in evaluating the quality of the workpiece, they are the best choices. If however it is more important to obtain information about the average quality of the surface, then the *roughness average*, which is defined as the integral of the absolute values of the measurements on the line segment divided by the length of the segment, is more appropriate.

1.2.2 Roundness

Roundness measures the deviation of the machined hole from an optimal circle (Taylor Hobson Ltd.). It is measured by rotating either the measuring device or the workpiece around a fixed axis. The tip of the measurement device is set up close to the ideal radius of the workpiece, or in this case, of the hole relative to the fixed axis. Then the movement of the tip is traced within a plane. The output combines three kinds of signals; the instrument error, the set-up error of the workpiece, and form error of the workpiece. The first is reduced to a negligible amount by high-precision mechanics and stable electronics. The second is minimised by accurate centering and levelling of the workpiece. The form error can be magnified so that a good roundness measurement can be achieved.

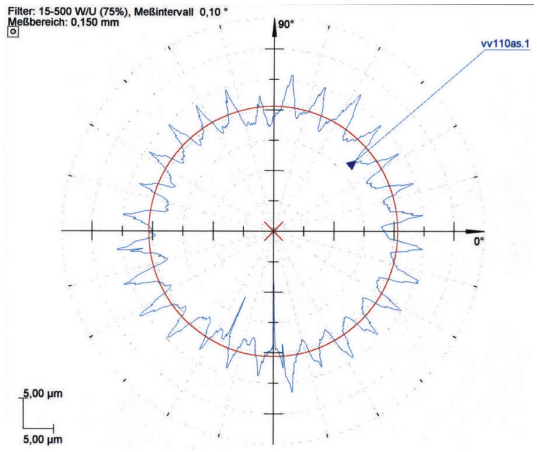

Figure 1.6: A roundness measurement plot from an experiment with extreme chatter vibrations

It has to be noted that several planes have to be measured to assess on the accuracy of the roundness measurements of a cylinder, otherwise any postioning errors still present cannot be checked, e.g. the tube may not be absolutely vertically, or it may be round at one end but not at the other (or in-between). To assess the roundness reference circles are used which are centered at the ideal axis, as shown in Figures 1.6 and 1.11 . In many cases the distance between the minimal circumscribed reference circle and the maximal inscribed reference circle is used as a roundness measurement.

1.3 Process-Disturbances

The project's main aims is how to deal with two dynamic disturbances (chatter vibration and spiralling) and more to the point, how to predict their occurence and prevent them by appropriate controls. The disturbances are described in the next subsections with some explanations from the literature.

1.3.1 Chatter Vibrations

As the name suggests, this disturbance is audible. The acoustic effect that accompanies chatter vibration can best be described as a high-pitched tone which occurs during the process. The tone suggests regularly interrupted cutting. A sawtooth pattern is produced at the bottom of the hole (Figure 1.7 a)). Chatter leads to significantly increased wear of the cutting edges and in more extreme cases it leaves so-called chatter marks on the hole surface. The patterns on the bottom of the hole are illustrated in Figure 1.7 a) and in Figure 1.7 b) chatter marks of varying kinds in the wall of the hole are shown (part 1: starting phase with no chatter vibrations; part 2: chatter type A; part 3: chatter type B). In the latter picture the marks repeat themselves periodically, but with varying intervals for different kinds of chatter.

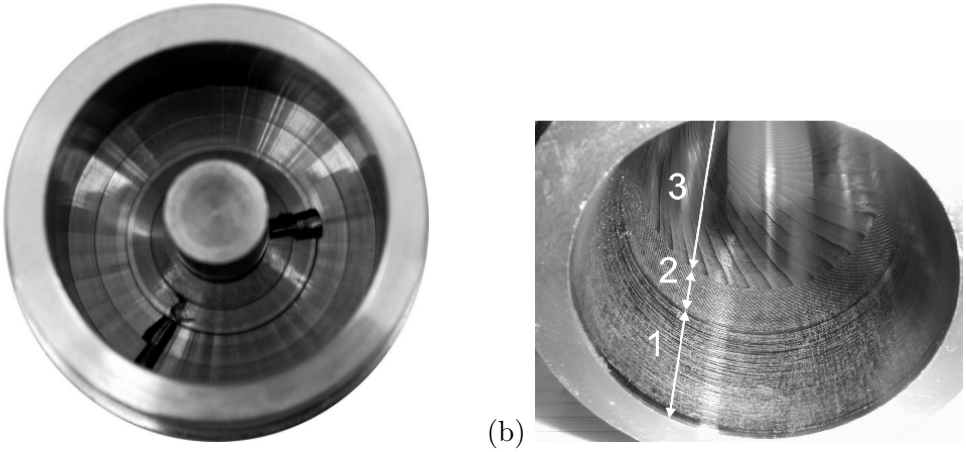

(a) (b)

Figure 1.7: (a) Chatter marks at the bottom of the hole; (b) chatter marks on boring wall

Figure 1.8 displays time series of the drilling torque from two experiments with the same machine parameters. From this view of the data it is already obvious that the drilling torque behaves quite differently for the same machine parameters. On the right-hand side an experiment with three kinds of chatter vibration is displayed and on the left-hand side an experiment with only one kind of chatter vibration.

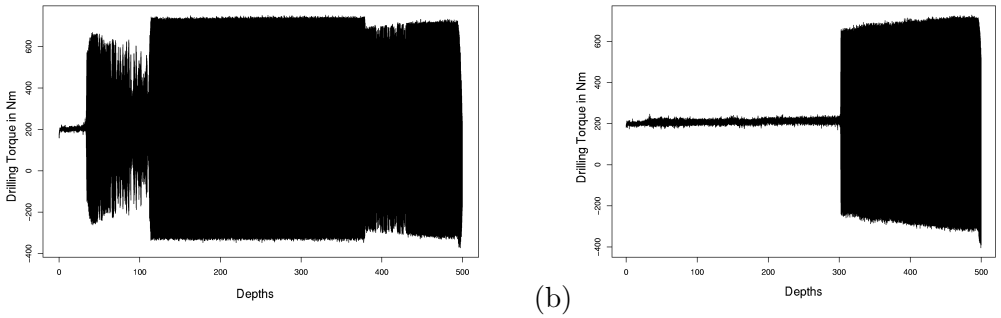

Figure 1.8: Two time series (Exp. 1 and 21a) of the drilling torque from experiments with the same parameters $f = 0.185\,mm/rev$, $v_c = 90\,m/min$ and $\dot{V} = 300\,l/min$

In Figure 1.9 the spectrograms of the drilling torque for the experiments above are depicted. The spectrogram is formed by calculating periodograms from sequences of fixed length from the time series, and then plotting them in a 2D-plot with time on the x-axis and frequencies on the y-axis using colours to distinguish the heights of the periodogram ordinates. As the spectrogram in Figure 1.9 shows the process is characterised by few frequencies.

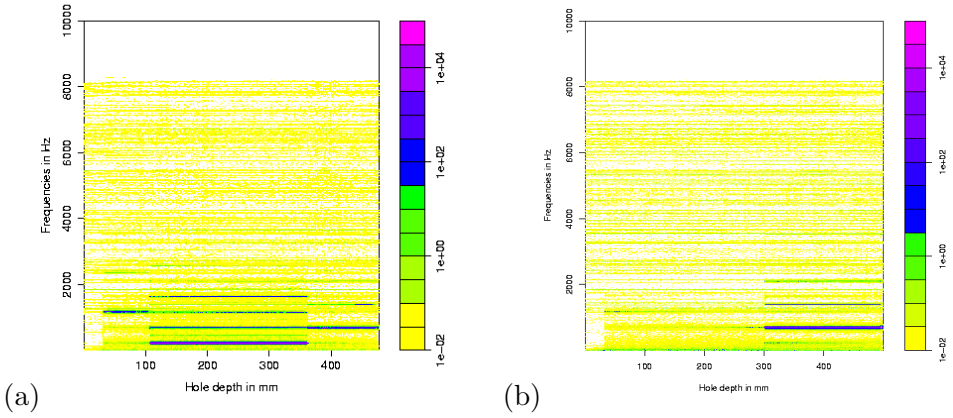

Figure 1.9: The spectrograms of the time series in Figure 1.8

Having observed out-of-phase torsional and longitudinal vibration during chatter, Thai (1983) traced this type of behavior of the BTA deep-hole drilling process back to the principle of coupled states. Furthermore, from the high dynamic content of the process torque, he inferred that the cutting parts periodically disengage from the workpiece when there is chatter vibration.

1.3.2 Spiralling

Spiralling is a periodic movement of the tool around the centre of the boring bar. This produces holes with three to five side-lobes (see Figure 1.11), which repeat themselves and turn slowly producing the characteristic spiralling marks shown in Figure 1.10.

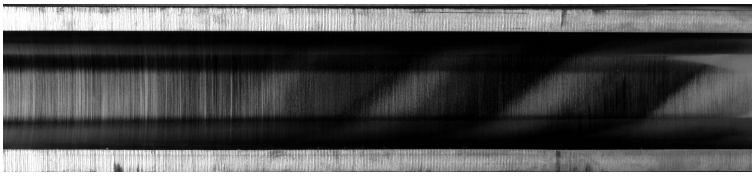

Figure 1.10: Spiralling marks

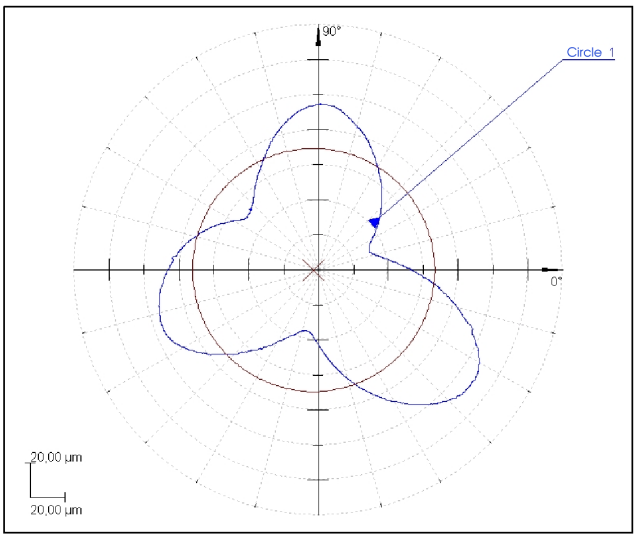

Figure 1.11: A roundness measurement plot from an experiment with spiralling

Results on Lack of Roundness and Spiralling

In the literature it is reported that spiralling in the BTA deep-hole drilling process is mainly observed with 5 lobes when there are three guiding pads regularly spaced on the circumference of the tool (cf. Pfleghar (1976), or Sakuma et al. (1981)). Therefore, the BTA deep-hole drilling process is compared to reaming when the tool has four cutting edges. This comparison is obvious in a way, since the guiding pads have

a transforming effect on the hole surface as well. In experiments with reaming Hermann (1970) found that the number of lobes N is linearly dependent on the number of cutting edges Z by $N = nZ \pm 1$. An explanation for this phenomenon is given in the following model (Sakuma et al., 1981):
The tool has a radius R_T and the angular velocity shall be v_T. It is also assumed that the axis of the boring bar is turning in a circle with radius R_A with an angular velocity of v_A. The path of (one) tip of a cutting edge can therefore be described by the following formulas:

$$x_{S1} = R_A \cos(\varphi_0 + v_A t) + R_T \cos(\theta_0 + v_T t) \tag{1.1}$$
$$y_{S1} = R_A \sin(\varphi_0 + v_A t) + R_T \sin(\theta_0 + v_T t) \tag{1.2}$$

When the cutting edges and guiding pads, respectively, are positioned regularly around the circumference of the tool, the path of the following edge/pad can be derived as follows:

$$x_{S2} = R_A \cos(\varphi_0 + v_A t) + R_T \cos(\theta_0 - \frac{2\pi}{Z} + v_T t) \tag{1.3}$$
$$y_{S2} = R_A \sin(\varphi_0 + v_A t) + R_T \sin(\theta_0 - \frac{2\pi}{Z} + v_T t) \tag{1.4}$$

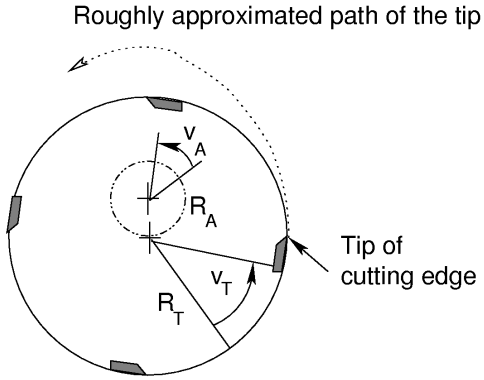

Figure 1.12: Schematic picture of the described mechanism for the development of spiralling.

From this it can be derived that to make the two positions $S1$ and $S2$ coincide the following equation must hold:

$$x_{S2}\left(t = t_0 + \frac{2\pi}{Z v_T}\right) = x_{S1}(t = t_0) \tag{1.5}$$
$$y_{S2}\left(t = t_0 + \frac{2\pi}{Z v_T}\right) = y_{S1}(t = t_0) \tag{1.6}$$

From equation 1.5 it follows directly that $\frac{v_A}{v_T} = nZ$ must hold, with $n \in \mathbb{N}$ if the angular velocities point in the same direction, and $-n \in \mathbb{N}$ if otherwise. From this it can be deduced, that the cutting edges/guiding pads follow identical paths if the axis revolves with a velocity nZ times the cutting velocity. Then the path of the tip of the cutting edge can be described by

$$R = \left(R_A^2 + R_T^2 + 2R_A R_T \cos((nZ-1)v_T t + \varphi_0 + \theta_0)\right)^{\frac{1}{2}}.$$

It is thus clear that this produces a hole with $|nZ-1|$ lobes.
This explains the number of lobes for regularly spaced cutting edges/guiding pads. Since this is such an obvious geometrical explanation for the development of spiralling mechanical engineers have changed the geometry of the drilling tool so that regular spacing of cutting edge and guiding pads on the circumference is avoided.
Stockert (1978) differentiates between three types of spiralling according to their occurrence: at the start of the process, repeatable at the same drilling depth, and seemingly at random. More recent investigations of Gessesse et al. (1994) have shown a connection between the bending modes of the boring bar and spiralling for the second type of occurrence.

2 Modelling Quality Measures in BTA Deep-Hole Drilling

In this chapter the effects of machine parameters on quality measures are investigated. The necessary design considerations are described and the study that resulted from these considerations and its results are discussed in detail.

2.1 Design Considerations

In experimental design it is necessary first to define response variables and how they should be modeled and which variables are influencing factors. Secondly it has to be decided on the aim of the experiment so that a decision can be made for which model of the response variables a design should be selected. These steps are now descibed for the problem of the deep-hole drilling process.

2.1.1 Response Variables

The first target in the project was to determine the effect of the machine parameters on quality measures. The mean roughness depth, the roughness average and roundness were chosen as quality measures, because as pointed out in Section 1.2 these measures are connected in a way to the dynamic disturbances chatter vibration and spiralling.
To model the dynamics of BTA deep hole drilling, time series of quantities characterizing the process were recorded. Chatter vibration and spiralling can be detected in the variation of the cutting and friction forces acting upon the cutting parts and guide pads respectively. In previous investigations this type of measurement was found to be very difficult to achieve, due to, among other things, the restricted space available in the tool head. Therefore, the process forces were measured in terms of feed force and drilling torque transmitted via the boring bar. To this end, the strain gauges were applied to the clamped end of the bar.
These measurements were not to be modeled directly, but were investigated in an exploratory fashion. They are:

- Drilling torque
- Feed force
- Airborne and structure-borne sound

– Realized number of revolutions of the workpiece

The realized number of revolutions of the workpiece are controlled by an engineering process control. Therefore, we wanted to investigate whether the variation in this factor might be correlated to the variation of the other measurements.
In Figure 2.1 the positions of the different sensors is shown.

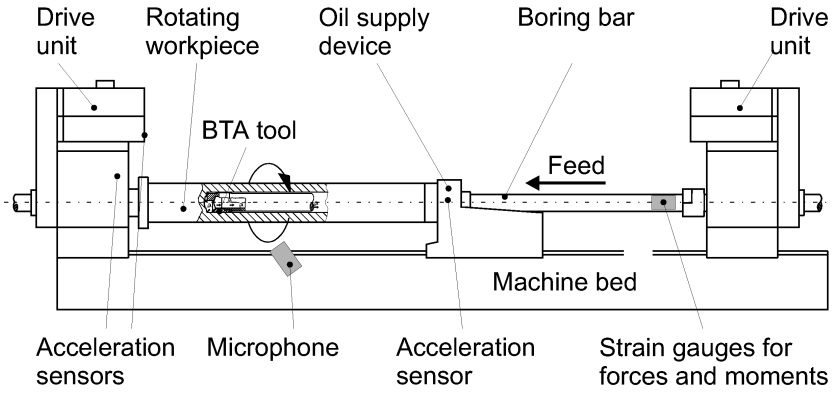

Figure 2.1: Experimental Setup.

2.1.2 Influencing Factors

In Section 1.1.1 it was described, which possibilities exist to influence the BTA-deep-hole-drilling process. These possibilities shall be considered again under the viewpoint of the goal of the experiments and some further practical considerations.
Of the three different modes of operation only one was considered, namely the rotating workpiece/stationary boring tool. This was chosen because an appropriate measuring device to transmit the signals of drilling torque and feed force from the rotating boring bar was not available. The mode of operation is mainly determined by the kind of workpiece, which is to be manufactured. So it is more of a boundary condition than an independent parameter of the process.
The damper was not considered in the first step because its position could not be determined beforehand. Therefore, it was not possible to define one or two treatments of its parameters, which would have allowed a proper inclusion into the experimental design without increasing the number of experiments too much.
This left the following three controllable influencing factors for the design:

– feed f

– cutting speed v_c

– flow rate of the drilling oil $\dot{V}$

Finally there are some uncontrollable influences such as the temperature of the boring oil and more importantly the wear of the cutting edges and the guiding pads.

2.1.3 Model

Since Astakhov et al. (1997a) and Astakhov et al. (1997b) already investigated the quality measures for the BTA-process with respect to the most important influencing factors and found out that these are exactly the three named above, it was decided to find optimal parameter settings for these parameters. In experimental design it is standard to use models for response surfaces in this situation. In this case a quadratic model was chosen, which included the influencing factors feed, cutting speed and oil flow rate.
An important consideration was to account for known uncontrollable factors. Since the temperature of the oil changes only slightly during the boring process, and has no impact on the cooling effect, it was ignored. The wear of the guiding pads is a very slow process, so it could be ignored as well.
Wear of the cutting edges of the tool was expected to be a serious problem. So this was added to the model as a blocking factor, blocking the experiments by the succession of the experiments on the cutting edge — this means the first experiments with the cutting edges were blocked together and so forth.
The complete model for each of the quality measures (here denoted by R) considered thus reads:

$$R = \mu + \beta_1 f + \beta_2 v_c + \beta_3 \dot{V} + \beta_{12} f v_c + \beta_{13} f \dot{V} + \beta_{23} v_c \dot{V} + \beta_{11} f^2 + \beta_{22} v_c^2 + \beta_{33} \dot{V}^2 + (\eta +)\varepsilon \tag{2.1}$$

with μ a constant term, $\eta \sim \mathcal{N}(0, \sigma_\eta^2)$ a block effect, and $\varepsilon \sim \mathcal{N}(0, \sigma_\varepsilon^2)$ a random error term.

2.1.4 Experimental Design

For the estimation of the described model it is necessary to choose an experimental design, which makes it possible to estimate all parameters in the model. Such a design is the central-composite design (cf. Box and Draper (1987) pp.508-512). This design consists of the so-called cube, which here is a full 2^3 factorial design, and the star with points on the axis in a distance α from the centre, and some experiments in the centre. Figure 2.2 shows a 3-dimensional central-composite design in coded factors as it is used here. Coded means that the centre is the point $(0, 0, 0)^T$ and the cube has points with coordinates $1, -1$.
By choosing α correctly this design can have two desirable properties: Rotatability and orthogonal blocking.
Rotatability means that the variances and covariances of the parameter estimates are invariant with respect to arbitrary rotations of the design region. This is desirable because it cannot be determined in which direction the largest variance will occur before the experiments have been run.
Orthogonal blocking makes it possible to estimate variance components of the block effect and the random error in the error structure independently. Possible blocks in the described central-composite design are the star points with some centre

points and the cube itself or two fractions of the cube with some centre points as well.

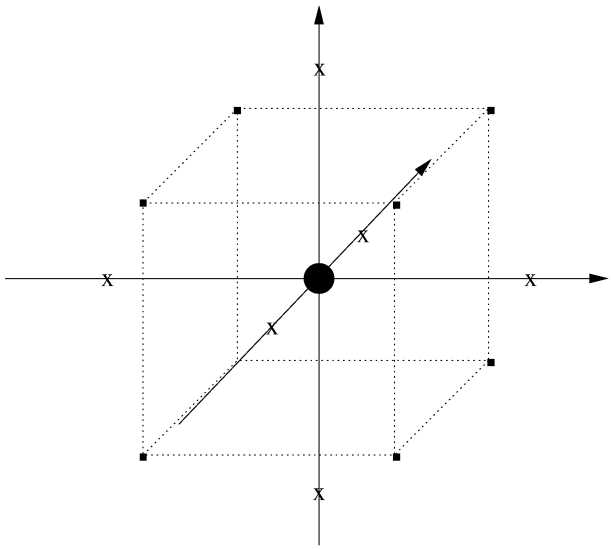

Figure 2.2: Central-composite design

Both properties could almost be fulfilled by choosing $\alpha = 1.68$ and three repetitions in the centre. But to fulfill the blocking condition for the inclusion of the wear of the cutting edges seven cutting edges were needed for the block consisting of the star, but only five for the half fractions of the cube. So the blocks from the cube got two additional repetitions in the centre each. A correction on α was therefore required. This led to $\alpha = \sqrt{2}$ (cf. Box and Draper (1987), pp. 509-511).
The following values for the machine parameters were chosen as borders of the experimental region:

	f in mm/rev	v_s in m/min	$\dot{V}$ in l/min
min.	0.12	60	200
max.	0.25	120	400

Table 2.1: Minimal and maximal values of the machine parameters

As a comparison for common settings of these parameters Figure 2.3 shows the tool manufacturer's recommended region for cutting speed and feed, the recommondation of the VDI and the total range of physically possible values.

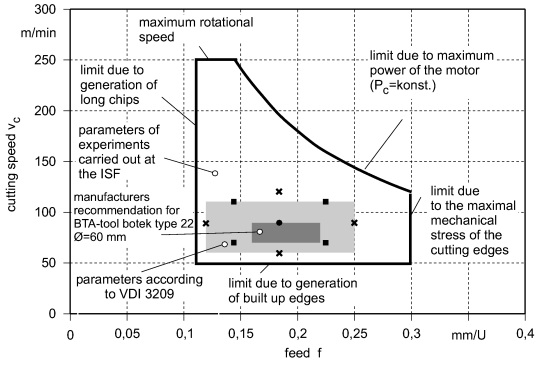

Figure 2.3: Plan in the region of all possible parameter values and recommended parameter regions.

This results in the following Table 2.2 of experimental settings in the original values for the machine parameters:

Exp.	f in mm/rev	v_c in m/min	$\dot{V}$ in l/min
1	0.185	90.00	300.00
2	0.185	90.00	300.00
3	0.185	90.00	300.00
4	0.139	111.21	370.71
5	0.12	90.00	300.00
6	0.231	111.21	370.71
7	0.231	68.79	370.71
8	0.185	90.00	400.00
9	0.139	68.79	370.71
10	0.231	111.21	229.29
11	0.185	60.00	300.00
12	0.139	111.21	229.29
13	0.139	68.79	229.29
14	0.185	90.00	200.00
15	0.231	68.79	229.29
16	0.185	90.00	300.00
17	0.185	120.00	300.00
18	0.185	90.00	300.00
19	0.185	90.00	300.00
20	0.25	90.00	300.00
21	0.185	90.00	300.00

Table 2.2: Central-composite design in the original values of the machine parameters

2.2 Results of the Experiments

2.2.1 Results on Quality Measures

During the experiments, phases with different process dynamics were observed. These in turn lead to corresponding sections of the workpiece, which also showed different characteristics. For all quality measures (R) we therefore defined a weighted mean to obtain one value per experiment, which reflects the different surfaces from the observed phases of the process appropriately. The measurements from each homogeneous part of the hole are weighted by the length of the corresponding section:

$$\begin{aligned} g(R) &= \frac{l_{start}cm}{50cm} R_{start} + \frac{l_{good}cm}{50cm} R_{good} \\ &\quad + \frac{l_{chatt.A}cm}{50cm} R_{chatt.A} + \frac{l_{chatt.B}cm}{50cm} R_{chatt.B} \end{aligned}$$

'Start' stands for the first part of the drilling process until the guiding pads are completely contained in the hole. 'Good' means a part where no chatter marks are visible. Two different sorts of chatter have been observed, chatter type A which leaves chatter marks in the surface and chatter type B which leads to the formation of a pattern along the bore hole wall which could be described as high frequency spiralling.
For the assessment of the models we used the Akaike Information Criterion AIC and the R^2_{adj}, both criteria for the prediction ability of the models. These criteria were chosen because the main goal of a response surface model is the prediction of optimal parameter values for the influences.
The AIC is defined as

$$AIC = -2 \log L + 2p \,,$$

where L denotes the likelihood function and p the number of estimated parameters in the model. And the R^2_{adj} is defined as (cf. eg. Weihs and Jessenberger (1999)):

$$\begin{aligned} R^2_{adj} &:= 1 - \frac{\hat{\sigma}^2}{\hat{Var}(y)}, \text{ where} \\ \hat{\sigma}^2 &= \frac{1}{n-p-1} \sum_{j=1}^{n} \varepsilon_j^2 \text{ and} \\ \hat{Var}(y) &= \frac{1}{n-1} \sum_{j=1}^{n} (y_i - \bar{y})^2 \end{aligned}$$

ε are the residuals of the model, $y_i, i = 1, \ldots, n$, the observations and p the number of parameters in the model.
Since the complete model described above did not provide satisfactory values of our model selection criteria for some of the used quality measures, a stepwise regression was performed by the function step in the statistical software package **R** (Ihaka and Gentleman, 1996) to select the best possible model. This selection was based on the

Akaike Information criterium as objective. The chosen model should minimize the AIC.

Roughness

For the two selected measures of roughness (mean roughness depth (R_z) and roughness average (R_a)) the following models were selected as optimal:

- For mean roughness depth ($g(R_z)$):

  $$3.89 - 0.53f^2 + 0.77v_c^2 - 0.29\dot{V}^2 + 0.29f + 0.49v_c - 0.18\dot{V} + 0.26fv_c - 0.37f\dot{V} + 0.2v_c\dot{V}$$

  with $R^2_{adj} = 0.77$ and AIC $= -32.19$

- For roughness average ($g(R_a)$):

  $$0.69 - 0.12f^2 + 0.27v_c^2 - 0.10\dot{V}^2 + 0.09f + 0.16v_c - 0.04\dot{V} + 0.08fv_c - 0.08f\dot{V}$$

  with $R^2_{adj} = 0.83$ and AIC $= -90.84$

The given parameter values are estimated for the coded influences to make them comparable within the models.
Furthermore, it was tested whether using the blocks as a random parameter could improve the found models. This only resulted in an increased number of parameters in the model and no reduction in variability.

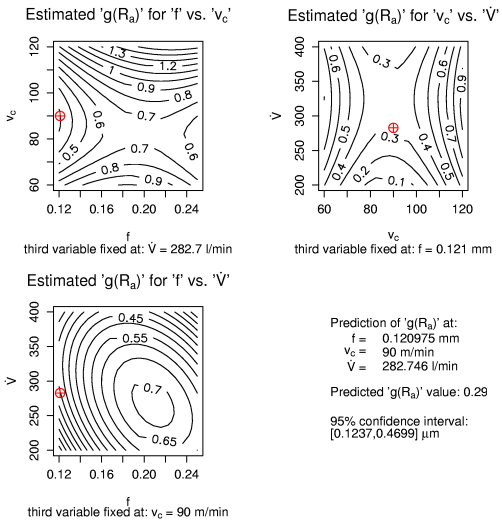

Figure 2.4: Contourplots with optimum for roughness average

Since the better fit was reached for R_a this model was also fitted for R_z to make the results comparable. This only affected the fit slightly ($R^2_{adj} = 0.76$ and AIC

$= -30.87$). These models were therefore used to calculate the optimal values for the influencing factors. The result can be seen in figure 2.4.
The optimum is realized at one of the borders of the chosen experimental region and the common practice would be to then move the experimental region now in that direction. But since the chosen values were already quite extreme, it seemed more appropriate to move on to the usage of the Lanchester damper.

Roundness
The full model was unsatisfactory for our model selection criteria with regard to the weighted mean of the roundness ($g(f_R)$), and so again the best model had to be found by a stepwise regression. The result including the coefficients of the terms scaled for the original factor values is:

$$g(f_R) = 1.05 + 0.32f + 0.38v_c + 0.11\dot{V} + 0.18v_c\dot{V}$$

and has an $R^2_{adj} = 0.53$ and AIC $= -41.49$. These values were not satisfactory but the residuals displayed no hint of further structure and therefore unreflected influences, as can be seen in Figure 2.5.

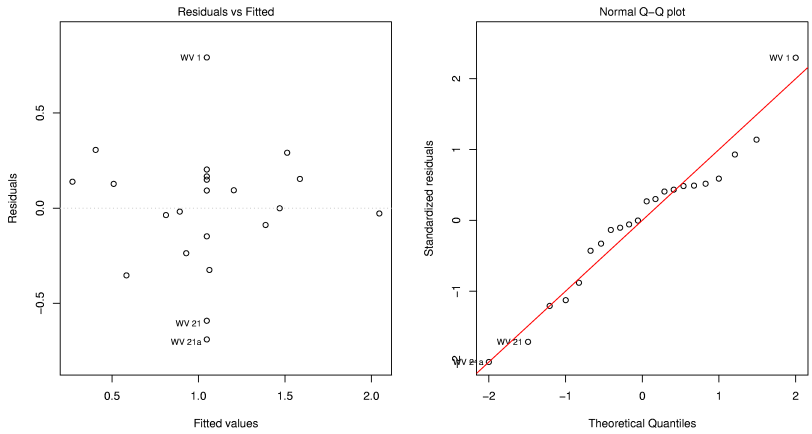

Figure 2.5: Residual- and Normalplot of the model for roundness

2.2.2 Results of On-line Measurements

The on-line measurements were to be explored with a view to explaining, understanding and forecasting chatter and spiralling. The first approach was to look at spectrograms of the drilling torque. It turned out that the different marks on the boring wall correspond to regimes of different frequencies. Figure 2.6 (a) shows an experiment at the centre point of the experimental design (number 21 from Table 2.2), where two dynamic regimes are recognizable: In the first part of the process a frequency near 1200Hz is prominent and then slowly a second frequency near 700Hz becomes visible

and finally dominates the process to the end. Figure 2.6 (b) displays experiment 19 which has the same parameter settings but has just one kind of chatter vibration from the moment that the guiding pads leave the starting bush until the end of the process.

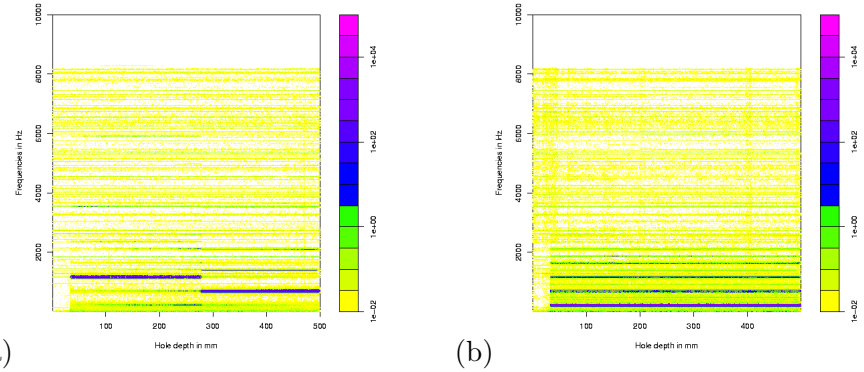

Figure 2.6: Spectrograms of two experiments on the centre point of the design; (a) Chatter right after guiding pads leave starting bush and change to a different kind at the end; (b) chatter right after guiding pads leave starting bush but constant until the end.

Comparing these spectrograms to the spectrograms in Figure 1.9, which are two other examples of experiments with the same machine parameters, it is obvious that the behaviour of the BTA-deep-hole-drilling process is quite dynamic. Figure 2.7 shows a spectrogram of the experiment (number 5) with the lowest cutting speed of $60 m/min$ which was undisturbed for the first 30cm, and then chatter was observed. This chatter appears to have the same frequency as the second kind of chatter in Figure 2.6.

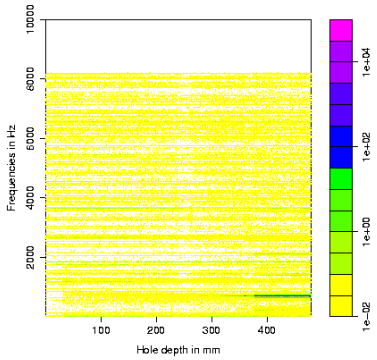

Figure 2.7: Spectrogram of an experiment on the point with the lowest cutting speed of the design

When looking at the other spectrograms it appeared that only a few frequencies,

which were the same for all settings of the influencing factors in the design, really determined the process. This was investigated by determining significant frequencies on segments of a length of 4096 observations and draw histograms on these. Figures 2.8-2.9 show the results.

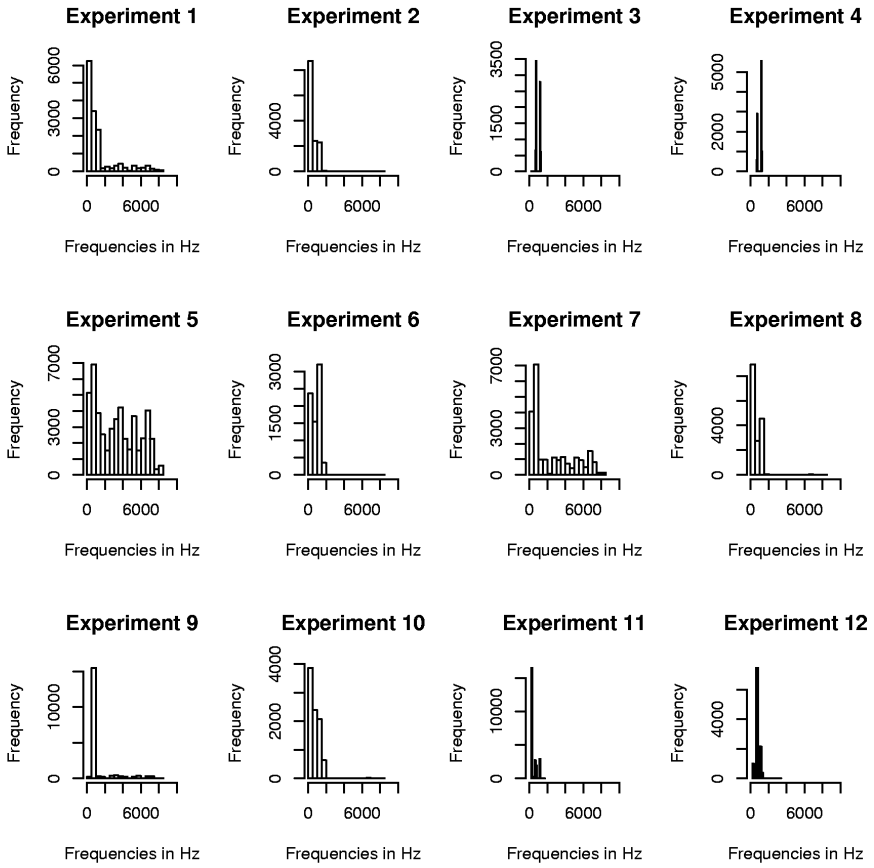

Figure 2.8: Histograms of the significant frequencies of the experiments 1 to 12

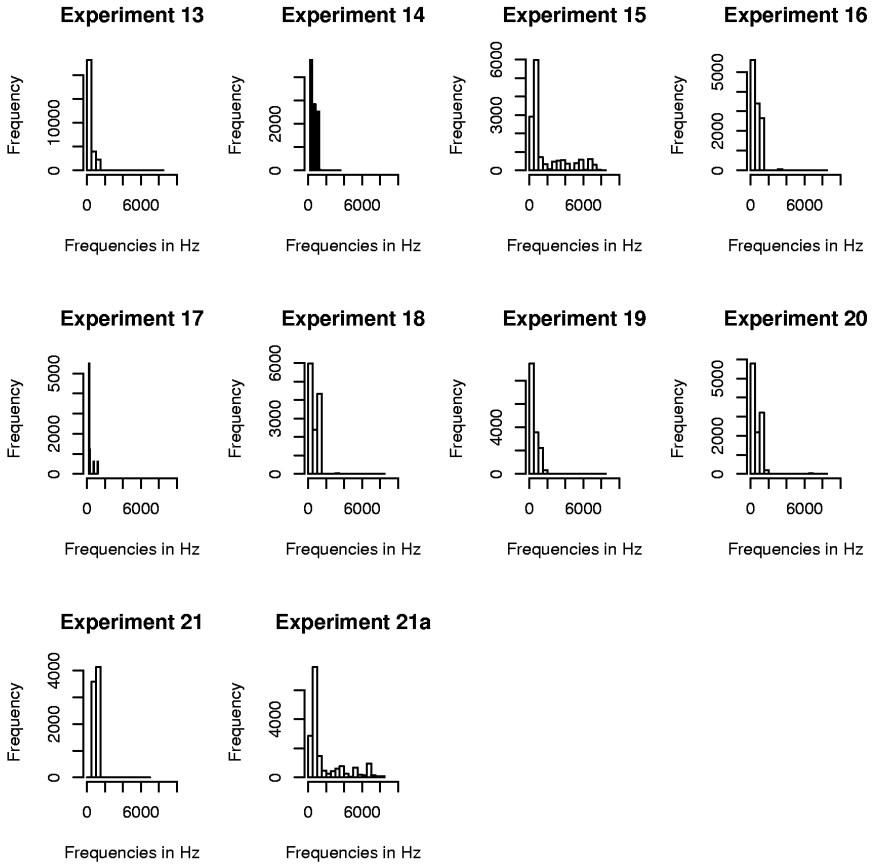

Figure 2.9: Histograms of the significant frequencies of the experiments 13 to 21a

It is obvious from Figures 2.8-2.9 that closer investigation of the region between 0Hz and 2000Hz suffices since the higher frequencies are only important in experiments, where chatter was only observed for a short time. The bar-width in Figures 2.10-2.11 is standardized to 50Hz to make comparison easier.

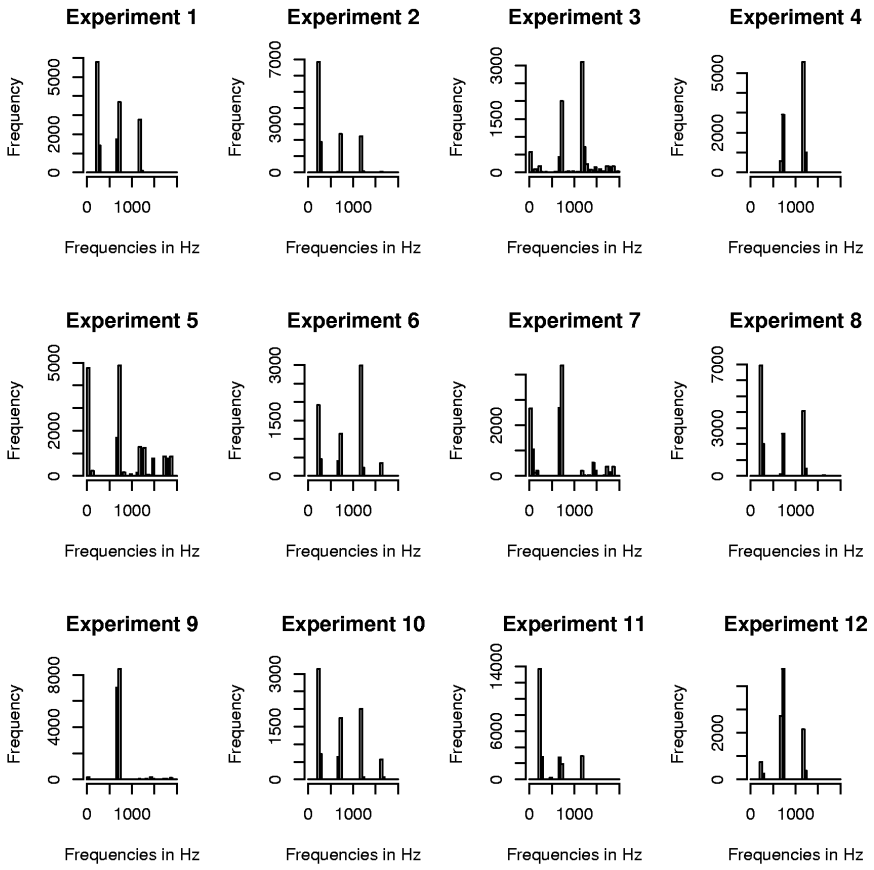

Figure 2.10: Histograms of the significant frequencies smaller than 2000Hz of the experiments 1 to 12

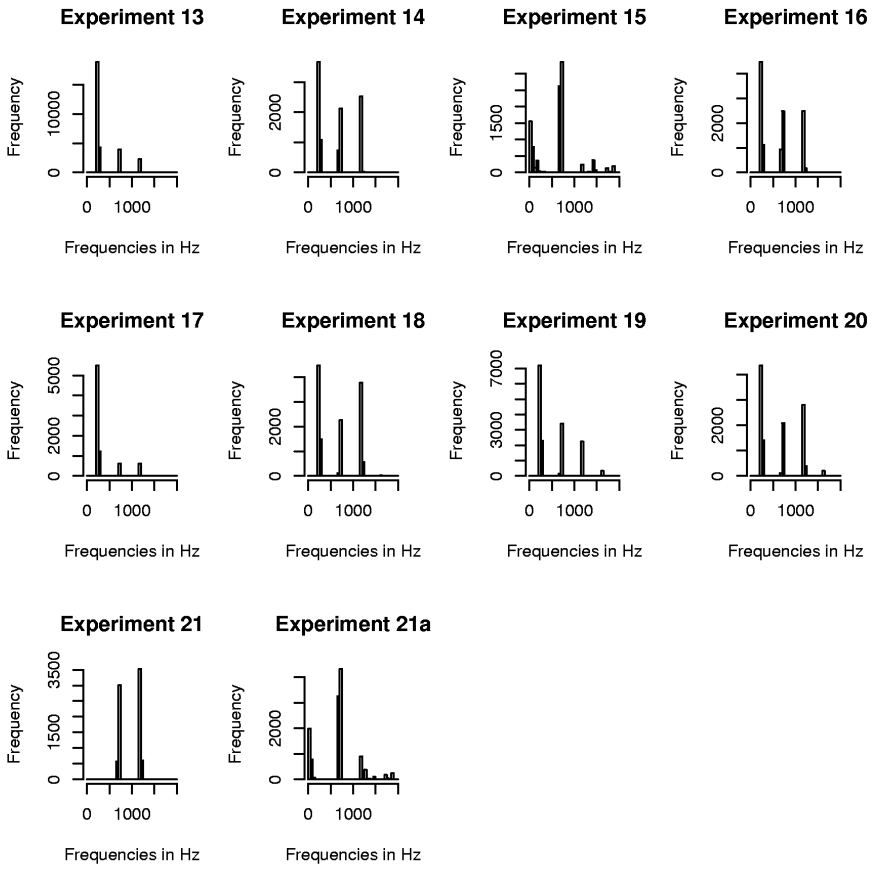

Figure 2.11: Histograms of the significant frequencies smaller than 2000Hz of the experiments 13 to 21a

Figure 2.12 is a summary of the preceding histograms, where the frequency that a bar is larger than 2 is counted. So the bars most prominent in Figure 2.12 are especially important for the process. The corresponding centre values of the bars are:

`25 Hz  225 Hz  275 Hz  675 Hz  725 Hz  1175 Hz  1225 Hz  1625 Hz`

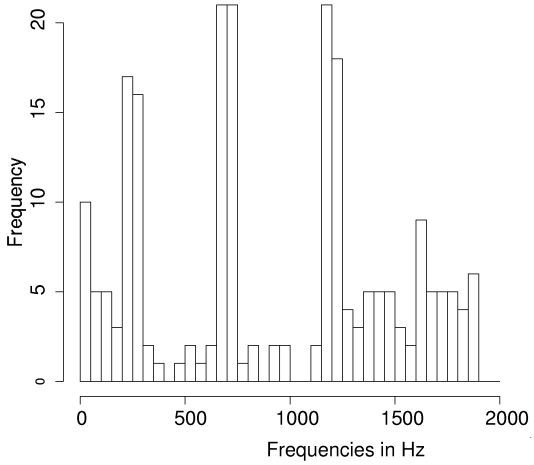

Figure 2.12: Histogram of the most frequent frequencies in the experiments.

When looking at the frequencies in the most prominent bars in the histogram in Figure 2.12 the following frequencies are found to be significant in these intervals:

```
> 0 - 50 Hz
  4.9  9.8 14.7 19.5 24.4 29.3 34.2 39.1 43.9 48.8

> 200 - 300 Hz
 200.2  205.1  210.0  214.9  219.7  224.6  229.5  234.4  239.3  244.1
 249.0  253.9  258.8  263.7  268.6  293.0  297.9

> 650 - 750 Hz
 659.2  664.1  668.9  673.8  678.7  683.6  688.5  693.4  698.2  703.1
 708.0  712.9  717.8  722.7  727.5  732.4  737.3  742.2  747.1

> 1150 - 1250 Hz
1152.3  1157.2  1162.1  1167.0  1171.9  1176.8  1181.6  1186.5  1191.4
1196.3  1201.2  1206.1  1210.9  1215.8  1220.7  1225.6  1230.5  1235.4
1240.2  1245.1

>  1600 - 1650 Hz
1601.6  1606.4  1611.3  1616.2  1621.1  1626.0  1630.9  1635.7  1640.6
1645.5
```

In the following Figure 2.13 the variation of the amplitudes over three of these intervals are depicted for the experiment at the centre point from Figure 1.9 (a). In Figure 2.14 the corresponding picture for the experiment from Figure 1.9 (b) is shown.

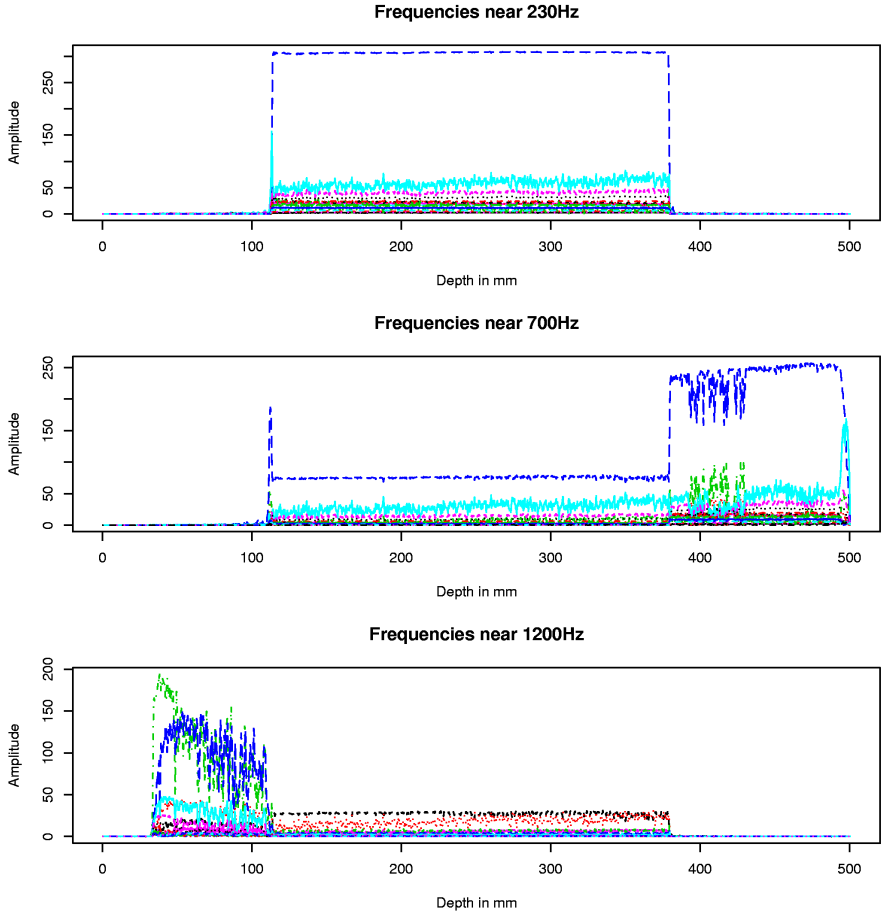

Figure 2.13: Variation of the amplitudes for frequencies top 190-273Hz, middle: 659-747 Hz, and bottom: 1143-1406 Hz

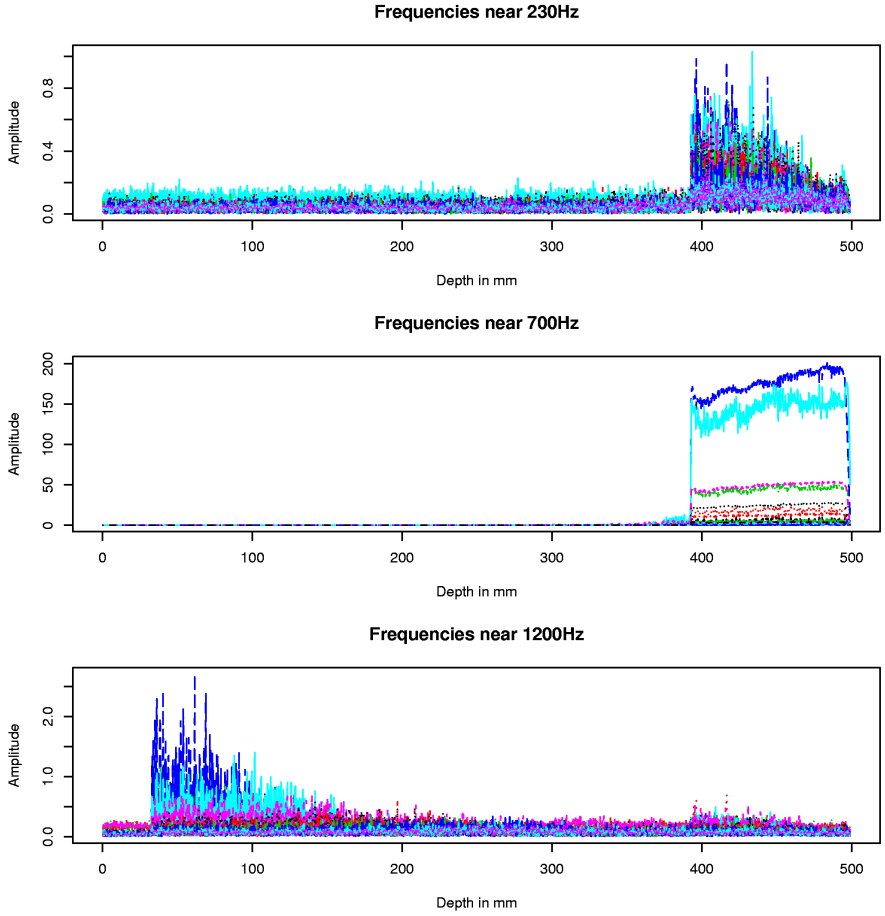

Figure 2.14: Variation of the amplitudes for frequencies top: 190-273Hz, middle: 659-747 Hz, and bottom: 1143-1406 Hz

These led to the idea to model time-varying amplitudes. The models will be discussed in Chapter 4.

2.3 Second Experimental Design

The results from the first design made it possible to determine likely effective positions for the damper. Therefore, it was decided to perform a second experimental design using one of these positions to compare the results regarding roughness and roundness to the results from the first design. Since the oil flow rate exerted a minor influence on the responses and is not always changeable in practice, the design was reduced by setting the oil flow rate at the optimal value found in the experiments at $300 l/min$. The rest of the design was projected into the plane of the cutting speed and the feed, thereby preserving $\alpha = \sqrt{2}$ the optimal value in the two-dimensional case for

orthogonal blocking and rotatability (Box and Draper (1987), p. 511). The number of repetitions in the centre was set at two.
First the different positions were tested and the most efficient was chosen. As can be seen from Figure 2.15 the frequencies dominating the chatter are completely gone. But this does not mean that further research on the problem of chatter is unnecessary, because in many practical situations the most efficient position for the damper cannot be achieved. This is the case, when extremely long workpieces are machined or the position is too close to the oil supply device.
In these experiments spiralling occurred with all settings of the influencing factors. It turned out that this was due to the wear of the guiding pads. Although this should not happen usually, it gave a good insight into the dynamics of spiralling which develops slowly as well as the chatter. Again only a few frequencies are prominent in the drilling torque in Figure 2.15(b). In the bending moment in Figure 2.15(a) single frequencies are important for any time slice but they change with time. A closer inspection reveals that some of the very low frequencies increase slowly over time. So they could be used similarly to the chatter dominating frequencies to detect and predict spiralling.

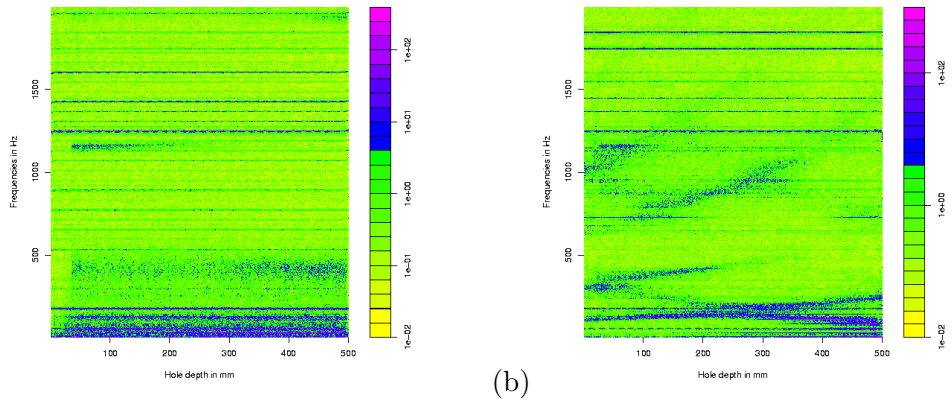

Figure 2.15: Spectrograms of the drilling torque (a) and one bending moment (b) for an experiment with $v_c = 111m/min$ and $f = 0.231mm$, both spectrograms are restricted to the frequencies 0–2000 Hz.

Because of the worn guiding pads the experimental design was completely repeated. This time no chatter or spiralling was observed. Therefore, the damper efficiently suppressed chatter and the appearance of spiralling was truely due to the worn guiding pads. But since the damper cannot be placed at the most efficient place in all tasks encountered in deep-hole drilling, it is of interest to avoid it without using the damper.

3 Overview on Experimental Design Methods for Time Series Experiments

When planning experiments with time-dependencies, it is necessary to distinguish between time-dependent and time-independent influences. If the response in such an experiment is time-dependent but the influences are time-independent the time may be modelled as a further influence variable. In some cases it may be possible to eliminate the time completely by using summary statistics, which are time-independent, for the response, e.g. the parameters of an assumed time series model, or the spectrum of a time series. Another way of looking at time-dependencies is to attribute these dependencies to autocorrelation in the error structure.
From this description four situations arise:

(1) No time-dependent influences exist and the response can be transformed into a time-independent measurement.

(2) No time-dependent influences exist, but the response can not be summarised time-independently or time-independent modelling leads to information loss.

(3) No time-dependent influences exist, but a time-dependency in the error-structure is assumed to generate the time-dependency in the response.

(4) Time-dependent influences exist and the error structure could be time-dependent as well.

In the last situation the model can be viewed as a discrete time observation of a stochastic dynamic system. In the case of dynamic systems the notion of an estimable model is replaced by the notion of identifiability.
In the first situation standard procedures for experimental design for regression models can be used, like factorial or D-optimal designs. The greatest difficulty here is determining the correct error model, as it is not always obvious, how a chosen summary statistic is distributed, given the assumed noise process in the response.
In the literature the problem of experimental design for responses measured over time is considered mainly for repeated-measurement designs with auto-correlated errors. For most of the other situations the literature is rather sparse. In the next sections this literature will be briefly reviewed and finally assessed according to the usefulness for the experimental design problem in the deep-hole drilling process.

3.1 Evaluation of Time Series collected in an Experimental Design

The two papers described in this subsection tackle one specific way to deal with a problem of the first of the four types mentioned above.
Brillinger (1973) derives F-tests for the situation of analysis of variance (ANOVA) type models on the discrete Fourier-transform in his article 'The Analysis of Time Series collected in an Experimental Design'. First he considers the following fixed effects model

$$y_{ij}(t) = \mu_{ij} + \gamma(t) + \delta_i(t) + \varepsilon_{ij}(t),$$

where μ_{ij} is the overall mean, $\gamma(t)$ is a time effect and $\delta_i(t)$ are the effects of the I levels of treatment. $\varepsilon_{ij}(t)$ are realisations of a stationary process with mean 0, power-spectrum $f_{\varepsilon\varepsilon}(\lambda)$, $0 \leq \lambda \leq \pi$, and all moments exist and are finite. This model is extended to a random effects model by assuming that $\gamma(t)$ and $\delta_{ij}(t)$ are stationary processes with the same properties as $\varepsilon_{ij}(t)$.
As a further modification the model with fixed effects and transients is considered:

$$y_{ij}(t) = \mu_{ij} + \omega_{ij}(t) + \gamma(t) + \delta_i(t) + \varepsilon_{ij}(t),$$

with the same assumptions as in the fixed effects model above and the additional condition that $\omega_{ij}(t)$ are constants, which fulfill the following property:

$$\sum_{t=0}^{\infty} |t||\omega_{ij}(t)| < \infty$$

Furthermore, he also considers stationary point processes in the case of one-way ANOVA with one repetition per class. The considered model has the following form:

$$n_i(t) = m_i(t) + p_i(t),$$

where $p_i(t), i = 1, \ldots, I$, are independent realisations of a stationary point process with power spectrum $f_{pp}(\lambda)$, while $m_i(t), i = 1, \ldots, I$, are independent of $p_i(t)$, and they are components of an I-vector-valued stationary point process $\mathbf{m}(t), t \in \mathbb{Z}$, which are symmetrically dependent.
$F-$statistics are derived for all these models , so that it is possible to perform ANOVA in all cases. In this article no further comments on the construction of suitable experimental designs are made.
In 'Time Series obtained according to an Experimental design' Gallant et al. (1974) describe a way to analyse time series obtained in a block design. The time series from the experiments are transformed into periodograms and these are further transformed by the function $\varphi_\alpha = z^\alpha$, $\alpha \in (0, 1)$. The latter transformation is chosen to ensure a better approximation to the normal distribution than is given by the simple argument, that the periodogram ordinates are χ^2-distributed for a stationary Gaussian process. The authors chose $\alpha = \frac{1}{4}$, because this seemed to be appropriate for the observed data. Like Brillinger (1973) they construct $F-$statistics on the Periodogram ordinates and perform an ANOVA. Again nothing is said about the consequences for experimental design.

3.2 D-optimal Design for Time Dependencies

The Time Series Problem

The article of Papakyriazis (1978) is one of the very few articles concerned with optimal experimental design for time series experiments. In the article he describes designs for time dependencies in the influences as well as for time dependencies in the errors and combinations of both types, thus the models fall into the last three categories mentioned above. Papakyriazis restricts himself to AR and MA processes. A significant limitation to the applicability of these considerations is the necessity to have precise information about the order and the parameters of the AR/MA process. If such information is not available or incorrect, the proposed methods will lead to inefficient or even completely misleading designs.
The following models are considered:

(1) Lagged–independent variables: Consider a model with a finite, known and small lag τ

$$y_t = \sum_{i=1}^{K} \sum_{j=1}^{\tau+1} \beta_{ij} x_{i,\tau-j+1} + \varepsilon_t \,\text{mit}\, \varepsilon_t \sim N(0, \sigma) \tag{3.1}$$

the influences $x_{i,\cdot}$ are deviations from the respective means of the variables. Moreover, the following assumptions are made:

(a) $(x_{i,t})$ and ε_t are independent,

(b) $(x_{i,t})$ is stationary for all i during the experiments and for the infinite past,

(c) $var(x_{i,t}) = 1$ for all i and t,

(d) the estimates of the variances and covariances of the model parameters must converge to the true values for growing sample size T.

Going on these assumptions it is proved that an experimental design is D–optimal if and only if the correlation matrix is equal to the identity matrix.

(2) Auto-correlated errors: The model in formula (3.1) is modified in this case so that $\varepsilon_t = [\theta(L)/\phi(L)]a_t$, where $\theta(L)$ and $\phi(L)$ are polynomials of the lag–operator L (defined as $L^k x_{i,t} = x_{i,t-k}$). Designs are constructed especially for the following models:

(a) A simple AR(1)–process, i.e. $\tau = 0$, $\theta(L) = 1$ and $\phi(L) = 1 - \phi L$, $\phi \in (-1, 1)$,

(b) for an ARMA(1,1)–process,

(c) a model with a lag of one period, one independent variable and an AR(1)–process on the error term, i.e.

$$y_t = \beta_1 x_t + \beta_2 x_{t-1} + (1 - \phi L)^{-1} a_t$$

For all these models correlation structures for the control process are given.

(3) the mixed autoregressive–regressive model with correlated errors, i.e.

$$y_t = \delta y_{t-1} + \beta x_t + (1 - \phi L)^{-1} a_t$$

If ϕ is known, it exists a function, which has to be maximized with respect to the auto-correlation at lag 1 to get a D–optimal design.

Therefore, various models of types (2)–(4) are tackled in this article. However, all designs described have the aforementioned drawback of the exactness of information on the model.

Factorial Designs and Auto–Correlation

The problem of optimal factorial designs in the presence of autocorrelation has been considered in a series of articles in the 1990s. These models have time-dependent influences i.e. the influencing factors are changed in time but correlation over time is only introduced in the error process (type (4)). The articles will be described briefly here.

Saunders and Eccleston (1992) dealt with 'Experimental Design for continuous Processes'. They consider models of the form

$$Y_{t_i} = x_i'\beta + \varepsilon_{t_i} \,,$$

where ε_{t_i} is a continuous time process with variogram $V(t)$. The variogram is a function of the following form:

$$V(t) = \frac{1}{2} E(Y_s - Y_{s+t}).$$

Additionally the authors make the following assumptions:

(1) the process has stationary increments, so that the variogram exists.

(2) the error process is not influenced by the treatments applied.

The authors are interested in the common case that it is not the effect of single influences that are of interest, but only specific contrasts. In factorial designs these are the main effects and the interactions of low order; in Taguchi experiments these are the interactions of controlled and uncontrolled factors. The variance of the estimation of a contrast is only dependent on the time points of the measurements, since it is assumed that the variance structure does not depend on the level of the factors. Saunders and Eccleston prove that the variances and covariances of a set of interesting contrasts K are given by the expression $-K^T V K$ with $V = V(t_i - t_j)$. Therefore, the following procedure is proposed:

(1) Determine the contrasts with low variance from $-K^T V K$.

(2) Assign the influencing factors so that the most interesting effects (parameter estimates) are assigned to the contrasts with low variance.

Then it is proved that the variances and covariances, which have to be controlled to obtain an optimal design, only depend on the chosen contrasts and the form of the variogram. A- and D-optimality can therefore be expressed directly by the variogram as suggested by the above formula.
Optimal time points for the measurements are determined theoretically for the case of equally spaced time points and increasing variogram. The time points are optimal iff $E\left((\varepsilon_{t_i} - \varepsilon_{t_j})^2\right) = \lim_{t\to 0, t\geq 0} V(t)$ for $i \neq j$. But the authors point out that level changes of influencing factors in a continuous process show effects after some time so that very short distances in time are not realistic. This leads to the problem that optimal contrasts cannot be determined only with respect to the optimal time points but over a stretch of time points. This can lead to different optimal contrasts, and therefore it is not possible to determine uniformly optimal contrasts for all variograms.
Saunders (1994) constructs algorithms for the determining irregularly spaced optimal time points for the linear and the exponential variogram. He proves that his algorithms lead to minimal variance of the parameter estimates at least locally. The restriction to local optimality is of no interest for practical purposes, because experiments are always limited in time.
Saunders and Eccleston (1992) roughly describe an algorithm for constructing optimal contrasts. This algorithm is formulated in more detail in Saunders et al. (1995). In this article it is shown that contrasts with many level changes lead to small variances of the parameter estimates under the named circumstances. It is shown that so-called paired contrasts of the form $(k_1, -k_1, \ldots, k_n, -k_n)$ are often optimal. On the one hand a restriction to paired contrasts reduces the number of contrasts under consideration. On the other hand it means that constructing a design to estimate two main effects and their common interaction is not possible. This is easily seen by considering the elementwise product of paired contrasts, which is obviously no longer paired. For the algorithm they further restrict the search space by considering only balanced designs. The examples they give show impressively the variance reduction gained by using optimal contrasts.
These investigations are continued in Martin et al. (1998b). Here not only the aforementioned AR(1)-correlation structures, but AR(q) and other kinds of structures are considered. Most of the examples considered, are models with a MA(1)-structure or a 'linear variance' structure (with a covariance of the form: $I_{n-1} + \nabla'\nabla$ with ∇ a $n - d \times n$ difference matrix) with positive dependencies. In this case, the authors prove explicit connections between the number of level changes and the optimality criteria for A-, D- and E-optimality. Their results on the connection between designs for different models are highly interesting. In Lemma 7 (page 374) they demonstrate the special form of the information matrices, which makes it possible to construct an optimal fractioned 2^{p-q}-design from a complete optimal 2^p-design.
Finally Martin et al. (1998a) demonstrate that similar criteria for the construction of multi-level designs in this framework exist. Adequate generalisations for the number of level changes and a suitable neighbourhood definition lead to easily determinable parameters, which mainly influence the optimality criteria. They also managed to

generalise the result on the connection between a complete and a fractioned design.

3.3 Experimental Design and Dynamics

So far only models of a classical statistical point of view, which do not include continuous time or even non-linear models, have been considered. In this section results concerned with one or both of these topics will be mentioned. Again these models may fall into the categories (2)-(4).

Connection to the other Approaches
Fedorov and Nachtsheim (1995) consider the design problem for dynamic experiments, i.e. the models under consideration depend upon time and control variables. They consider only additive error structures and linear models. The difference to the other articles discussed is that they allow for continuous time. First they consider the same models as Papakyriazis (1978) and get the same results using a slightly different approach. The section on parameterization of the trajectories is the most interesting. Parameterizationof the trajectories reduces the dimensionality of the design problem by replacing the general series of r different settings of the control variable with a parametric function of time for which only the parameters have to be determined. Secondly they also discuss algorithmic problems in optimising designs formed by trajectories.

3.3.1 Experimental Design for Dynamic System Identification

Dynamic system identification is a concept of control theory, and translates as the estimation of parameters in a dynamic system from a statistical point of view.

Linear Dynamic Systems
In 'Optimal Experiment Design for Dynamic System Identification' Zarrop (1979) constructs ϕ-optimal designs for the identification of linear dynamic systems of the form

$$y_k = L^s \frac{b(L)}{a(L)u_k} + \frac{d(L)}{c(L)}\varepsilon_k \,,$$

where a, b, c, d are polynomials of degrees n, m, q, r, and L is again the lag operator as defined in section 3.2. The power s of L means that it is applied s times. $(\varepsilon_k)_{k\in\mathbb{N}}$ is a white noise process. Additionally it is assumed that the polynomials a, b, c, d are relative prime, and that their degrees and the power s are known.
Under these assumptions Zarrop derives geometric properties of the space of all informationmatrices for this model. He proves that this space is embedded in $\mathbb{R}^p$. It turns out that this property can be used to obtain canonical representations of input trajectories in form of Tschebycheff systems. He derives algorithms for constructing D-optimal designs of input trajectories. Finally he generalizes this approach to continuous time,and tackles the question of simultaneous optimization of sampling rate and input trajectories.

Non-linear Dynamic Systems

Leontaritis and Billings (1987) discuss the problem of optimal experimental design in the case of non-linear systems. They show that in the case of open-loop operation (i.e. there is no feedback control applied) Gaussian white noise is optimal when a power constraint on the input is given, and a uniformly distributed process is optimal when an amplitude constraint has to be respected. Furthermore, they proved that the use of trajectories that are optimal for the identification of linear systems may lead to a complete loss of identifiability. Additionally they give practical guidelines for designing experiments in a closed-loop situation.

3.4 Repeated-Measurements Designs in the Presence of Auto-Correlated Errors

In repeated-measurements (RM) models in particular, the question of auto-correlation in the errors is considered frequently in the literature. This is not surprising, since it would seem natural to take into account a possible time dependency when making several observations over time on the same experimental unit.
In this section only a few articles are mentioned to complete this overview on methods for experimental design respecting time dependencies.
There are several articles on the search for optimal designs in the case of first-order auto-regressive processes in cross-over experiments. They all assume the following kind of model:

$$y_{ijt} = \alpha_i + \beta_t + \tau_j + \varepsilon_{ijt}\,,$$

where α_i is the effect of the i^{th} subject or experimental unit, β_t is the effect of time t, τ_j the effect of treatment j, and ε_{ijt} the error process with correlation matrix V.
Several articles consider the optimality properties of Williams-Designs. Berenblut and Webb (1974) show that Williams designs are the best possible choice when, in a repeated-measurements situation, it is not known whether or not the errors are uncorrelated. They show by simulations that in this situation the Williams designs are the most efficient under both conditions, uncorrelated errors or errors with first order autocorrelation. Kunert (1985) shows, using the same model assumptions, that E-optimality for weighted least-squares analysis is obtained with an additional balancing property. More generally Kunert and Martin (1987) prove A- and D-optimality for Williams (IIa) block designs with extra plot.
Based partly on the above cited papers Martin and Eccleston (1991) develop the concept of strongly equineighboured designs and prove that designs fulfilling this concept are weakly universally optimal BIB (balanced incomplete block) designs under ordinary least-squares for any dependence structure of the errors.
The cited literature covers a wide variety of situations in designs for repeated-measurement models with dependence of the errors.

3.5 Assessment of Methods for Experimental Designs for the BTA Deep-Hole Drilling Process

All experimental designs covered in this chapter so far deal with the problem of correlation between experiments. Experiment means here observation from a period with a constant treatment of the experimental unit. However, they do not deal with experiments which have time series as the result or observation of a single experiment. Thus, these experimental designs were of minor interest for the first experiments on the deep-hole drilling process but some may be of interest in later stages of the project. The first two articles on the evaluation of time series collected in an experimental design provided the general idea for the developments of the models on varying amplitudes described in Chapter 4.

In general, it can be said that the categories (2)-(4) from the beginning of the chapter are covered well by the literature presented here. The first category is not extensively covered.

The D-optimal designs on time series in the first part of Section 3.2 have the major draw-back that the correlation coefficients of the time series need to be known in order to construct the design. These coefficients are not known for the time series of the drilling torque for the deep-hole drilling process, and the diverse outcomes of the time series of the drilling torque at the centre point of the design point more towards a dynamic process.

The second part on factorial designs and auto-correlation could be of interest for the design of experiments to test the effect of on-line changes of the machine parameters. Such factorial designs appear quite promising for detecting the most effective change in the machine parameters for different kinds of chatter vibrations. Since the series of articles not only includes all relevant theoretical proofs but also an algorithm to construct the appropriate contrasts it should be possible to apply these designs in the future.

The experimental designs for system identification could not be applied because the first formulations of dynamic systems for the deep-hole drilling process were not in the form of input-output systems. This may change after the first experiments with time-varying machine parameters have been accomplished. It should then be possible to distinguish between linear and non-linear dynamic systems which is crucial as the results of Leontaritis and Billings (1987) show.

Finally the repeated-measurements designs are of interest when thinking about experimental designs for the models on varying amplitudes. This is because a combination of time-stationary and time-varying effects lead to a data situation which is best described as a repeated-measurements model and certain error structures on harmonic processes may lead to correlation between the periodograms estimated for the spectrogram data. For more details see Section 4.3.

3.6 Experimental Design Solutions for Experiments with Time Series as Output

The investigation of dynamic problems or problems where the measurements are obtained in the form of time series can be compared to spatial analyses. Müller (2001b) points out in Chapter 4 of his book 'Collecting Spatial Data' that optimal design of experiments is often criticised for the necessity to exactly specify the model to be fitted to the data. This is often impossible in spatial problems because the models used there are only rough approximations of the actual highly complex phenomena. Furthermore, the experimental designs are criticised for 'leaving large parts of the experimental region unobserved'. W. G. Müller suggests exploratory designs to address this criticism. Since these designs may also be valuable in the situation discussed here, the next subsection is dedicated to the brief introduction of several possible definitions of such designs and a more extensive description of Coffeehouse designs. Coffeehouse designs were chosen because they have an especially easy construction rule.

3.6.1 Model-free or Exploratory Designs

When no model assumptions can be made because there is no information on possible connections between influencing variables and the chosen response or the investigation has several different goals, a way of exploring a wide variety of combinations of the influencing variables is called for. The simplest form of such a design would be a grid across all interesting levels of influencing variables. It should be noted however that even with a small number of variables (less than five) and levels this amounts to very large numbers of experiments.
Exploratory designs must therefore be able to:

(1) Explore the space of possible values as 'completely' as possible

(2) Deal with the restricted number of experiments

One approach to constructing such designs is to define regions of interest for each variable, define a common sampling distribution for this restricted space, (e.g. a multivariate uniform distribution), and then draw a sample of the requested number of experiments with this distribution. Alternatively define a distribution for each variable, take one-dimensional samples, construct a grid from all these one-dimensional samples, and sample again with a uniform distribution from this grid. These are called random designs, cf. Esbensen et al. (1998). The results from these designs are then typically evaluated with Principal Component Analysis (PCA) or Partial Least Squares (PLS) because this makes it possible to identify the subspaces of large variance contribution to the response variable. This kind of space-filling design is probably not the best choice if only a small number of experiments can be accomplished because then it may happen that the random realisations are clustered within the design space. Additionally it is not clear how to define an appropriate measure

of variability for the use of PLS or PCA, when the outputs of the experiments are time series. It should be noted however that the results of Leontaritis and Billings (1987) on the identification of non-linear dynamic systems could be included in this framework in the following sense:
Define a random set of time-stationary experimental conditions, and random input samples to the dynamic system drawn from the appropriate distribution.
Another approach is to use optimal space-filling designs, or maxmin-distance designs. These designs try to 'fill' the given space of input values with the given number of experiments. The construction rules try to identify a set of points which has the property to maximise the minimal distances between all points. This is done to ensure that not more space than absolutely necessary is left void. There are various ways of constructing space-filling designs, cf. e.g. Morris and Mitchell (1995) or Johnson et al. (1990). An easy way of constructing such a design is described below. It was also applied in the simulation study described in Chapter 5.

Coffeehouse Designs

Müller (2001a) proposed the so-called Coffeehouse Designs. These are maxmin-distance designs constructed as follows:

(1) Choose two points in the design region with maximum distance.

(2) Find all points which maximise the minimal distance from all points selected so far.

(3) Select one of the points found in step 2.

(4) Repeat step 2 and 3 until the number of experiments is achieved.

Figure 3.1 illustrates the steps on an irregularly shaped region. Points 1 and 2 have the maximal possible distance in this region. Since the region is concave on the lower left-hand side, the minimal distances cannot be maximised in this part of the region. Thus the first guess is that the next point should lie on the blue curve on the upper border. In this region therefore the point with equal distances to the first two points is the correct choice. By finding the maximal width of the region it becomes clear that point 4 with equal distance to point 1 and 3 is correct.

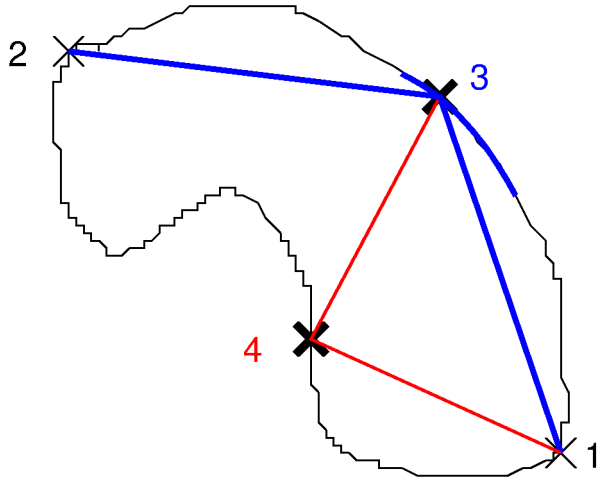

Figure 3.1: Coffeehouse design on an irregularly shaped region.

This approach can be implemented much more easily, when a grid is applied to the search space, thus candidate points are not constructed by computationally challenging optimisations.
Projection optimality is another interesting property in space-filling design (Morris and Mitchell, 1995). Projection optimality means that any projection of the design into a canonical subspace of the experimental space is a space-filling design with the same number of experiments in this subspace. This property can be obtained by the Coffeehouse Design in the following way:

(1) Determine candidate points from each one-dimensional interval by the Coffeehouse rule,

(2) construct a grid from these one-dimensional candidate points,

(3) apply the Coffeehouse rule to this grid,

(4) eliminate the elements of the chosen point from the one-dimensional candidate points,

(5) repeat until number of experimental points is reached.

Of course this construction rule can only be applied when each variable can take at least n levels. Figure 3.2 illustrates this algorithm for a design with six points on points 3 and 4. The final position of point 4 is uniquely defined by the distances in the two-dimensional space.

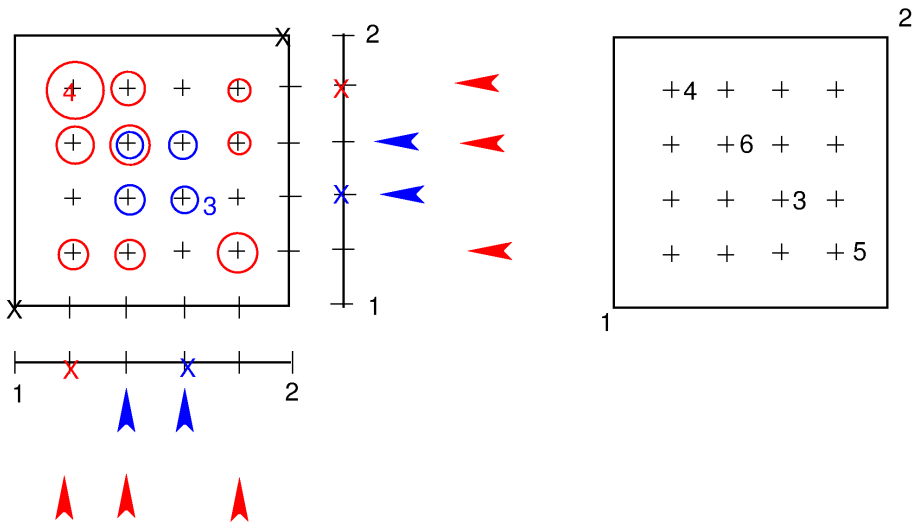

Figure 3.2: Construction of a projection-optimal Coffeehouse design with six points.

4 Models on Periodogram Ordinates for Harmonic Processes

This chapter provides the theoretical background for the models on periodogram ordinates. First the distribution of periodogram ordinates at significant frequencies of a harmonic process with normal disturbances is determined. Then a procedure for the determination of so-called relevant frequencies is derived and finally regression methods to fit models on varying amplitudes are introduced.

4.1 Determination of the Distribution of Periodogram Ordinates

Gallant et al. (1974) and Brillinger (1973) consider analysis of variance (ANOVA) models on periodograms. Their argument – based on a Taylor series extension of the distribution function – is to transform the observed ordinates with $g(x) = x^{\frac{1}{4}}$ to increase the convergence of the χ^2_2-distributed measurements to a normal distribution and thereby make a common ANOVA sensible in this situation.
Since the basic idea of Gallant et al. (1974) is to use a normal approximation for the distribution of the periodogram ordinates, the distribution of Fourier-transforms of processes based on normal white noise is investigated more closely. This is the foundation for the construction of models on varying amplitudes.
The periodogram ordinate at frequency f equals n times the squared absolute value of the Fourier-transform F of the time series y_t at frequency f, that is

$$I[y_t](f) = n|F[y_t](f)|^2,$$

where n is the number of observations in the series.
If y_t is a Gaussian process with distribution $\mathcal{N}(0, \sigma^2)$, $F[y_t](f)$ as a linear transformation of y_t has again a normal distribution. $|F[y_t](f)|^2 = (\mathrm{Re}(F[y_t](f))^2 + (\mathrm{Im}(F[y_t](f))^2$ is therefore χ^2 distributed with 2 degrees of freedom, which equals an exponential distribution (cf. e.g. Fisz (1970)). On the basis of this argument and using the fact that the Fourier-transform is a linear operator it follows that periodogram ordinates of AR(p) processes are χ^2_{2p}-distributed.
The expected value of $|F[y_t](f)|^2$ can be calculated using the formula $Var(X) = E(X^2) - E(X)^2$:

$$E(|F[y_t](f)|^2) = E((\mathrm{Re}(F[y_t](f)))^2 + (\mathrm{Im}(F[y_t](f)))^2) \quad (4.1)$$

$$
\begin{aligned}
&= && E((\mathrm{Re}(F[y_t](f)))^2) + E((\mathrm{Im}(F[y_t](f)))^2) && (4.2)\\
&\overset{E(F[y_t](f))=0}{=} && Var(\mathrm{Re}(F[y_t](f))) + Var(\mathrm{Im}(F[y_t](f))) && (4.3)\\
&= && 2\sigma^2 && (4.4)
\end{aligned}
$$

Now consider a harmonic process of the following form:

$$h_t = \sum_{k=1}^{K} R_k cos 2\pi(f_k t + \varphi) + \varepsilon_t, \tag{4.5}$$

where $\varepsilon_t \sim \mathcal{N}(0, \sigma^2)\, \forall t \in \mathbb{Z}$ and R_k are the amplitudes at the relevant frequencies f_k , $k = 1, \ldots, K$.
The Fourier-transform of $R_k cos 2\pi(f_k t + \varphi)$, $t = 0, \ldots, n-1$, is (cf. Bloomfield (2000), p.46):

$$F[R_k cos 2\pi(f_k t + \varphi)](f) = R_k \exp\left(2\pi i (f_k - f)\frac{n-1}{2}\right) \frac{\sin(\pi(f_k - f)n)}{sin(\pi(f_k - f))} \tag{4.6}$$

Because the equation $\dfrac{\sin(\pi(f_k - f)n)}{sin(\pi(f_k - f))} = 0$ is true for all Fourier frequencies $f \neq f_k$ and, $\dfrac{\sin(\pi(f_k - f_k)n)}{sin(\pi(f_k - f_k))} = 1$ holds for the relevant frequencies f_k, $k = 1, \ldots, K$,, it follows that the Fourier-transform of h_t is

$$F[h_t](f) = \begin{cases} F[\varepsilon](f) + B_f & \text{for } f \neq f_k\,,\ k = 1, \ldots, K \\ R_k + F[\varepsilon](f) & \text{for } f = f_k\,,\ k = 1, \ldots, K \end{cases}, \tag{4.7}$$

where $B \neq 0$ is only true for frequencies near to one of f_k , $k = 1, \ldots, K$, and possibly harmonics of these frequencies.
Again a result on the distribution of the periodogram ordinates is readily gained by the same arguments as above: they are χ^2-distributed. It is only close to the relevant frequencies that you get non-central χ^2-distribution with non-centrality parameter $\nu = n(R_k^2 + 2\sigma_\varepsilon^2)$. The latter can be derived from formulas (4.4) and (4.7) in the following way:

$$
\begin{aligned}
E(|F[h_t](f_k)|^2) &= E\left(\mathrm{Re}(R_k + F[\varepsilon](f_k))^2\right) + E\left(\mathrm{Im}(R_k + F[\varepsilon](f_k))^2\right) && (4.8)\\
&= E(\mathrm{Re}(R_k + F[\varepsilon](f_k)))^2 + E(\mathrm{Im}(R_k + F[\varepsilon](f_k)))^2 && (4.9)\\
&\quad + Var\left(\mathrm{Re}(R_k + F[\varepsilon](f_k))\right) + Var\left(\mathrm{Im}(R_k + F[\varepsilon](f_k))\right) && (4.10)\\
&= R_k^2 + 0 + \sigma_\varepsilon^2 + \sigma_\varepsilon^2 && (4.11)
\end{aligned}
$$

A more general determination of the distribution of periodogram ordinates can be found in Wittwer (1986). In her paper G. Wittwer determines the moment generating function and the general properties of the distribution of the periodogram ordinates for stationary sequences.

4.2 Regression Models on Periodogram Ordinates

When the amplitudes at the relevant frequencies f_k , $k = 1, \ldots, K$, of a harmonic process are influenced by some input variables $\vec{x}$, it is of interest to investigate the form of this influence. So the following model is considered:

$$G_t(\vec{x}) = \sum_{k=1}^{K} g_k(\vec{x}) cos 2\pi(f_k t + \varphi) + \varepsilon_t, \tag{4.12}$$

With equation (4.7) the Fourier-transform is essentially the following:

$$F[G_t(\vec{x})](f) = \begin{cases} F[\varepsilon](f) + B_f & \text{for } f \neq f_k \text{ , } k = 1, \ldots, K \\ g_k(\vec{x}) + F[\varepsilon](f) & \text{for } f = f_k \text{ , } k = 1, \ldots, K \end{cases}, \tag{4.13}$$

where $B_f \neq 0$ is only true for frequencies near to one of f_k , $k = 1, \ldots, K$ and possibly harmonics of these frequencies.
With equation (4.11) it is clear that the expected value of the periodogram ordinates at the relevant frequencies is

$$E(I_{G_t(\vec{x})}(f)) = n(|e^{i\pi\varphi}| \, g_k(\vec{x})^2 + 2\sigma_\varepsilon^2) \text{ for } f = f_k \text{ , } k = 1, \ldots, K. \tag{4.14}$$

4.2.1 Effect of the Phase

The phase is of no interest in this model because it contributes only a constant factor in the complex Fourier transform equal to $e^{i\pi\varphi}$ of which the absolute value is 1. So the phase does not contribute to the estimates described above, and is ignored in the following sections and subsections.

4.2.2 Estimating the Variance of ε (σ_ε^2)

When constructing an estimator for the functions $g_k(\vec{x})$, $k = 1, \ldots, K$, an estimate of σ_ε^2 is required. If the frequencies are known, it is then possible to fit a harmonic process in those frequencies at different values of the input variables $\vec{x}$, and use the least-squares residuals to estimate σ_ε^2. However, there are two reasons against this: On the one hand the relevant frequencies need to be known, which might not be the case. On the other hand the least-squares fit also needs a constant phase, albeit unnecessary for the periodogram ordinates to be constant. If the phase varies only slightly this leads to very large residuals and thereby to a bias of the variance estimate. So another procedure is required, which does not rely on known relevant frequencies and is not as vulnerable to faulty pre-steps for its calculation.
The Fourier-transform of a harmonic process with a small number of relevant frequencies K compared to the number of observations n can be viewed as a sample from a χ^2-distribution contaminated by some non-central χ^2-distributed observations, where the distributions have the same degrees of freedom. As shown in formula (4.4) the expected value of the majority of observations is directly connected with the variance

of the disturbance process. A robust estimator of the expected value of this distribution is also proportional to an estimator for the variance of the disturbance process with known proportionality factor.
Since it is assumed that in a regression situation the error processes are independent between experiments and identically distributed over all experiments, the following procedure looks promising:

(1) Estimate the periodogram $I[G_t(\vec{x_l})]$ for all input values x_l , $l \in 1, \ldots, L$

(2) Merge all $I[G_t(\vec{x_l})](f)$ into one sample

(3) Calculate a robust estimator for the expected value of $I[G_t(\vec{x_l})](f)$, e.g. the standardized median $med_{stand.}(X) = \frac{1}{\log(2)} med(X)$ on the merged sample

Step 2 enlarges the database for the robust estimate, because it is assumed, that the observations with different input values are independent and the realisations of $I_{G_t(\vec{x_l})}(f)$ for different Fourier frequencies are independent due to the orthogonality relations of the Fourier transform. If $K \ll n$ and $\frac{K}{n}$ is lower than the breakdown point of the robust estimator, which equals $\frac{1}{2}$ for the standardized median (Gather and Schultze, 1999), one gets an estimator – in the case of Gaussian white noise – for $2\sigma_\varepsilon^2$.

4.2.3 Constructing Regression Estimates

Known Frequencies

If the relevant frequencies are known, it suffices to calculate the regressions on periodogram ordinates of the corresponding Fourier frequencies – if f_k are Fourier frequencies themselves only at those frequencies. If they are not Fourier frequencies, then at the nearest Fourier frequencies.

Unknown Frequencies

If the relevant frequencies are not known, they have to be estimated. This can be done by using the estimate of $2\sigma_\varepsilon^2$ to test for significant frequencies in all time series from the experiments and then selecting those frequencies present in all of them. Although the large number of significance tests could lead to a loss of power of the test it is not strictly necessary to correct for multiple tests because this is taken care of by checking if the frequencies test significant in all experiments. In the simulations described in Section 5.2, all really relevant frequencies are found in all the situations considered.

Transforming Periodogram Ordinates

Given that the goal of the regression on periodogram ordinates is to estimate the influences on the amplitudes, the observations have to be transformed in the following way:

(1) substract $2n\sigma_\varepsilon^2$ to eliminate the bias

(2) divide periodogram ordinates by n

(3) take the square root of the periodogram ordinates

(4) repeat for all realisations of the influences $\vec{x}$.

So the following estimator for $g_k(\vec{x})$ is used:

$$\hat{g}_k(\vec{x}) = \sqrt{\frac{I[G_t(\vec{x})](f_k) - 2n\sigma_\varepsilon^2}{n}},$$

Johnson et al. (1994) state several normal approximations of the non-central χ^2-distribution. One of these is simply to take the square-root of non-central χ^2-distributed variable. All these approximations depend on the value of the non-centrality parameter, which in this context depends on the value of the functions g_k , $k = 1, \ldots, K$ and the number of observations. So there is theoretical reason to use a normal approximation in these models. The impact of this approximation is tested in the simulation study in section 5.2.

4.3 Time-varying Amplitudes

In the deep-hole drilling process it is necessary to deal with time-varying amplitudes. Here a helpful tool is the so-called spectrogram. The spectrogram is formed by calculating periodograms from sequences of fixed length from the time series, and then plotting them in a 2D-plot with time on the x-axis and frequencies on the y-axis using colours to distinguish the heights of the periodogram ordinates. This kind of data can be used to construct models to approximate time-dependent functions of the amplitudes.
Now the model in time domain has the following structure:

$$H_t(\vec{x}) = \sum_{k=1}^{K} h_k(\vec{x}, t) \cos 2\pi(f_k t + \varphi) + \varepsilon_t, \tag{4.15}$$

for $t \in 0, \ldots, n-1$ and $K \ll n$. The functions of the amplitudes of the relevant frequencies are now time-dependent. Since only discrete time is considered, they are defined by $h_k : \mathbb{R}^d \times \mathbb{N} \to [0, \infty)$. For h_k only the existence of a Fourier-transform is assumed.
The corresponding model in frequency domain is in terms of the complex Fourier-transform:

$$F[H_t(\vec{x})](f) = \begin{cases} F[\varepsilon](f) + B_f & \text{for } f \neq f_k,\ k = 1, \ldots, K \\ F[h_k(\vec{x}, t) \cos 2\pi(f_k t + \varphi)](f) + F[\varepsilon](f) & \text{for } f = f_k,\ k = 1, \ldots, K \end{cases}, \tag{4.16}$$

where again $B_f \neq 0$ is only true for frequencies near to one of f_k , $k = 1, \ldots, K$ and possible harmonics. Now the transform is not as simple as before and therefore more assumptions about $h_k(\vec{x}, t)$ are needed to analyse ways to estimate them.

4.3.1 Modelling Amplitudes of Fourier Frequencies

The periodogram is only able to estimate Fourier frequencies, so it is of interest to know what happens when the relevant frequencies are Fourier frequencies. This turns out to be especially easy, because the finite Fourier transform of h_k – omitting the factor introduced by the phase – is:

$$\begin{aligned} F[h_k(\vec{x},t)\cos 2\pi(f_k t)](f) &= \frac{1}{n}\sum_{t=0}^{n-1} h_k(\vec{x},t)\cos 2\pi(f_k t)e^{-i2\pi f} \\ &\overset{(*)}{=} \frac{1}{2n}\left(\sum_{t=0}^{n-1} h_k(\vec{x},t)e^{i2\pi(f_k-f)t} + \sum_{t=0}^{n-1} h_k(\vec{x},t)e^{-i2\pi(f_k+f)t}\right) \\ &= \frac{1}{2n}\sum_{t=0}^{n-1} h_k(\vec{x},t)(1+e^{-i4\pi f_k t}) \text{ for } f = f_k \\ (*)\cos(2\pi f_k t) &= \frac{1}{2}\left(e^{i2\pi f_k t} + e^{-i2\pi f_k t}\right). \end{aligned}$$

When all relevant frequencies are Fourier frequencies the important part of the periodogram is greater than $1/2$ and less than or equal to the mean of the values of h_k over the time points $0,\ldots,n-1$ – or the chosen part of the time series:

$$\frac{1}{2n}\sum_{t=0}^{n-1} h_k(\vec{x},t) \ll \sqrt{\frac{I[h_k(\vec{x},t)\cos 2\pi(f_k t)](f_k)}{n}} \leq \frac{1}{n}\sum_{t=0}^{n-1} h_k(\vec{x},t)$$

So using the periodogram to estimate the function of the amplitudes over time possibly underestimates the values of the function.

Linearity in Time

As usual in statistics linearity means here linearity in the parameters of the time model, and not that time has a linear effect on the amplitudes. The linearity of the Fourier transform preserves this kind of linearity, and thereby makes these functions of the amplitudes tractable by regression methods.
First consider a simple linear time-trend:

$$h_k(\vec{x},t) = \mu + l_k(\vec{x}) + \sum_{i=1}^{j}\beta_{ki}x_i t + \alpha_k t.$$

If $f_k, k = 1,\ldots,K$ are Fourier frequencies, it is easy to calculate the Fourier transform:

$$\begin{aligned} F[h_k(\vec{x},t)cos2\pi(f_k t+\varphi)](f_k) &= \mu + l_k(\vec{x}) + \frac{1}{2}\left[\sum_{i=1}^{j}\beta_{ki}x_i\frac{n-1}{2} + \alpha_k\frac{n-1}{2}\right. \\ &\quad \left. + \frac{1}{n}\sum_{i=1}^{j}\beta_{ki}x_i\left(\sum_{t=0}^{n-1} te^{-i4\pi f_k t}\right) + \frac{\alpha_k}{n}\sum_{t=0}^{n-1} te^{-i4\pi f_k t}\right] \end{aligned}$$

Divide a time series of length N into chunks of equal length n, then for the m^{th} chunk $\frac{n-1}{2}$ in the formula is replaced by $\frac{2m+n-1}{2}$. So this means that a linear function in the amplitude is transformed into a linear function over several periodograms.
When t is replaced by a function $\phi(t)$, the transform at the Fourier frequencies stays a linear combination of the Fourier-transform of ϕ.

4.3.2 Non-Fourier Frequencies

When f_k is a non-Fourier frequency the finite Fourier transform introduces additional non-zero terms to the periodogram because it only considers Fourier frequencies. This comes from the fact that $e^{i2\pi(f_k-f)}$ is not only non-zero at the nearest Fourier frequencies but also in a neighbourhood.

$$\begin{aligned} F[h_k(\vec{x})\cos 2\pi(f_k t)](f) &= \frac{1}{n}\sum_{t=0}^{n-1} h_k(\vec{x},t)\cos 2\pi(f_k t)e^{-i2\pi ft} \\ &= \frac{1}{2n}\sum_{t=0}^{n-1} h_k(\vec{x},t)\left(e^{i2\pi(f_k-f)t} + e^{-i2\pi(f_k+f)t}\right) \end{aligned}$$

Because of the term $e^{i2\pi(f_k-f)t} + e^{-i2\pi(f_k+f)t}$ it is clear that a larger value of h_k influences the estimates of the amplitudes around f_k in an exponentially decaying way with growing distance to f_k. This has to be taken into account when deciding how many significant appearances of a frequency in an experiment are necessary to make that frequency a relevant frequency.

4.3.3 Constructing Regression Estimates

Since the distribution of the spectrogram data with varying amplitudes is the same as the distribution of the periodogram ordinates the same procedure as described in Subsection 4.2.3 can be applied to this situation. The only difference is that the time series of the amplitudes on the varying frequencies have to be extracted from the spectrogram data. Then Repeated Measurement models have to be applied, if fixed influences $\vec{x}$ are included in the model for the amplitudes. Otherwise, it is possible to use the time t as single regressand. It is also necessary to check whether the assumption of independence holds for the observations – at least conditionally for the periodogram ordinate estimates on the same frequencies. If the recorded time series are long enough it is of course possible to ensure the independence of the single periodograms by leaving gaps between the parts of the series which are used for the estimation of the periodograms. Otherwise, if the series are short or such spacing is not feasible repeated measurement models allow for auto-correlation in the observations if a sensible guess of the order of autocorrelation can be made. Overlap of the parts on which the periodograms are calculated can be a remedy for an insufficient resolution in the frequencies, e.g. a good guess of the relevant frequencies exists and two of them fall between two Fourier frequencies when no overlap is allowed. In this case auto-correlation has to be included in the model. For

the general estimation of repeated measurement models compare e.g. Lindsey (1993) 'Models for repeated measurements'.

5 Simulation Studies on Regression Models on Periodogram Ordinates

All situations considered in Chapter 4 shall be assessed for their correctness and practical usefulness by two extensive simulation studies. A general introduction to the design of computer experiments, simulations, resp., is given. The actual design considerations for selecting of input variables and their respective realisable values are presented. Exemplary results of the studies are shown and discussed and the chapter ends with a general assessment of the results of the studies.

5.1 Experimental Design and Simulation Studies

Simulation studies are the experiments of the statistician. So it is an obvious question to ask, how statistical experimental design can be applied in the construction of simulation studies. A similar but more detailed discussion of the topic can be found in the book Santner et al. (2003): 'The Design and Analysis of Computer Experiments'.

5.1.1 Design Considerations

The first step for experimental design is to define possible influencing variables on some response. This may appear a difficult task for an arbitrary statistical problem but typically there are natural choices for the response as well as for influencing variables. Natural choices for the responses include:

- **Bias** of a point estimator
- **Variance** of an estimator
- **Power** of a test
- **Fit** of a model
- **Predictive power** of a model

All these possible responses are typically measured in numerical variables.
Natural candidates for influencing variables include:

- Number of observations
- 'True' distribution of random variables

– Deviation from the proposed model – stochastic or deterministic

– Signal-to-Noise ratio

In many cases it can be difficult to make proper assumptions on the distribution of the above-mentioned response variables. Therefore, only designs are of interest which do not heavily depend on distribution assumptions when constructing simulation studies. The next subsection deals with possible designs.

5.1.2 Designs for Simulation Studies

Factorial Designs

To use factorial designs for a simulation study a unimodal distribution of the response, and independent observations have to be assumed so that the typical way of analysis in the form of a linear regression makes sense. The latter assumption would seem sensible in simulation studies, although pseudo random numbers are not independent in a strict sense.
Factorial designs are the simplest orthogonal designs, and therefore ensure that the estimated parameters of a chosen linear model are independent stochastic variables. This independence and the comparability of the estimated parameters in a coded model at least make it possible to state the 'most influencing variables', even if no significance test is applicable.

Model-free or Exploratory Designs

As pointed out in Section 3.6 there are many situations in which factorial designs are too restricted in the number of levels, and no model-oriented experimental design is applicable because the form of the influence of the interesting parameters on the response is not theoretically tractable. This is especially true in a statistical simulation study when the impact of wrong assumptions on a procedure is to be tested. Or another reason often met in simulations are diverse goals of a study which make a common modelling impossible. So again the designs discussed in Section 3.6, such as the random designs or the space-filling designs and especially the Coffeehouse design, are appropriate designs when planning computer experiments. This is also discussed in the book of Santner et al. (2003), Chapter 5.

Uniform information not always desirable?! – Transforming input variables

When considering the mentioned influencing variables it is obvious that for some of these variables a uniform spread of experiments – whether random or systematic – does not always make sense. For example the behaviour of a model fit close to a signal-to-noise ratio of one is more interesting – i.e. the signal is harder to discern from the noise – than with very large values of the signal-to-noise ratio. A uniform distribution would therefore be more appropriate on a log scale than on a usual scale. The necessity to transform some of the variables can be incorporated in the plan by choosing the plan on $[0,1]^p \subset \mathbb{R}^p$, where p is the number of influencing variables, and

transforming each variable back into its appropriate scale. This approach makes it possible to apply the projection optimal space-filling design to all situations if the transformations are allowed not to be injective. For example the transformation could be a step function, with k levels. With the projection optimal Coffeehouse-Design this would lead to a uniform sampling of the k levels. To use the projection optimal Coffeehouse-design is advantageous because it is computationally easier to construct for higher dimensions.

5.2 Simulation Study on Linear Regression on Periodogram Ordinates

The first study is designed to reveal the properties of a stationary influence of the input variables on the relevant amplitudes. In this setting the question is answered whether an assumption of normally distributed errors is sensible and thus a normal distribution is implied for the estimated parameters of a linear regression. Furthermore, the proposed technique to estimate the error variance is tested, and the results are used for the determination of the relevant frequencies. The corresponding programs are reproduced in the Appendix, Section C.2.

5.2.1 Design Considerations

Since the goals of this simulation study were wide spread and no clear idea of the impact of the different influencing variables could be stated, a Coffeehouse design was chosen for this simulation study.
When looking at the harmonic model with influenced amplitude, the following parameters determine this model:

- The functions g_k, $k = 1, \ldots, K$
- The relevant frequencies f_k, $k = 1, \ldots, K$
- The phases φ_k, $k = 1, \ldots, K$
- The error variance σ_ε^2

The phases are of no interest for the models on periodogram ordinates. For the models on periodogram ordinates the following properties are of interest:

- The length of the observed series n
- The number of relevant frequencies f_k, $k = 1, \ldots, K$
- The distance δ_f of the relevant frequencies to each other
- Whether or not the frequencies are Fourier frequencies
- The functions g_k, $k = 1, \ldots, K$

– The error variance σ_ε^2

The last two points are closely related, since they determine the signal-to-noise ratio in this model. To keep things simple for the simulation the chosen functions g_k, $k = 1, \ldots, K$, are all equal:

$$g_k(\vec{x}) := 2 + 3x_1 + 4x_2 + 0.001x_3$$

The parameters $b_1 = 2$, $b_2 = 3$, $b_3 = 4$ were chosen arbitrarily in this way, $b_4 = 0.001$ was chosen to test whether an unimportant influence on influenced but time-stationary periodogram ordinates could be detected with this model .
All influencing variables x_1, x_2, x_3 are set to levels 0 and 1 in a 2^3 full factorial design. Then the smallest signal is reached for $x_1 = x_2 = x_3 = 0$ and therefore the signal-to-noise ratio SNR may be calculated by

$$SNR = \frac{2}{\sigma_\varepsilon} \tag{5.1}$$

For the lengths of the series powers of 2 are chosen to allow for very fast Fourier transforms. The smallest number of observations is 64, the largest 4096, the lower bound was chosen to investigate cases where the number of observations is a hard bound for the experiments. The number of frequencies is varied between 1 and 5, the distance of the frequencies between 1 and 10 Fourier frequencies. Those numbers are chosen with respect to the chosen range of numbers of observations.
For the signal-to-noise ratio values between 1.11 and 101.11 are chosen. Setting the lower bound of the SNR at 1.11 ensures that a signal is present although not prominent in the series. The chosen transformation $x^3 * 100 + 1.11$ leads then to the upper bound. This function ensures that more situations with a low signal-to-noise ratio are investigated than those with a high signal-to-noise ratio because it is more interesting to see if the method works even in those more difficult situations.
Whether or not the frequencies are Fourier frequencies is assured by always selecting the Fourier frequency $\frac{5}{n}$ as first frequency and the next frequencies $\frac{5+\delta_f k-1}{n}$, and in case the non-Fourier frequencies, adding $\frac{1}{\sqrt{2}}$ in the numerator. The underlying design is a Coffeehouse design constructed in a standard hypercube $[0,1]^d$ from which all variables are transformed to fit the requirements. The transformation functions are:

(1) For the number of frequencies: $[10x] \bmod 5 + 1$

(2) Fourier Frequencies yes/no: $\frac{[x]}{\sqrt{2}}$

(3) Distance of frequencies δ_f: $[10x] \bmod 10 + 1$

(4) Length of series: $2^{[10x] \bmod 7+6}$

(5) Signal-to-Noise ratio: $x^3 * 100 + 1.11$

Here $[x]$ denotes the function:

$$[x] = m \text{ for } m - 0.5 \leq x < m + 0.5\ ,\ m \in \mathbb{Z}$$

The complete experimental design is displayed in Table 5.1.

	# freq.	Fourier	dist. freq.	n	SNR
1	1.00	0.00	1.00	512.00	101.11
2	1.00	0.71	1.00	64.00	1.11
3	1.00	0.00	6.00	2048.00	15.69
4	3.00	0.71	4.00	64.00	2.93
5	3.00	0.00	9.00	256.00	50.32
6	2.00	0.71	2.00	4096.00	72.74
7	5.00	0.71	10.00	128.00	1.23
8	2.00	0.71	10.00	256.00	1.23
9	5.00	0.00	10.00	256.00	1.23
10	5.00	0.00	8.00	128.00	1.23
11	5.00	0.71	10.00	256.00	33.14
12	2.00	0.00	8.00	256.00	1.23
13	2.00	0.00	5.00	128.00	1.23
14	2.00	0.71	5.00	256.00	33.14
15	5.00	0.71	5.00	128.00	33.14
16	4.00	0.71	5.00	128.00	1.23
17	2.00	0.71	10.00	128.00	33.14
18	2.00	0.00	10.00	256.00	33.14
19	5.00	0.00	10.00	128.00	33.14
20	4.00	0.00	7.00	128.00	33.14

Table 5.1: Experimental Design

For each experiment 100 data sets are simulated from the model and then evaluated by the algorithm described in Chapter 4, as well for known frequencies as for unknown frequencies.

5.2.2 Results

Known Frequencies

In the simulations it was found that in most cases the assumption of normal distribution of the regression parameters could not be rejected at a 5% niveau in a Shapiro-Wilk test (Shapiro et al., 1968). Only 22 out of 368 estimated parameters showed significantly non-normal behaviour in 100 repetitions according to this test. Thus some non-normality was found in only 6% of the considered samples. At most two regression parameters were found to be distributed non-normal. By checking the

situations in which such rejections of the normality assumption appeared, no recognizable pattern as to which parameter was affected could be found. Common to the experiments with rejections of normality in some parameters were the small number of observations, and several relevant frequencies and a low SNR.
The proposed estimator for the error variance turned out to be generally biased. The bias is, as expected, dependent on the number of relevant frequencies and the number of observations. It seems that the amount of leakage is higher than presumed, even for only one relevant Fourier frequency σ_ε^2 is overestimated, as can be seen in Figure 5.1.

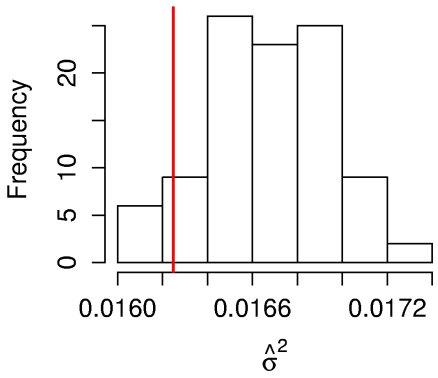

Figure 5.1: Estimated σ_ε^2 and true value $\sigma^2 = 0.01625$, depicted by vertical red line, for experiment 3 from Table 5.1.

Looking at the estimated parameter values, it turned out that they are distributed around half the set value which is correct because the used design leads to the estimation of half-effects. Only a slight underestimation of the parameters is observable which is most likely due to the overestimation of σ_ε^2. As an example, Figure 5.2 shows the results from experiment 1 in Table 5.1 with only one relevant Fourier frequency and the highest possible SNR. But at least the significance of the regression parameters is not heavily influenced by this finding. In all situations the parameter for variable x_3 was found insignificant.

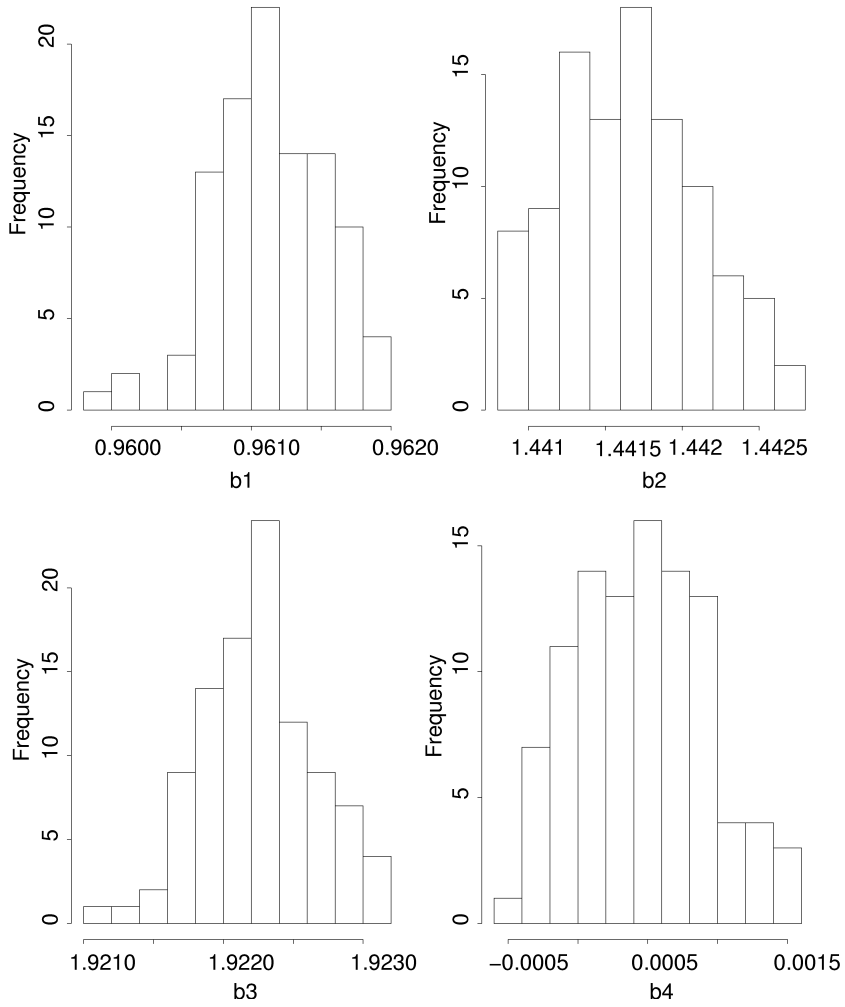

Figure 5.2: Histograms of parameter estimates for the linear model.

Unknown Frequencies

Despite the overestimation of the error-variance, the determination of relevant frequencies by using a significance test based on this estimate was found to be very efficient. In all situations at least all relevant frequencies were found and the number of frequencies which were considered relevant additional the true frequencies was low. So the over-estimation allowed only very strong leakage frequencies to appear relevant.

5.3 Simulation Study on Time-Varying Amplitudes

The goal of this simulation was to check how strongly typical properties of the data with time-varying amplitudes affect the goodness of fit in a linear model and a non-linear model. Furthermore, the method to detect relevant frequencies was evaluated in the presence of slow change in the amplitudes. The corresponding programs are reproduced in the Appendix in Section C.3.

5.3.1 Design Considerations

In this case the strength of the influences on the fit measured by the residual sum of squares have been evaluated. Therefore a full factorial design was applied. Again the influences of interest are the signal-to-noise ratio, the number of frequencies, number of observations, Fourier or non-Fourier frequencies, and the distance between the relevant frequencies. Additionally the effect of AR(1)-disturbances was checked.
For the influences the following values for treatment low, high, respectively were chosen:

(1) Number of frequencies: 1 or 5

(2) Fourier Frequencies no/yes add 0 or $\frac{1}{\sqrt{2}}$ in the calculation of the frequencies

(3) Distance of frequencies δ_f: 3 or 10

(4) Length of series: 2560 or 102400

(5) Signal-to-Noise ratio: 1.1 or 100

These choices were made to ensure comparability with the choices in the preceding simulation. The calculation of the frequencies considered is again $\frac{5+\delta_f k-1}{n}$ with, in the case of non-Fourier frequencies, addition of $\frac{1}{\sqrt{2}}$ in the numerator.
The following functions were chosen as 'true' models for the variation of the amplitudes:

$$R_{lin}(t) = 2 + 0.001 * t \tag{5.2}$$

$$R_{nonlin}(t) = 2 + \frac{2}{(1 + \exp\left(\frac{m-t}{d}\right))} \tag{5.3}$$

The parameters m, d in equation (5.3) are changed for each frequency if 5 frequencies are included in the model. This is done in the following manner:

$$m = 5 * l \text{ or } m_i = (2 + i) * l \text{ and } d = l \text{ or } d_i = \frac{l}{i}$$

where $i = 1, \ldots, 5$. These different values for the parameters in the nonlinear function were chosen to test whether differing functions on the frequencies can be found in the data.

The choice of these functions had two reasons: the first slow linear trend may be useful as approximation for a slow nonlinear trend in the amplitude. Generally it can be assumed that amplitudes have an upper bound because oscillating systems break down when the amplitude becomes too large. This is one reason for the chosen logistic function. The other reason is that we use a product of logistic functions in Chapter 6 to describe the development of amplitudes in the BTA deep-hole drilling process. The inclusion of a mean intercept of 2 in both cases is done to ensure a true harmonic process right from the start of the observations.
For all settings 100 repetitions were evaluated. The function nls from **R** was used to fit the nonlinear models. Since it is well known that nonlinear regressions tend to fail with some starting values, ten randomly chosen starting values were tested and the first successful set was used for the fit.
As experimental design we used a 2^7 full factorial design. So the number of relevant frequencies changed for every experiment, the Fourier or non-Fourier property changed every two experiments, the distance of the relevant frequencies every four experiments, the number of observations every eight experiments, which model changed every 16 experiments, the signal-to-noise ratio changed after 32 experiments, and finally the kind of disturbance splitted the design into the first 64 experiments with AR(1) disturbance and the second half with normally distributed disturbances.

5.3.2 Results

First we checked whether the procedure to find the relevant frequencies was influenced by the time varying amplitudes, or the AR(1) disturbances. Both influences did not show an effect on the performance of the method in the sense that the correct frequencies are always found. This becomes obvious from the histograms of the found relevant frequencies in Figures 5.3 to 5.5. In these histograms of relevant frequencies the bars are set to a width of 0.0025 which equals a number of two or three possible frequencies in the case of 1024 observations per periodogram.

Figures 5.3 and 5.4 show the results on relevant frequencies for experiments with the high level of observations, 10240, and high signal-to-noise ratio of 100 and five non-Fourier frequencies with a distance of ten Fourier frequencies in the simulated model that is, the true values of the frequencies are:

```
0.00557 0.0251 0.03487 0.04463 0.0544
```

The left hand side panels are from linear models, the right hand side panel from nonlinear models. The difference between Figures 5.3 and 5.4 is the disturbance term which is an AR(1) process in Figure 5.3 and a normal white noise process in Figure 5.4. The graphics show no obvious difference for these four cases, and it is the same for all other similar situations.

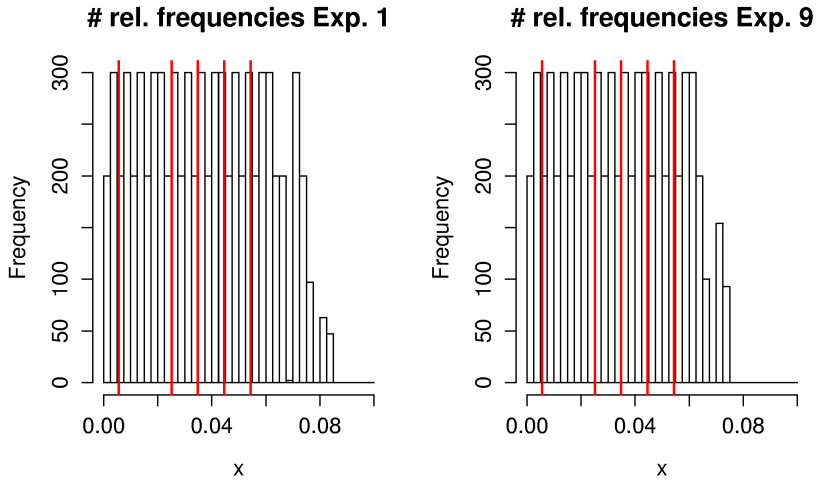

Figure 5.3: There are only slight differences visible between the histograms of the linear (Exp. 1) to the nonlinear (Exp.9) case in the found relevant frequencies.

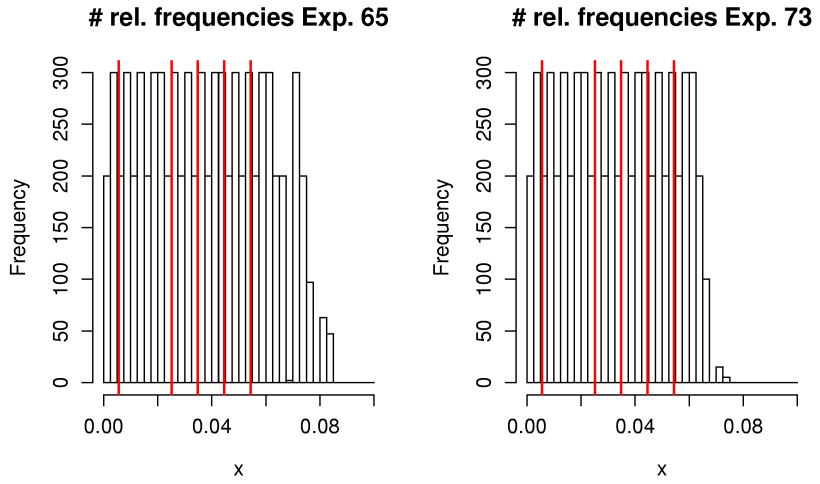

Figure 5.4: Compared to Figure 5.3 the differences are even less recognizable in the histograms of the linear (Exp. 65) to the nonlinear (Exp. 73) case in the found relevant frequencies with normal error.

Figure 5.5 gives an impression of the more difficult situation with only 2560 observations and AR(1) disturbances but Fourier frequencies. From these panels it is clear

that at least the true frequencies are found by the method for the detection of relevant frequencies. In this case the true frequencies are (the first frequency is the single frequency from experiment 52):

```
0.0195 0.0977 0.1367 0.1758 0.2148
```

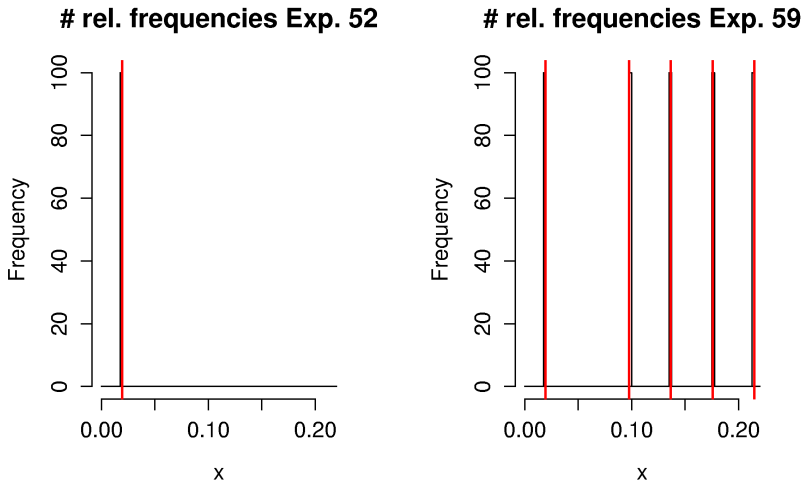

Figure 5.5: At least the true relevant frequencies in the case of Fourier frequencies are found (linear Exp. 52, nonlinear Exp. 59).

The goodness of fit in the different settings was summarised by calculating the individual residual sums of squares for all fitted models and calculating the mean of these per setting. Then these results were split between the linear and the nonlinear model and within these groups again in those cases with AR(1) disturbance and those with normal disturbances. After this a linear model was fitted in the influences of the design and their two-factor interactions on each of the groups.
The most important influences are the number of observations and the signal-to-noise ratio, and their interaction in all four cases. We found the distance of the relevant frequencies and the interaction of number of relevant frequencies with Fourier/non-Fourier important only in the case of the nonlinear function of the amplitude and AR(1) disturbances.

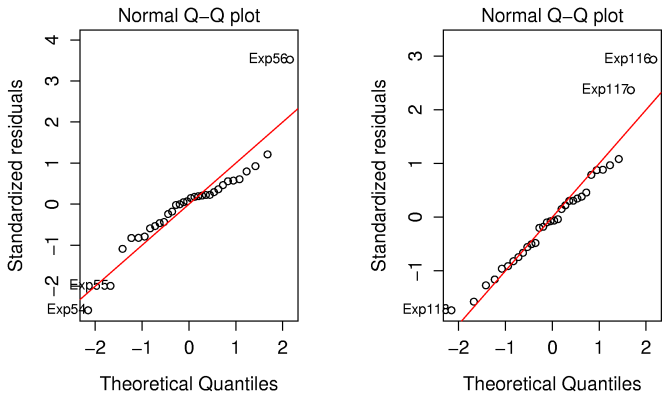

Figure 5.6: Normal plots of the residuals from the regressions on the RSS for the linear trend without and with AR(1) disturbance.

This result is not surprising as the signal-to-noise ratio should influence the residual sums of squares and the number of observations determine the exactness of the found relevant frequencies. Both influences have a decreasing effect on the residual sum of squares, which is to be expected because a high signal-to-noise ratio and a large number of observations should result in low residual sums of squares.

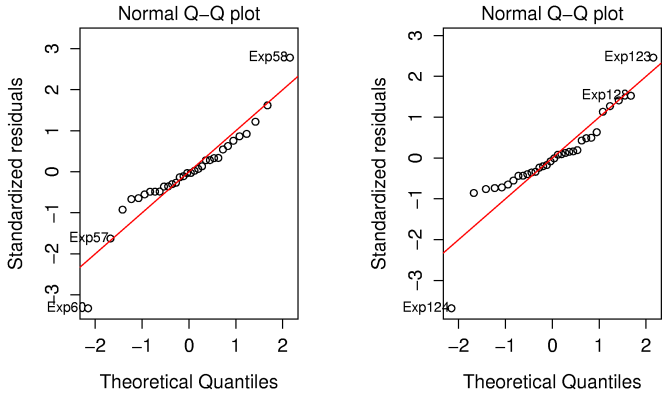

Figure 5.7: Normal plots of the residuals from the regressions on the RSS for the nonlinear trend without and with AR(1) disturbance.

As in Section 5.2 the normality approximation proposed in Chapter 4 was checked for appropriateness. As before we applied a Shapiro-Wilk test to test this assumption. First we checked whether the observations were normally distributed. To achieve this

goal for each true relevant frequency and each of the ten observations the 100 repetitions were collected and tested for normality on a 5%−niveau. The Shapiro-Wilk test rejected the hypotheses for the case of the linear influences only in 4.86% of a total of 2880 tested cases. With 5.82% in 2680 tested cases this value was slightly higher for the case of the nonlinear influence on the amplitudes. The differing number of observations is due to the fact that in two experiments with a 2560 observations, five non-Fourier frequencies and normal disturbances the lower neighbouring frequency was not detected as relevant in a small number of repetitions and therefore no general comparisons were possible.
In both cases – linear and nonlinear influences – exists a difference with respect to the kind of disturbance term. The number of rejections of normality of the observations for the normal disturbances is slightly higher than with AR(1) disturbances (linear case: 5.21% vs. 4.51% of 1440 observations; nonlinear case: 6.04% of 1240 observations vs. 5.63% of 1440 observations). This was expected by the theoretical model because the goodness of the approximation is influenced by the number of stochastic components, i.e. the order of the disturbance process and the value of the non-centrality parameter.
Since the percentage of rejections is slightly higher than the chosen niveau of the test we investigated, whether there was a clear and assignable pattern to the rejections. One such pattern could have been a higher number of rejections on the first three or four observations in the simulated data sets due to the smaller non-centrality parameter, but no such pattern was found. A hint of a pattern appeared in the nonlinear case for the second to fifth observation in the simulated data sets, where more rejections occurred but the difference was only slight compared to the other observations.
The distribution of the parameter estimates was also investigated. In the linear case the parameters displayed an even greater degree of normality. The Shapiro-Wilk test rejected only in 3.47% of the situations.
In the nonlinear case it cannot be expected to find normality in the parameters. It is hard to define a distribution for the parameters in nonlinear regression, only when a linear approximation approach is chosen as fitting procedure normality is expected. Since this was not the case here, no further investigation was pursued. Ratkowsky (1990) remarks on page 20 in his 'Handbook of Nonlinear Regression Models':

'... The [nonlinear] estimators achieve this property [unbiased, normally distributed, minimum variance] only approximately, that is, as the sample sizes approach infinity. Some nonlinear regression models have estimators that are badly biased with a highly asymmetric long-tailed nonnormal distribution.[...]'

Figures 5.8 to 5.10 give an insight into the goodness of the fits of the functions on the truely relevant frequencies. In all cases it is obvious that the observations lie below the values of the true functions and therefore the fitted functions underestimate the true values as well.
Figure 5.8 compares the effects of the different disturbances and the effect of Fourier or non-Fourier frequency in the linear case. The figures are very similar with respect

to the apparent goodness of fit and the general behaviour of the fitted functions. The case of the non-Fourier frequency on the right hand side gives the impression that the underestimation may be cured by summing over neighbouring frequencies in an appropriate way. This is emphasized by the dotted blue line which is the sum of the fitted values.

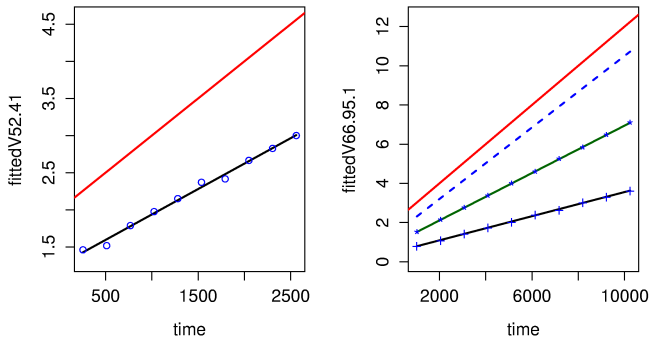

Figure 5.8: Fitted function on varying amplitudes in the linear case, on the left-hand side with AR(1) disturbances on a Fourier frequency; on the right-hand side with normal disturbances and originally on a non-Fourier frequency, therefore two lines on the neighbouring Fourier frequencies.

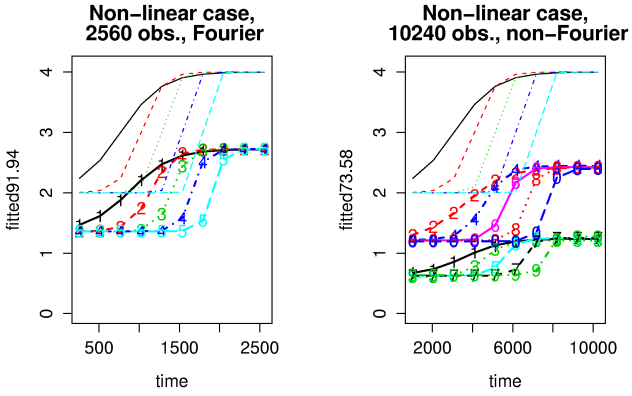

Figure 5.9: Fitted functions on varying amplitudes in the nonlinear case, on the left hand side on Fourier frequencies, with 256 observations per periodogram; on the right hand side on non-Fourier frequencies and with 1024 observations per periodogram estimation; normal disturbances.

Figure 5.9 underlines the last impression as well. Furthermore, it is obvious that the general form of the influences on the amplitudes is found even if they are different for the different frequencies. This is also not influenced by the number of observations or the kind of disturbances.

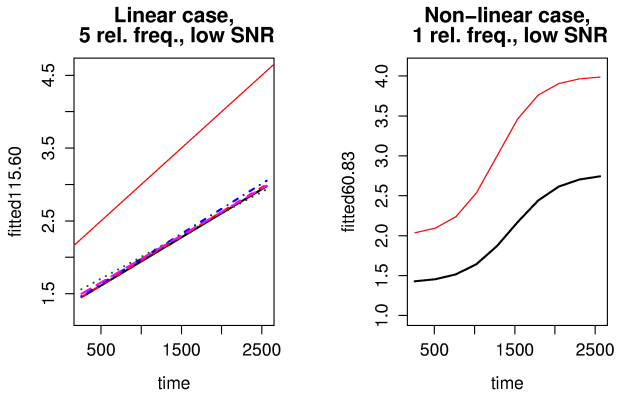

Figure 5.10: Fitted functions on varying amplitudes, on the left-hand side linear case with five frequencies, normal disturbances; on the right-hand side non-linear case, AR(1) disturbances; signal-to-noise ratio= 1.11 and Fourier frequencies in both cases.

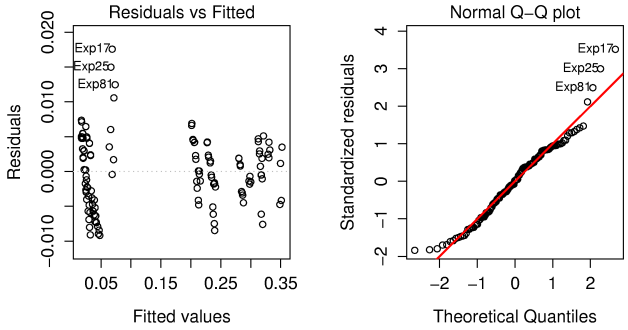

Figure 5.11: Residual plot and Normal plot for the regression on the difference of the estimated to the true σ.

Figure 5.10 shows that everything said before is also true for the more difficult cases with low signal-to-noise ratio.
The last thing investigated in this study was the effect of the varying amplitudes on the performance of the variance estimator proposed in Chapter 4. Compared

to the results from the simulation with fixed amplitutes in Section 5.2 slightly less overestimation of the true standard deviation σ occured. This can be seen from the residuals versus fitted in Figure 5.11 since the regression was performed for the difference $\hat{\sigma} - \sigma$.

	Estimate	Std. Error	t value	Pr(>|t|)
(Intercept)	0.1506	0.0005	299.87	0.0000
nrelfreq	0.0065	0.0005	13.02	0.0000
fourier	0.0001	0.0005	0.11	0.9125
distfreqs	0.0040	0.0005	7.98	0.0000
model	0.0004	0.0005	0.77	0.4409
rate	−0.0278	0.0005	−55.41	0.0000
StoN	−0.1164	0.0005	−231.87	0.0000
AR	−0.0079	0.0005	−15.73	0.0000
nrelfreq:fourier	0.0002	0.0005	0.30	0.7627
nrelfreq:distfreqs	0.0040	0.0005	7.97	0.0000
nrelfreq:model	0.0003	0.0005	0.58	0.5658
nrelfreq:rate	−0.0054	0.0005	−10.73	0.0000
nrelfreq:StoN	−0.0006	0.0005	−1.10	0.2752
nrelfreq:AR	0.0001	0.0005	0.19	0.8484
fourier:distfreqs	0.0001	0.0005	0.20	0.8397
fourier:model	−0.0000	0.0005	−0.06	0.9540
fourier:rate	−0.0001	0.0005	−0.17	0.8664
fourier:StoN	0.0010	0.0005	1.95	0.0536
fourier:AR	−0.0000	0.0005	−0.09	0.9260
distfreqs:model	0.0003	0.0005	0.53	0.5957
distfreqs:rate	−0.0035	0.0005	−6.90	0.0000
distfreqs:StoN	0.0012	0.0005	2.48	0.0148
distfreqs:AR	0.0002	0.0005	0.47	0.6393
model:rate	−0.0002	0.0005	−0.44	0.6639
model:StoN	−0.0001	0.0005	−0.10	0.9189
model:AR	−0.0000	0.0005	−0.02	0.9862
rate:StoN	0.0173	0.0005	34.48	0.0000
rate:AR	0.0014	0.0005	2.79	0.0063
StoN:AR	0.0065	0.0005	13.01	0.0000

Table 5.2: Regression on differences of the estimated from the true σ ($\hat{\sigma} - \sigma$), $R^2_{adj} = 0.9978$.

The two most important influences are the signal-to-noise ratio followed by the number of observations (rate) which influence the distance to the true σ negatively. This means that a high signal-to-noise ratio also leads to better estimates of the standard deviation of the disturbance term. Of course a higher number of observations leads

to a better estimation since then there are more observations following the distribution of the Fourier transformation of the AR(1) or white noise normally distributed disturbances.

5.4 Summary and Conclusions from the Simulations

In general the simulations in Sections 5.2 and 5.3 supported the theoretical results from Chapter 4. In both simulations the method for the estimation of the error variance in harmonic processes was found to be biased towards a general overestimation of the true values. However this did not influence the method proposed for the determination of the relevant frequencies since in all cases at least the true frequencies were found by the method. It may have influenced the parameter estimates for the functions on the amplitudes but this cannot be said for certain. This is because the theoretical observations give a hint that the leakage effect may weigh down the periodogram ordinates.
In both simulations the general form of the influences on the amplitudes could be rediscovered by the regressions. It was proved in Section 5.2 that the importance of the influencing variables is preserved. In Section 5.3 it was proved that the general form is also preserved and differing functions on amplitudes for different frequencies can be found as well. The observations at the end of Section 5.3 suggest that underestimation might be avoided by appropriately summarising the observations near the highest relevant frequencies with a weighted sum which would even improve the normality approximation further.
Furthermore, it was shown that the normality approximation for the distribution of the periodogram ordinates is already valid for small values of the non-centrality parameter. This makes it possible to generally assume normality when investigating varying amplitudes on a few relevant frequencies. The investigation into the autoregressive disturbance in Section 5.3 showed an even better approximation to normality as expected by the theoretical discussion in Chapter 4.

6 Modelling the Drilling Torque by Models with Varying Amplitudes

Now that the statistical properties of models on periodogram ordinates have been established in Chapter 4, and verified under a variety of situations in simulation studies in Chapter 5, this chapter is dedicated to the application of these models to the data from the deep-hole drilling process. First some more results from the exploration of the data on the drilling torque will be presented. The model building process is described on the basis of these results, and finally the results will be presented and discussed.

6.1 Features of the Development of Amplitudes of the Drilling Torque over Time

First the method to determine the relevant frequencies was applied to the time series of the drilling torque. So periodograms on sequences of 4096 observations were calculated. For each sequence the significant frequencies were determined by standardizing the data in the usual way, (i.e. substracting the mean and division by the standard deviation), and then testing against the 95% quantile of the standard exponential distribution. This was done so that the outcome would correspond with the results from Section 2.2.2. Then the frequencies that test significant in this procedure for more than 10 observations per experiment and more than 6 experiments were defined as relevant. That ensured the inclusion of all frequencies found in at least one third of the experiments. These frequencies in Hertz are given in Table 6.1.

4.88	195.31	200.20	205.08	209.96	214.84	219.73	224.61
229.49	234.37	239.26	244.14	249.02	253.91	258.79	263.67
268.55	468.75	664.06	668.95	673.83	678.71	683.59	688.48
693.36	698.24	703.12	708.01	712.89	717.77	722.66	727.54
732.42	737.30	742.18	1142.58	1147.46	1152.34	1157.23	1162.11
1166.99	1171.87	1176.76	1181.64	1186.52	1191.41	1196.29	1201.17
1206.05	1210.94	1215.82	1220.70	1640.62	1645.51	1650.39	2109.37
2114.26	2119.14						

Table 6.1: Relevant frequencies found by the first method from Chapter 2.

When compared with the results from the procedure described in Chapter 4 we found that the results from the procedure from Chapter 4 included most of the frequencies form the above procedure as well. The procedure from Chapter 4 has the clear advantage that it tests against the correct distribution for the periodogram ordinates and estimates the parameters of the distribution from the raw data. In contrast the above procedure standardizes the time series first, then uses the Fourier-transform and finally tests against a distribution that should be true for the Fourier-transform of the standardised data. But also it has to be noted that the results from Section 5.3 show that the variance is in general slightly overestimated. Nevertheless, much harder conditions can be applied in this procedure to make a frequency relevant because if the same conditions as above are used with only 10 significant observations per experiment in 6 experiments then 1687 frequencies are found relevant.
Therefore, we decided to demand for more than 1000 significant observations (corresponding to more than one half of the observations in most of the experiments), in more than 18 experiments and got 67 relevant frequencies. So we got the frequencies reported in Table 6.2.

4.88	9.76	14.65	19.53	24.41	29.30	34.18	39.06
43.95	48.83	53.71	58.59	63.48	78.13	87.89	234.38
239.26	249.02	253.91	673.83	678.71	683.59	688.48	693.36
698.24	703.13	708.01	712.89	717.77	722.66	727.54	732.42
737.30	742.19	1147.46	1152.34	1166.99	1171.88	1176.76	1181.64
1186.52	1191.41	1196.29	1201.17	1206.05	1450.19	1748.05	1752.93
1850.59	2148.44	2451.17	3251.95	3281.25	3286.13	3349.61	3549.80
3647.46	3652.34	3950.20	4150.39	5048.83	5351.56	5449.22	5649.41
6562.50	6567.38	6850.59					

Table 6.2: Relevant frequencies found with the new method described in Chapter 4.

Comparing the two lists of relevant frequencies it is obvious that more low and high frequencies are present in the second list than in the first. Since the two procedures agree on the most prominent frequency bands near 234Hz, 703Hz and 1200Hz, we keep on reporting the results on the frequencies from the first procedure to maintain the comparability with the results in Chapter 2, highlighting those frequencies found by both procedures.
When looking at the plots over time for various experiments we find that all these developments over time exhibit a common behaviour:

While the guiding pads are still in the starting bush none of the frequencies are significant, because the amplitudes are constraint by the fact that vibrations of the tool are strongly damped by the starting bush supporting the guiding pads. When the guiding pads leave the starting bush there is always an increase in all relevant amplitudes caused by the tool being freed. In most frequencies this increase is then immediately dampened again, forming a peak in the beginning and then declining

again. Under some experimental conditions certain frequencies increase very quickly which leads to chatter right after the start of the process. This chatter continues for some time until another frequency exceeds a certain threshold and dominates the process. The first chatter mostly occurs near 1200Hz but sometimes also near 234Hz while the second chatter can be near 234Hz or 703Hz. A stable chatter over the complete process is only observed when all relevant frequencies emerge directly after the guiding pads have left the starting bush.

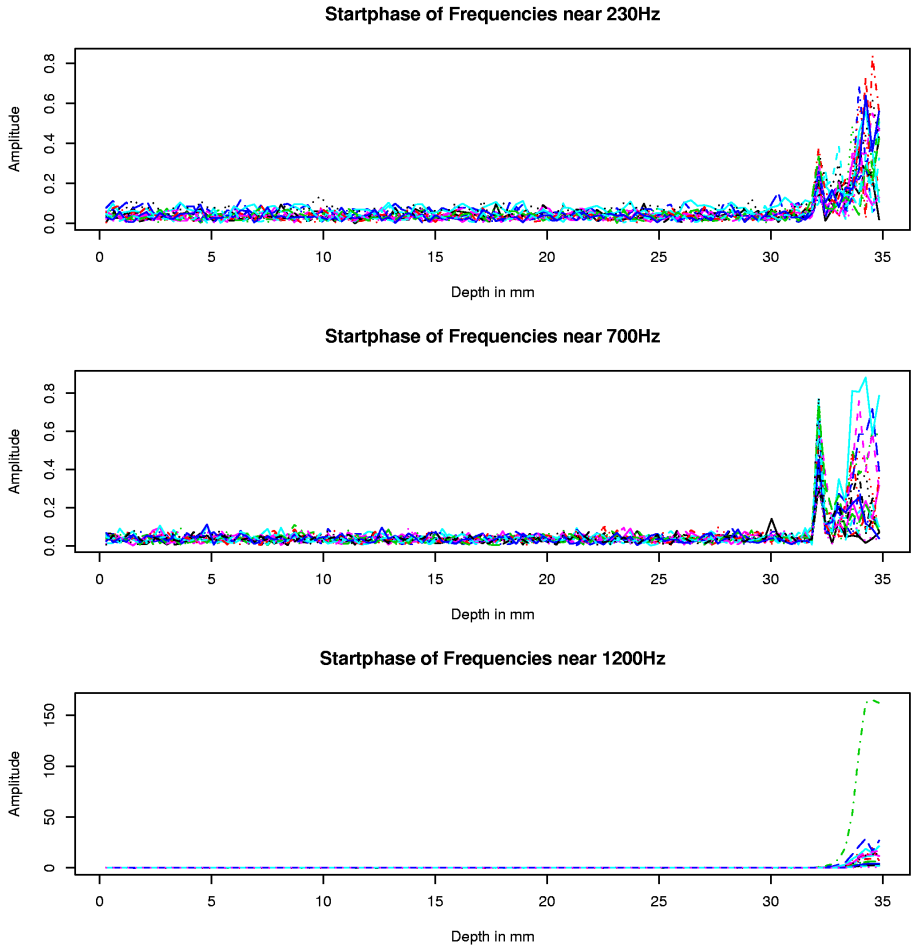

Figure 6.1: The development of the amplitudes on the first 35mm from Figure 2.13.

For a better impression of this behaviour consider again Figures 2.13 and 2.14, where the described behaviour can be seen. To get a more detailed insight Figures 6.1 and 6.2 show the first 35mm of these experiments. It is clear that the chatter right after the guiding pads leave the starting bush develops very quickly in one of the frequencies near 1200Hz. Yet in all frequencies a peak in the amplitude can be

observed at this point, independent of chatter occurrence. Two different behaviour patterns are observed after the first jump. If the jump turns out to be just a peak, it is followed by a slow descent. If the jump leads into chatter, the amplitude rises to a certain level and fluctuates around this level. When the chatter shifts to another frequency the amplitude drops but not necessarily to the level produced by the noise in the process, i.e. the frequency is still present but at a lower level. This behaviour can be observed in all relevant frequencies whenever there is a shift in the chattering frequency.

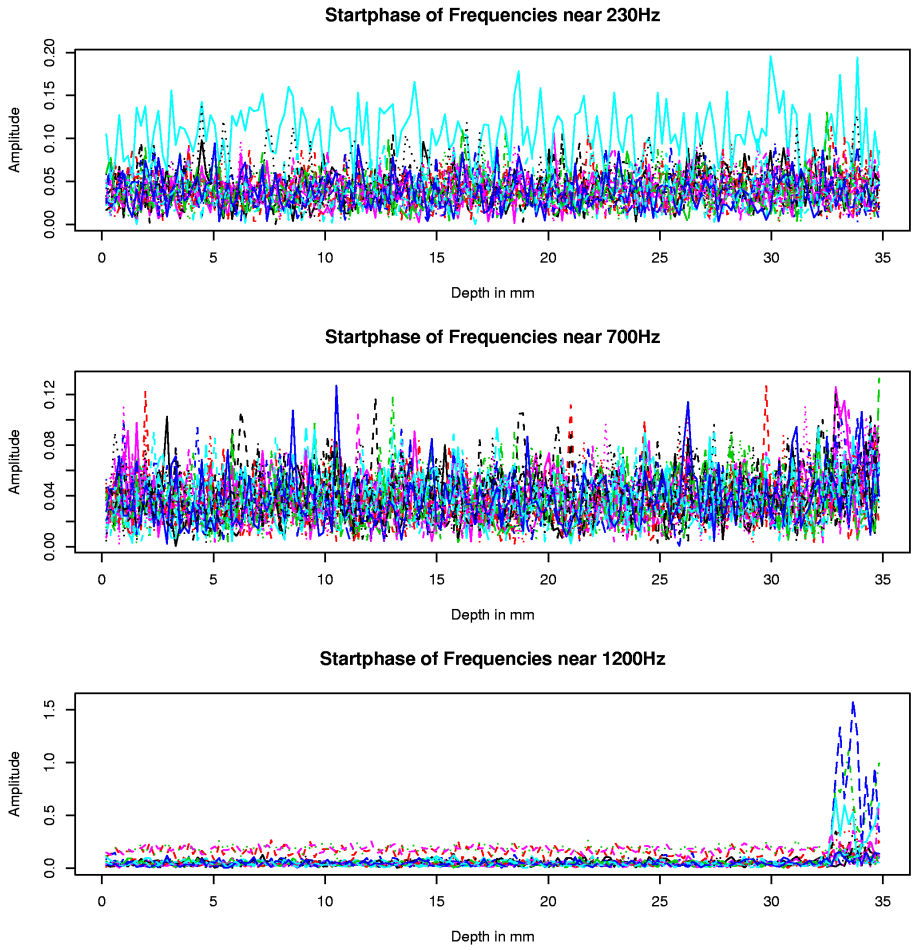

Figure 6.2: The development of the amplitudes on the first 35mm from Figure 2.14.

Chatter around 1200Hz was only observed directly after the guiding pads left the starting bush in our experiments. Only the frequencies near 1200Hz and higher frequencies are influenced significantly. The amplitudes have a high variance for this kind of chatter.

Chatter around 234Hz was observed at different stages of the process. In some cases it developed after the high-frequency chatter while in others it developed at different times from the stable process. In one case it also developed straight after the guiding pads left the starting bush. All other relevant frequencies are significant in this kind of chatter but with lower amplitudes.

Chatter around 703Hz develops at later stages of the process. If other kinds of chatter are present in the experiments then chatter around 703Hz always follows high-frequency chatter or low-frequency chatter and dominates the process completely.

One interesting question concerning the behaviour of the amplitudes on the relevant frequencies was whether there were features which are influenced by the machine parameters. The maximal value of the amplitudes was an obvious choice because it is bounded by the constant damping factor of the tool/workpiece assembly and the amount of energy introduced into the system by feed, cutting speed and the flow rate of the oil.
So for each experiment and each relevant frequency the maximal value was determined. The maximal values for each frequency were regressed on the three machine parameters used in the experimental design (cf. Section 2.1). For each frequency the best fitting model was searched for by stepwise regression based on AIC (cf. Subsection 2.2.1). The quadratic model with all interactions up to the three factor interaction was used as starting point. In Tables 6.3, and 6.4 the chosen parameters are reported and marked by '+' and if they are significant by 'X'. What is of note about these models is that the three main interesting frequency bands are each dominated each by a different group of machine parameters. For the low frequency chatter around 240Hz these parameters are the feed f and the flow rate of the oil $\dot{V}$ which are significant in most of the models in which they are present (13 of 18, and 13 of 16, resp.). The feed f arises also as a quadratic term in some models. In this frequency band the cutting speed v_c arises in the interaction $f : v_c$ and as the quadratic term v_c^2 in a significant way (4 of 16).
For the chatter around 703Hz the most dominant parameters are the feed f, the cutting speed v_c and their interaction $f : v_c$. The most frequently significant quadratic term is the feed (5 of 6). The flow rate of the oil is only present in 8 of 16 models and only significant in two of them.

Hz	μ	f^2	v_c^2	$\dot{V}^2$	f	v_c	$\dot{V}$	$f:v_c$	$f:\dot{V}$	$v_c:\dot{V}$	$f:v_c:\dot{V}$	$R^2_{adj.}$
5	.	+	.	.	+	+	X	+	+	.	.	0.375
195	X	.	.	.	X	+	X	+	+	.	.	0.409
200	X	.	.	.	X	+	X	+	+	.	.	0.371
205	X	.	.	.	X	+	X	+	+	.	.	0.346
210	X	.	.	.	X	+	X	+	+	.	.	0.307
215	.	+	.	.	+	+	+	+	+	.	.	0.265
220	.	+	+	.	+	+	+	+	+	.	.	0.201
225	.	X	X	.	X	X	.	.	.	.	.	0.134
229	X	X	X	.	+	X	+	X	+	.	.	0.644
234	X	.	.	.	X	+	X	+	+	.	.	0.341
239	X	.	.	+	X	+	X	X	+	.	.	0.464
244	X	.	.	.	X	+	X	X	+	.	.	0.452
249	X	.	.	.	X	+	X	X	+	.	.	0.411
254	X	.	.	.	X	+	X	+	+	.	.	0.369
259	X	.	.	.	X	+	X	+	+	.	.	0.334
264	.	+	.	.	+	+	X	+	+	.	.	0.318
269	.	+	+	.	+	+	+	+	+	.	.	0.232
469	.	.	.	.	+	+	+	+	.	.	.	0.133
664	X	.	.	.	X	X	.	X	.	.	.	0.302
669	X	.	.	.	X	X	.	X	.	.	.	0.277
674	.	.	.	.	X	X	.	X	.	.	.	0.216
679	X	.	.	.	+	X	+	X	.	+	.	0.164
684	.	.	.	.	.	.	.	.	.	.	.	#
688	.	.	.	.	.	.	.	.	.	.	.	#
693	X	+	.	.	X	X	X	X	X	X	X	0.226
698	X	X	.	.	X	X	X	X	X	X	X	0.717
703	.	.	.	.	+	X	.	X	.	.	.	0.239
708	.	X	X	.	X	X	.	.	.	.	.	0.473
713	.	X	X	.	+	X	.	X	.	.	.	0.436
718	.	.	.	.	X	X	.	X	.	.	.	0.306
723	.	.	.	.	+	X	.	X	.	.	.	0.251
728	X	.	.	.	+	X	+	X	.	+	.	0.203
732	.	.	.	.	.	.	.	.	.	.	.	#
737	.	.	.	.	.	.	.	.	.	.	.	#
742	.	.	.	.	.	.	.	.	.	.	.	#

Table 6.3: Results of the stepwise regressions on the maximal amplitudes per relevant frequency in the lower frequency bands. '+' means chosen for the model, but not significant at a 10% level, 'X' means significant influence.

In the models for the frequency band around 1200Hz the clearly dominating machine parameter is the cutting speed v_c, which is present in all models and in some ad-

ditionally as a quadratic term. The flow rate of the oil $\dot{V}$ is the second interesting parameter in this frequency band with 6 selections in the 16 models.
Finally the frequencies near 1650Hz display a clear common behaviour with $\dot{V}^2$, all main effects and interaction $f : v_c$ present in all models. All frequency bands not mentioned do not display a clear pattern.

Hz	μ	f^2	v_c^2	$\dot{V}^2$	f	v_c	$\dot{V}$	$f : v_c$	$f : \dot{V}$	$v_c : \dot{V}$	$f : v_c : \dot{V}$	$R^2_{adj.}$
1143	X	.	.	.	.	X	.	.	.	.	.	0.403
1147	X	.	.	.	.	X	.	.	.	.	.	0.348
1152	.	.	.	.	.	X	.	.	.	.	.	0.246
1157	.	.	.	.	.	X	.	.	.	.	.	0.158
1162	.	.	.	.	.	.	.	.	.	.	.	#
1167	.	.	.	.	.	.	.	.	.	.	.	#
1172	.	+	.	.	+	+	.	+	.	.	.	0.258
1177	.	.	X	+	+	X	+	.	.	.	.	0.448
1182	.	.	+	+	.	X	+	.	.	.	.	0.304
1187	.	.	.	+	.	X	+	.	.	.	.	0.342
1191	X	.	.	.	.	X	.	.	.	.	.	0.34
1196	X	.	.	.	.	X	.	.	.	.	.	0.336
1201	X	.	.	.	.	X	.	.	.	.	.	0.269
1206	.	.	.	.	.	X	.	.	.	.	.	0.165
1211	X	.	+	.	.	X	.	.	.	.	.	0.184
1216	.	.	X	X	+	+	X	+	.	.	.	0.5
1221	.	.	+	X	+	+	X	X	.	.	.	0.51
1641	.	.	.	.	.	.	.	.	.	.	.	#
1646	.	.	+	+	+	+	+	X	.	.	.	0.399
1650	X	.	.	X	X	X	X	X	.	.	.	0.637
2109	.	.	.	.	+	X	X	.	.	X	.	0.109
2114	.	.	X	.	+	+	.	+	.	.	.	0.447
2119	X	.	.	+	X	X	+	X	.	.	.	0.534

Table 6.4: Results of the stepwise regressions on the maximal amplitudes per relevant frequency in the higher frequency bands. '+' means chosen for the model, but not significant at a 10% level, 'X' means significant influence.

The next feature that was checked for correlations with the machine parameters was the depth of the jumps of the amplitudes at the start of the chatter. Since the chatter appeared at significantly different positions in the eight repetitions of the centre point (including observation 21a) no general connection was determined. We therefore investigated whether a change in the behaviour of the system is more likely at certain depths than at others. Of course the end of the starting phase was already established and well accounted for.
The bar plot in Figure 6.3 shows per bar the number of relevant frequencies, which

had a high jump within the segment of 5mm corresponding to the bar. 'High' jumps are defined here by the first differences of the amplitudes being lower/higher than the 5%/95% empirical quantiles of the first differences (cf. program code in Section B.2).

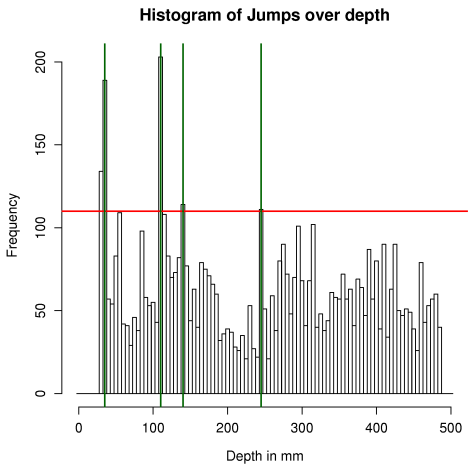

Figure 6.3: Number of frequencies with a jump in the amplitude within segments of 5mm.

The vertical lines at depths 35mm, 110mm, 140mm and 245mm indicate the most prominent jumps apart from those at the end of the process. The jumps at the end of the process are not counted in Figure 6.3 because they were significant in nearly all frequencies in all experiments and therfore made it impossible to properly see the structure of the other counts. It could be argued that there are other bars which are only slightly below the horizontal red line at 110 counts, like 50/55mm, 85mm, 295mm, 325 and 385mm. The cut-off point of 110 counts was chosen in order to restrict the number of vertical lines and thereby keep the structure of the plot visible.
It is interesting that the highest bar in the plot is at 110mm and not at 30/35mm depth. There appears to be a connection between this position and the machine assembly in that it is approximately the position where the tool enters the bore hole completely. This might lead to changes in the dynamic process because the boring bar is slightly thinner than the tool and therefore the pressures in the hole may change.
In several experiments (experiments 6,10, 12 and 17) a very slow oscillation could be observed in important chatter frequencies. Figure 6.4 shows the two most important chatter frequencies of experiment 6.

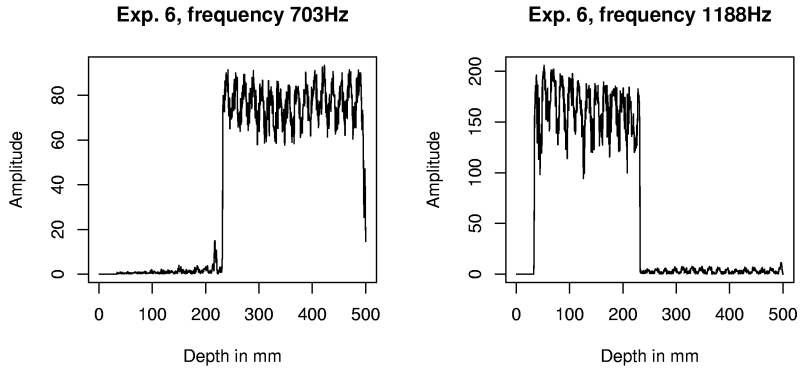

Figure 6.4: Amplitudes of frequencies 703Hz and 1188Hz from experiment 6 displaying a slow oscillation.

6.2 Model Building

It is assumed that the error process in the data of the drilling torque is a Gaussian process. Moreover it is assumed to be white noise. These assumptions are based on the fact that before the start of the drilling process the signal is fluctuating around 0. In the case of white noise we can apply the results from Chapter 4 and thereby know that there are two possible assumptions for the random part of the model: either one uses generalized regression models with a gamma distribution, or one uses the normal approximation and standard regression. In the simulations in Chapter 5 it was established that the normal approximations fit well. For this reason only the models using these approximations will be considered here.
To establish common models for all tested machine parameters a common 'time' axis needs to be defined. When time in seconds is used, different lengths of experiments are obtained, and the time point is of no meaning in a technological sense. Therefore, the depth of the hole was chosen as a common 'time'-axis for all experiments. This can be interpreted technologically because different depths can be related to changing physical conditions in the process (i.e. guiding pads leave the starting bush, the tool is completely in the hole).
Next, the functional form of the mean has to be tackled. It has to be flexible enough to be able to approximate all observed behaviours of the process. Furthermore it must be easy to parameterize with a small number of parameters to keep complexity low and avoid over-fitting. Two different important behaviours were observed. On the one hand the fast jump to a maximal value and then decline back to the start level in a similarly steep descent, on the other hand a smaller peak and then a slow descent to the start level. When searching for a smooth function which allows for both behaviours, the use of a three parametric logistic function suggested itself. This would allow for the steep rise, and when multiplied with a two parametric logistic

function on $-t$, would allow for the descending behaviour.
So the basic functional form for the model is the following:

$$h(t; a, \vec{m}, \vec{d}) = \frac{a}{1 + \exp\left(\frac{-t+m_1}{d_1}\right) + \exp\left(\frac{t-m_2}{d_2}\right) + \exp\left(-\frac{(d_2-d_1)t+d_1m_2-d_2m_1}{d_1d_2}\right)} \tag{6.1}$$

The following Figure 6.5 shows two parameter settings for this function, which exhibit the desired behaviour.

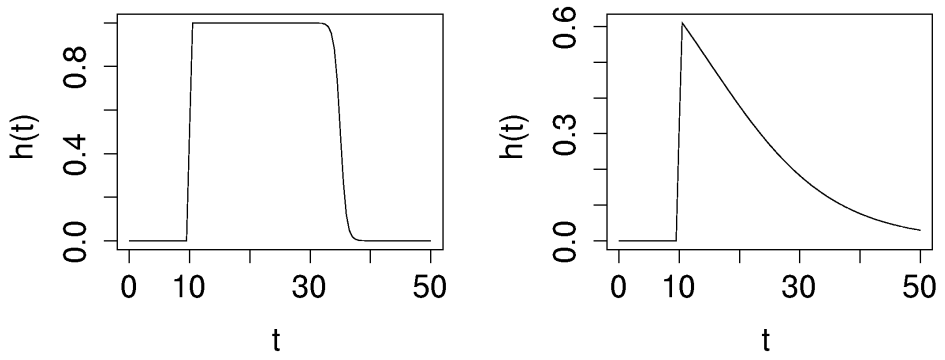

Figure 6.5: $h(t; a, \vec{m}, \vec{d})$ for $a = 1$, $m_1 = 10$, $m_2 = 40$, and $d_1 = 2 = d_2$ on the left-hand side, and $m_{1,2} = 10$ and $d_1 = 2$ and $d_2 = 1000$ on the right-hand side.

The several changes in the chatter frequencies observed in some experiments should be incorporated by summing up various functions of this form. So the complete model to be fitted to the periodogram ordinates reads:

$$H_k(t; \vec{a}, \vec{m}, \vec{d}) = \begin{cases} \mu_{A,k} & \text{, for } t < 30mm \\ \mu_k + \sum_{j=1}^{J} \frac{a_{j,k}}{\left(1 + \exp\left(\frac{-t+m_{1j,k}}{d_{1,j,k}}\right)\right)\left(1 + \exp\left(\frac{t-m_{2,j,k}}{d_{2,j,k}}\right)\right)} & \text{, else.} \end{cases} \tag{ii}$$

This function was fitted to each relevant frequency for each experiment. Because of the different dynamic behaviour observed it was not possible to fit a common model per frequency for all experiments including the machine parameters.

6.2.1 Fitting the Model

To fit the proposed model on each frequency per experiment the number of basic functions to describe the development of the amplitudes has to be established first. The number of basic functions should be as small as possible but as large as necessary.

The first step to achieving this goal is to find the jumps in the data. This is done by first calculating the means on 5mm sections of the time series, then calculating first differences of these means, and the empirical 5% and 95% quantiles. The position of the observations above or below these quantiles are then determined. So at most five jumps in each direction are included in this first step. Short peaks are not taken into account and a longer ascent or descent is modelled in one function. This is further supported by checking for consecutive observations in the jumps and if they are pointing in the same direction, they are merged into one jump. Narrow peaks are eliminated completely. One basic function was provided for each of these jumps except for those right at the end of the series.
After establishing the positions of jumps as starting values for m_1, m_2, their height to length ratio as starting value for the steepness parameters d_1, d_2 had to be quantified. For this the first difference divided by 5 was used if no merge had taken place. If a merge had occurred, the first differences were totalled up. The number of parts merged was multiplied by 5. The sum of the differences was then divided by the result of the multiplication. In many cases the starting values found by this method were astonishingly good, as can be seen from Figure 6.6.

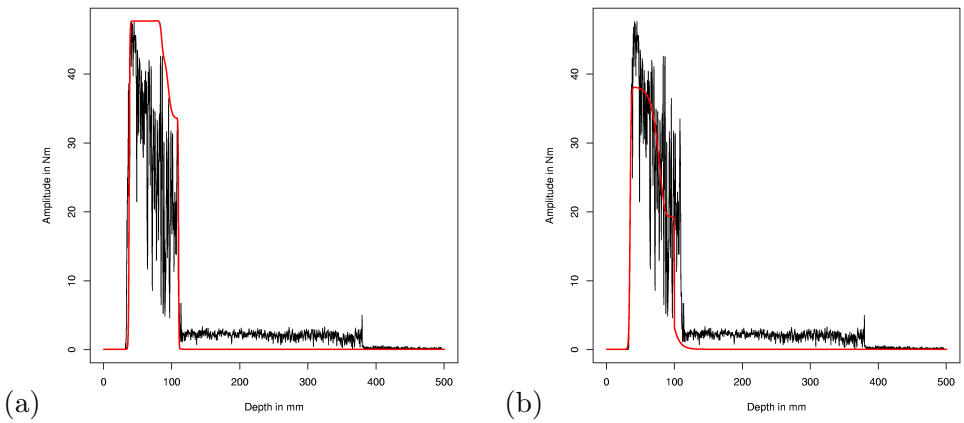

Figure 6.6: (a) Basic functions with start values (b) fitted by nonlinear regression with main jumps only

Since the positions of the jumps were determined at sections of 5mm or more, the starting point and end point of the jump were defined by this section. These points were used to define the part of the series on which the actual basic function was to be fitted to the data. For the first jump all the data up to the start of the second jump is used if the latter is upwards, if the second jump is downwards the endpoint is included. The rest of the time series is set to 0. After successfully fitting a basic function, the fitted values of this function are added to the already fitted values (starting from 0) and subtracted from the residuals (starting with the observed series).

Nonlinear regression had problems with the extreme values of the steepness parameters d_1, d_2 because these often led to singular gradients in parameters. To resolve this problem two approaches were implemented and then combined. The first approach was to relax tolerance of the comparison between numerical imprecision and the residual sum of squares varying from 10^{-3} to 1. The second consisted of testing several starting values for the steepness parameters. These values included the reciprocal of the determined starting value, ten times this value, the starting value itself and 10 uniformly distributed random values between the smallest and the largest of the named values. These two approaches were combined by first testing the different starting values, then changing the tolerance and again testing the starting values. Figure 6.6 displays the result of the algorithm described so far.
From Figure 6.6 one drawback of the described method is obvious: smaller steps in the development of the amplitudes are not explained. It was tested whether a larger quantile of jumps would help to explain these smaller steps, but this was not the case. So after the first fit of basic functions the remaining residuals were checked for larger parts of non-zero means. In these parts basic functions were again fitted. This procedure was applied at most three times or until no larger portion of the residuals with mean greater than zero was left. The portion had to be larger than 2% of the data or 10mm depth in this case.

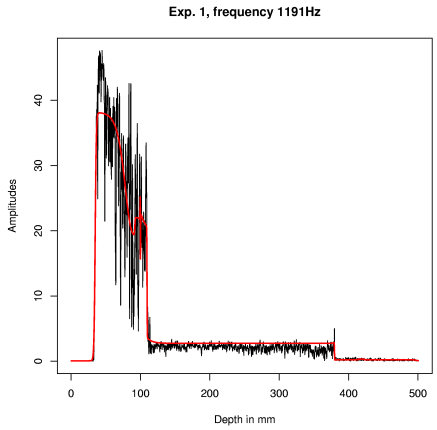

Figure 6.7: Final fit of the example from Figure 6.6

A second problem was that sometimes two or more basic functions were fitted to a section of the series where by inspection one should have sufficed. This was due to the empirical quantiles always forcing at least ten observations to be of interest. We therefore checked at each jump detected by the first method if the means on the actual section and the next were sufficiently different to need more than one basic function. Then we checked whether the difference between the means on the sections was lower than the jump found by the described method. If this was the case the

next section was added to the current data to be fitted and the check was repeated on the next section between jumps.
The result with the complete procedure for the example from Figure 6.6 can be seen in Figure 6.7. The commented code for the fitting procedure can be found in the Appendix in Section B.3.

6.3 Results from the Fits

6.3.1 Some Views of Fits

In general the fitting procedure worked very well, as can be seen from Figure 6.7 and Figure 6.8. In the latter figure it is obvious that the two forms of the development of the amplitudes can be fitted quite well.

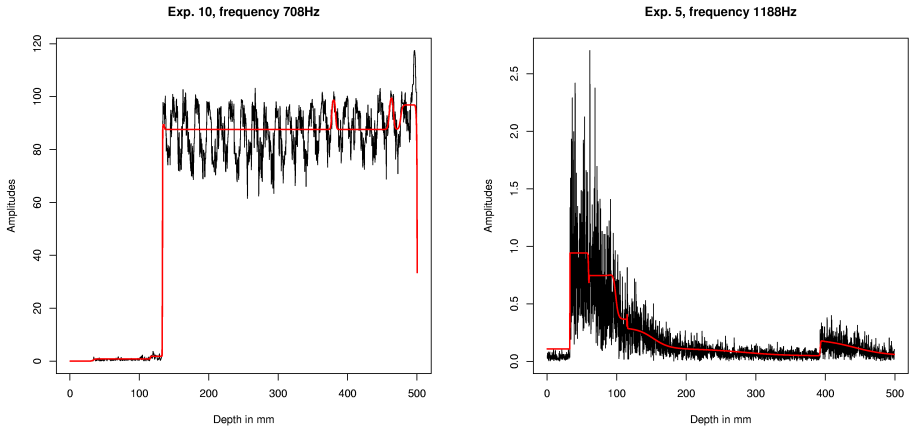

Figure 6.8: Fit on the Amplitudes for Experiment 10, frequency 708Hz, displaying the jump and the a plateau, and for Experiment 5, frequency 1188Hz, displaying two peaks followed by slow descent.

But the model is even flexible enough to approximate more complicated forms, like the two plots in Figure 6.9. On closer examination of these plots it is obvious that some features can only be explained by fitting additional basic functions. For example the 'hill' in the amplitude for 2109Hz on the depths 300-500mm is impossible to describe with just one of the basic functions. It is well approximated however using two functions.

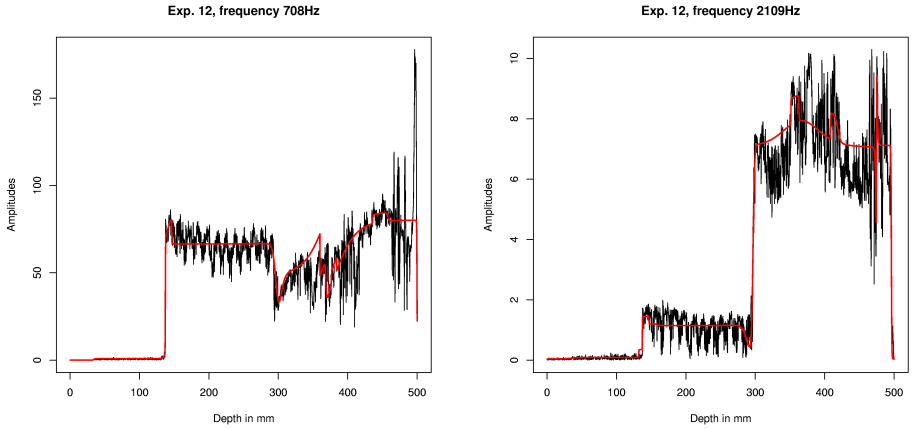

Figure 6.9: Two complicated developments of the amplitudes from Experiment 12.

It has to be said however that the procedure was not completely fail-safe. Consider Figure 6.10 for example. Since in some situations the tolerance level had to be relaxed considerably to get any result at all, in a few cases the results were totally unsatisfactory. In Figure 6.10 the panel on the left-hand side displays the first result (which is far off the mark) from the fitting procedure. The final result, which is used in the following analysis, is shown in the right-hand panel. This result was gained by simply reusing the fitting procedure several times on this data.

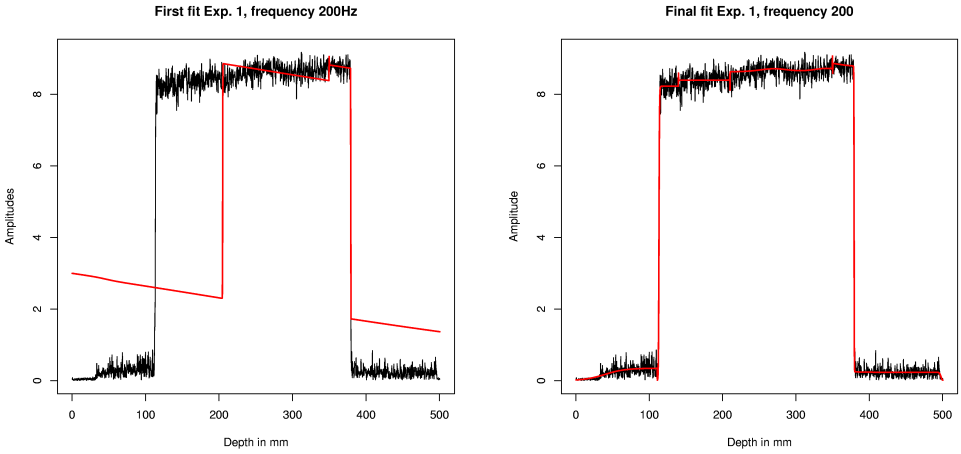

Figure 6.10: Failed and successful fit on frequency 200Hz in Experiment 1.

General failure even after several applications of the fitting procedure was only observed for series of amplitudes which had no obvious development – only two of the

1276 series. In the first automatic run 24 series turned out to be difficult to fit, but in 12 cases this could be cured by reusing the fitting procedure. The remaining 12 series were only partially fitted, typically only one insufficient basic function was fitted. Fits where the maximal parameter was not changed in the optimisation constituted another persisting problem of the fitting procedure. This only happened for the later fitted lower parts of the developments, as can be seen from Figure 6.11. Since this occurred in 90 of the fits which was only a small fraction of the series, and only for the parts of lesser importance a further improvement was not sought.

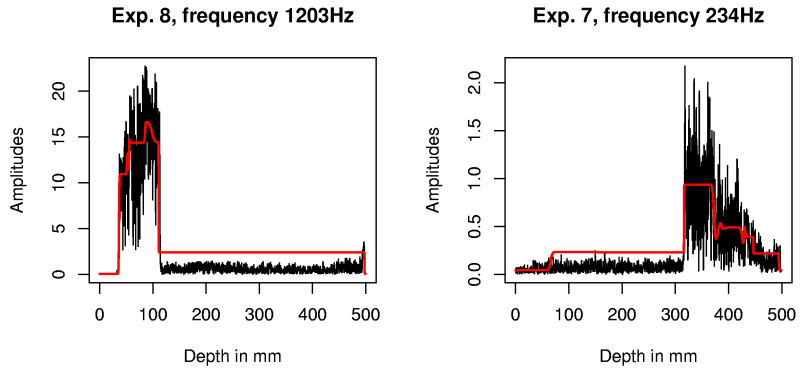

Figure 6.11: Series of amplitudes where the lower parts are overestimated by the fitting procedure.

6.3.2 Summarising Results

Numbers of Basic Functions

Before analysing the fits we had expected that the number of basic functions needed to describe the development of the different amplitudes would somehow be connected to the number of chatter states in the experiment. This was not the case, however. The differences when comparing the results from e.g. experiment 21a (which showed only a short period of chatter at the end) with those of experiment 1 (which had three different chatter phases) were negligible. For experiment 1 it took 13 basic function in median to approximate the behaviour of the amplitudes, while for experiment 21a 10 were needed. No obvious structure was found in the necessary number of basic functions, so it will not be discussed any further. The complete tables can be found in the Appendix, Chapter A.

Parameters m_1 and m_2 of the Basic Functions

The parameters m_1 and m_2 in the basis functions mark the two turning points of this function. In the fits they give the positions of steep rise or steep fall, respectively. So the histograms in Figure 6.12 give the number of amplitudes for the relevant frequencies which had a realisation of m_1 or m_2, respectively, within the section. Realisations

of m_1 or m_2 outside 0-500mm range have been cut because they cannot be interpreted sensibly. Furthermore, they are mainly due to basic functions corresponding to very low shifts in the amplitude.

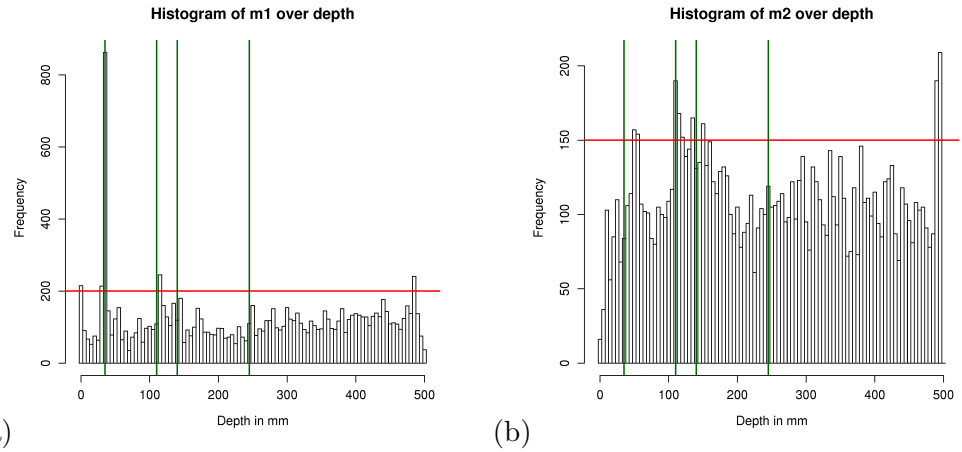

(a) (b)

Figure 6.12: Number of fits of basic functions with a realisation of m_1 on the left-hand side, and m_2 on the right-hand side, within segments of 5mm.

In Figure 6.12 (a) the depth of 35mm has become as important as expected, compared to Figure 6.3. The 110mm depth is still one of the highest bars, while 140mm and 250mm do not stand out any more. The same is true for all other afore-mentioned depths. So upward jumps only happen more often near 0mm, 35mm, 110mm and interestingly near 485mm depth.
In Figure 6.12 (b) it is obvious that the downward jumps are slightly more fuzzy than the upward jumps because there are two types: the slow descent from a peak, and the steep fall from a plateau. Here a possible explanation for the order of the counts in Figure 6.3 can be found: depth 35mm is only important for the rise, but depth 110mm is important for rise and descent. In Histogram 6.12 (b) all other peaks from Figure 6.3 are present which are not present in Figure 6.12 (a).

Machine Parameters and Parameters a, d_1 and d_2
One of the goals of analysing the development of the amplitudes over time was to find possible connections to the machine parameters. Since each experiment had its own specific number of chatter phases and even within the experiments the number of basic functions per frequency was not constant, the parameters of basic functions with maximal upper value a were investigated for connections to the machine parameters. In some basic functions m_1 and m_2 switched positions, i.e. a no longer reflects the maximal value of the fitted values. So only those basic functions, for which $m_1 < m_2 - 5\text{mm}$ was true, were considered in this analysis. The maximal parameter a was expected to display a similar behaviour as the maximal amplitude in Tables 6.3 to 6.4. This is indeed the case when the general selection of the variables is compared. For

the lower frequencies near 234Hz it is obvious from Table 6.5 that instead of the feed f and the flow rate of the oil, the cutting speed v_c is now the most significant influence.

	μ	f^2	v_c^2	$\dot{V}^2$	f	v_c	$\dot{V}$	$f:v_c$	$f:\dot{V}$	$v_c:\dot{V}$	$f:v_c:\dot{V}$	$R^2_{adj.}$
5	X	.	.	.	+	X	+	.	X	.	.	0.385
195	X	.	.	.	+	X	+	+	+	.	.	0.39
200	X	.	.	.	+	X	+	+	+	.	.	0.366
205	X	.	.	.	+	X	+	+	+	.	.	0.348
210	X	+	.	.	+	X	+	+	+	.	.	0.316
215	X	+	.	.	+	X	+	+	+	.	.	0.252
220	X	+	+	.	+	+	+	+	+	.	.	0.149
225	X	X	X	.	.	.	.	.	.	.	.	0.169
229	X	X	X	.	+	+	+	X	.	.	.	0.53
234	X	.	.	.	+	X	+	+	+	.	.	0.334
239	X	.	.	.	X	X	+	+	+	.	.	0.392
244	X	.	.	.	X	X	+	+	+	.	.	0.384
249	X	.	.	.	+	X	+	X	+	.	.	0.4
254	X	.	.	.	+	X	+	+	+	.	.	0.363
259	X	.	.	.	+	X	+	+	+	.	.	0.336
264	X	+	.	.	+	X	+	.	+	.	.	0.197
269	X	+	.	.	+	X	+	+	+	.	.	0.213
469	.	.	.	.	.	.	.	.	.	.	.	#

Table 6.5: Model fits of machine parameters to the maximal parameter a per frequency, lower frequencies.

For the frequencies near 703Hz the feed f and the interaction of feed and cutting speed $f:v_c$ are the most influencing factors. The cutting speed v_c is less important than for the maximal value of the series of amplitudes. The maximal parameter a for the frequency band near 1200Hz is also clearly dominated by the influence of the cutting speed v_c. Tables 6.6 and 6.4 are also very similar with respect to the selected albeit relatively unimportant influences.

	μ	f^2	v_c^2	$\dot{V}^2$	f	v_c	$\dot{V}$	$f:v_c$	$f:\dot{V}$	$v_c:\dot{V}$	$f:v_c:\dot{V}$	$R^2_{adj.}$
664	X	+	.	.	X	+	.	X	.	.	.	0.363
669	X	.	.	.	X	+	.	X	.	.	.	0.296
674	X	.	.	.	X	+	+	X	.	+	.	0.385
679	X	.	.	.	X	+	.	X	.	.	.	0.174
684	.	.	.	.	.	.	.	.	.	.	.	#
688	.	.	.	.	.	.	.	.	.	.	.	#
693	X	.	.	.	+	+	+	+	+	+	X	0.108
698	X	.	+	.	+	X	X	X	X	X	X	0.651
703	X	.	.	.	X	+	.	X	.	.	.	0.27
708	X	X	X	.	+	X	.	.	.	.	.	0.414
713	X	+	X	.	X	+	.	X	.	.	.	0.39
718	X	.	.	.	X	+	.	X	.	.	.	0.33
723	X	.	.	.	X	+	.	X	.	.	.	0.284
728	X	.	.	.	X	+	.	+	.	.	.	0.193
732	.	.	.	.	.	.	.	.	.	.	.	#
737	.	.	.	.	.	.	.	.	.	.	.	#
742	.	.	.	.	.	.	.	.	.	.	.	#
1143	.	.	.	.	.	.	.	.	.	.	.	#
1147	X	.	+	.	.	X	.	.	.	.	.	0.347
1152	X	.	.	.	.	X	.	.	.	.	.	0.168
1157	X	.	+	.	.	X	.	.	.	.	.	0.172
1162	.	.	.	.	.	.	.	.	.	.	.	#
1167	.	.	.	.	.	.	.	.	.	.	.	#
1172	X	X	.	.	+	+	.	+	.	.	.	0.178
1177	X	+	.	+	X	X	+	X	.	.	.	0.652
1182	X	.	X	.	.	X	.	.	.	.	.	0.44
1187	X	.	.	+	.	X	+	.	.	.	.	0.461
1191	X	.	.	.	.	X	.	.	.	.	.	0.381
1196	X	.	+	.	.	X	.	.	.	.	.	0.355
1201	X	.	X	.	.	X	.	.	.	.	.	0.292
1206	X	.	.	.	+	X	+	.	.	.	.	0.313
1211	X	.	.	.	.	X	.	.	.	.	.	0.248
1216	X	.	X	.	X	X	.	.	.	.	.	0.376
1221	X	X	.	X	X	X	.	X	.	.	.	0.645
1641	.	.	.	.	.	.	.	.	.	.	.	#
1646	X	.	.	.	X	X	.	X	.	.	.	0.315
1650	X	.	.	X	X	X	X	X	+	X	+	0.646
2109	.	.	.	.	.	.	.	.	.	.	.	#
2114	X	.	X	.	.	X	+	.	.	.	.	0.478
2119	X	.	.	+	X	X	+	X	.	+	.	0.496

Table 6.6: Model fits of machine parameters to the maximal parameter a per frequency, high frequencies.

It was of interest whether the slope parameters d_1 and d_2 displayed a connection to the machine parameters. While it is expected that d_1 displays a similar behaviour to a because all ascents are steep up to the maxima, d_2 may show a different behaviour. Tables A.1 and A.4 in the appendix summarise the results for d_1 and d_2. The presumed behaviour of d_1 was not found. It is interesting that for most frequencies where a model was found all parameters and interactions were selected. In some cases quadratic terms were also added to the models.
In general the results on the parameters d_1 and d_2 are hard to interprete and do not tell a story of their own since they are correlated to the maximal parameter a. So it is much more interesting to base further studies on the clearer results from the maximal parameters a.

6.3.3 Predicting early Chatter by Fitted Values

One of the challenging problems encountered when modelling the BTA deep-hole drilling process is the chatter vibrations starting directly after the guiding pads leave the starting bush. We therefore tried to use the fitted values of the varying amplitudes to predict whether or not the occurrence of such chatter vibration was likely.
This problem was analysed as a classification problem. The 22 experiments were classified into two groups – chatter vibration right after the guiding pads leave the starting bush (16 observations), and no such chatter (6 observations). The median of the fitted values between 25mm and 35mm depth was calculated for all the frequencies detected by both procedures described in Section 6.1, and additionally for the frequencies 2109Hz to 2119Hz. Inclusion of the frequencies 2109Hz to 2119Hz was due the fact that they are the highest harmonics of the eigen-frequency 234Hz detected significant. The high frequencies appeared more important because the strong damping effect of the starting bush only allows small movements of the tool.
The small number of observations especially in the group with no chatter restricted the choice of the classification method. We chose the well-known linear discriminant analysis (LDA) (cf. e.g. Venables and Ripley (2002) pp. 332-339) because it is one of the most stable methods and hard to beat with respect to prediction ability even in difficult situations (cf. Pouwels et al. (2002)). Because the number of classificator variables was, with 37 variables, still too high a stepwise variable selection procedure based on a 4-fold cross validation was performed.
The described procedure led to the following set of frequencies to classify the experiments into early chatter or none: 234Hz, 249Hz, 2109Hz, 2114Hz and 2119Hz. With this set of classificator variables a leave-one-out error rate of 13.6% was reached. A closer inspection of the posterior probability for the classes showed that one of the three wrong classifications was based on 50.4% for the wrong class. Therefore, we decided to check whether the discrimination could be improved by adding the machine parameters to the set of discriminators, and then reusing the variable selection procedure. This led to the inclusion of the cutting speed in the variable set which in turn led to the correct classification of the above mentioned observation. With this final set of variables the leave-one-out error rate was reduced to 9.1% and the two

wrongly assigned observations were assigned to the class of no chatter.

6.4 Summary and Conclusions

The relevant frequencies for the BTA deep-hole drilling process were established by applying the concepts from Chapter 4. Characteristic features, namely that there are always several phases in the development of the amplitudes, were then described. First there is the phase when the amplitudes are low because all frequencies damped by the fact the bore tool is firmly clamped in the starting bush by the guiding pads. After the guiding pads leave the starting bush there is the potential for high frequency chatter near 1200Hz. This chatter is either followed by chatter near 234Hz or chatter near 703Hz. For the different phases in the development of the amplitudes two typical forms were identified.
Connections between features of the machine/tool/workpiece assembly and the features of the development of the amplitudes included the more frequent occurence of large jumps near 35mm, 110mm and 250mm. The 35mm depth has already been pointed out as corresponding to the point at which the guiding pads leave the starting bush and thus a change in the dynamics is inevitable. The jump at 110mm is particularly interesting because it occurs shortly after the tool head with a length of 95mm is completely in the bore hole. One possible explanation for this is that the bore tool head is slightly thicker than the boring bar and for this reason the damping changes close to this point.
The results of the connection between machine parameters and the maximal amplitudes also prove interesting in that the maximal amplitudes of frequencies in the same frequency band are dominated by a distinct combination of the machine parameters, and could be used to construct control actions as a reaction to changes in specific frequency bands.
The product of two logistic functions as the basic function for the approximation of the developments of the amplitudes proved to be flexible enough to describe nearly all series of amplitudes save for twelve, which were uninteresting. As a summarising result we chose the maximal parameter a of the basic functions with the property that $m_1 < m_2 - 5\text{mm}$. These values should be connected to the maximal amplitudes because the condition ensures that a gives the maximal value for the basic function. It turned out that these parameters were similarly linked to the machine parameters as the maximal amplitudes. Only a slight shift in the importance of the parameters for the frequencies near 234Hz was observed. This supports the idea of using this information to design of control actions.
When analysing the steepness parameters d_1 and d_2 of the basic functions with maximal parameter a the most prominent common feature of the models was that all main effects and interactions were present in most of them. Because of the direct link to the maximal parameter – it is not possible to change the steepness without changing the maximum of the function – not a lot of insight is gained from this analysis.
More insight was gained from the consideration of the position parameters m_1 and

m_2. Since m_1 stands for the rise of the basic function and m_2 for its descent, the positions can be divided into upward and downward changes in the amplitudes. This made it clear that 110mm depth is a point where not only many upward changes occur like at the 35mm depth but also downward jumps occur just as frequently.
Overall it must be said that the dynamics of the process are much to variable to be captured with the fairly simple model used here. Especially the differing numbers of basic functions, and the variation of the places where a certain kind of chatter vibration occurs, make it impossible to define common sections of depth for all experiments, on which basic functions could be fitted including the machine parameters. The inclusion of the machine parameters could have been done by a linear function of the machine parameters in place of the maximal value parameter a.
But many of the discovered regularities in the approximations of the developments of the amplitudes make it possible to search more easily for interpretations of the observed behaviour in connection with the machine parameters and the machine/workpiece assembly. This makes the models for varying amplitudes useful in circumstances like the ones encountered above.
The most helpful result of the analysis of the varying frequencies is the result from the linear discriminant analysis which clearly makes it possible to predict chatter vibrations immediately after the end of the starting phase. This supports the idea of modelling and monitoring all frequency bands close to the eigenfrequencies of the boring bar and their harmonics.

7 Connection to Stochastic Differential Equation

A common approach to modelling dynamics in Physics and Mathematics is the use of stochastic differential equations. The change from one dynamic state of a system to another is called bifurcation. G. Schöner and M. Hüsken proposed the following differential equation as a general model to describe the bifurcation into chatter vibration in one frequency (Weinert, Webber, Hüsken, Mehnen, and Theis, 2002):

$$\frac{d^2M(t)}{dt^2} + h(t)(b^2 - M(t)^2)\frac{dM(t)}{dt} + \omega^2 M(t) = W(t) \tag{7.1}$$

where $M(t)$ is the drilling torque and $W(t)$ is a white noise process.
Since this is an alternative way to describe the development of the drilling torque over time this chapter aimes to prove that it is directly connected to the basic functions used in Chapter 6. In the next section the corresponding amplitude equation is derived. This is followed by the proof that there is a function $h(t)$ such that the logistic function is a solution of the amplitude equation. Finally a discrete version of the equation is derived and the closeness to the real data is demonstrated by a simulation.

7.1 Derivation of the Amplitude Equation

This equation is considerably simplified when $M(t)$ is taken as a harmonic process. The following calculations are based on Davies (2003). Let

$$M(t) := g(t)\cos(\omega t + \phi). \tag{7.2}$$

$$\frac{dM(t)}{dt} = \frac{dg(t)}{dt}\cos(\omega t + \phi) - \omega g(t)\sin(\omega t + \phi), \tag{7.3}$$

$$\frac{d^2M(t)}{dt^2} = \frac{d^2g(t)}{dt}\cos(\omega t + \phi) - 2\omega g(t)\sin(\omega t + \phi) - \omega^2 g(t)\cos(\omega t + \phi) \tag{7.4}$$

First, we note that the term $\omega^2 g(t)\cos(\omega t + \phi)$ vanishes. Second, all terms without ω may be omitted because ω is large compared to the change in the first and second derivative of $g(t)$. In other words $\frac{dg(t)}{dt}$ does not contain high-frequency components and thus, the following holds

$$\int \frac{dg(t)}{dt}\cos(\omega t + \phi)dt \approx 0.$$

Therefore, (7.1) can be replaced by

$$-\sin(\omega t+\phi)\left(2\frac{dg(t)}{dt}+h(t)g(t)(b^2-g(t)^2\cos^2(\omega t+\phi))\right). \tag{7.5}$$

Now $\cos^2(\omega t+\phi)=(1-cos(2\omega t+2\phi))/2$, and the term $g(t)^2(1-cos(2\omega t+2\phi))$ can be omitted as well. So we get

$$-\sin(\omega t+\phi)\left(2\frac{dg(t)}{dt}+h(t)g(t)(b^2-\frac{g(t)^2}{2})\right).$$

Now this is equalled to 0 or white noise $W(t)$, it becomes

$$-\sin(\omega t+\phi)\left(2\frac{dg(t)}{dt}+h(t)g(t)(b^2-\frac{g(t)^2}{2})\right)=W(t). \tag{7.6}$$

Multiply (7.6) with $\sin(\omega t+\phi)$, and note that $W(t)\sin(\omega t+\phi)$ behaves similarly to white noise. Moreover, note that $\sin^2(\omega t+\phi)\approx 1/2$. It follows for the amplitude that

$$2\frac{dg(t)}{dt}+h(t)g(t)(b^2-\frac{g(t)^2}{2})=\frac{W(t)}{\omega}. \tag{7.7}$$

This is the amplitude-equation for the differential equation in (7.1) if there is only one frequency present in the process.

7.2 Connection to Logistic Function

Now assume that the logistic function is the right form for $g(t)$. It has to be shown that there is a function $h(t)$ so that equation (7.7) has a solution. To show this, the white noise is replaced by 0 to make the calculations more straightforward.
Set

$$g(t):=\frac{a}{1+\exp\left(-\frac{t-t_0}{d}\right)},$$

it follows that

$$\frac{dg(t)}{dt}=\left(-\frac{\exp\left(-\frac{t-t_0}{d}\right)}{d}\right)\frac{a}{\left(1+\exp\left(-\frac{t-t_0}{d}\right)\right)^2}.$$

Inserting these formulas into (7.7) we get

$$-2\frac{\exp\left(-\frac{t-t_0}{d}\right)a}{d\left(1+\exp\left(-\frac{t-t_0}{d}\right)\right)^2}+h(t)\left(\frac{ab^2}{1+\exp\left(-\frac{t-t_0}{d}\right)}-\frac{a^3}{2\left(1+\exp\left(-\frac{t-t_0}{d}\right)\right)^3}\right)=0$$

Adding the first term on both sides:

$$h(t)\left(\frac{2ab^2\left(1+\exp\left(-\frac{t-t_0}{d}\right)\right)^2-a^3}{2\left(1+\exp\left(-\frac{t-t_0}{d}\right)\right)^3}\right)=2\frac{\exp\left(-\frac{t-t_0}{d}\right)a}{d\left(1+\exp\left(-\frac{t-t_0}{d}\right)\right)^2}.$$

Because the term in brackets on the left-hand side is never 0, it is possible to divide by it. It follows that

$$h(t) = 2\frac{\exp\left(-\frac{t-t_0}{d}\right)\left(1+\exp\left(-\frac{t-t_0}{d}\right)\right)}{d\left(b^2\left(1+\exp\left(-\frac{t-t_0}{d}\right)\right)^2 - \frac{a^2}{2}\right)}\,. \tag{7.8}$$

This solution is well-defined for $t \in \mathbb{R}$. So (g, h) is a pair of functions, which solves equation (7.7).
Of course the same procedure could be applied to the product of the two logistic functions from Formula (6.1). This establishes the link between the two approaches to describe the development of the amplitudes.

7.3 Making the Amplitude Equation Discrete and Simulations

Changing from continuous time to discrete time in equation (7.7) we get

$$g(t+1) - g(t) = -\frac{b^2 h(t)}{2} g(t) + \frac{h(t)}{4} g(t)^3 + \varepsilon_t \tag{7.9}$$

$$\Leftrightarrow g(t+1) = \left(1 - \frac{b^2 h(t)}{2}\right) g(t) + \frac{h(t)}{4} g(t)^3 + \varepsilon_t. \tag{7.10}$$

The latter relation is used to estimate $h(t)$ from the amplitudes for frequency 703 Hz in experiment 5 of the experimental design. Taking 21 consecutive observations of the amplitude and using only the linear part of the equation the coefficient of $g(t)$ displays the behaviour shown in Figure 7.1.

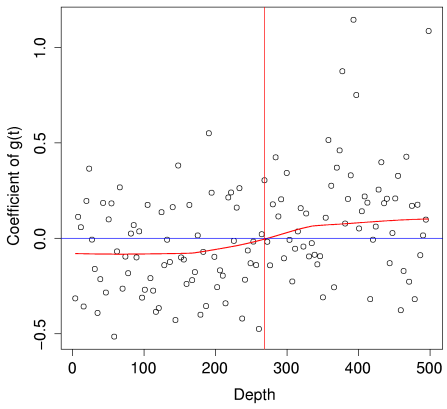

Figure 7.1: Coefficients of $g(t)$ in (7.9) over time

The horizontal red curve in Figure 7.1 shows the result of the Loess-smoother (Cleveland et al., 1992) including 75% of the data in the fit. This curve is similar to a logistic

function like the function $h(t)$ found in the last section. The sign change indicated by the vertical red line marks the change from stable to instable behaviour of this recursive formula. As shown by Davies (1983) the actual shift from one state of the system to another is postponed by the noise. Comparing the point of change in Figure 7.1 to the red line in Figure 7.2, which shows the development of the amplitude of 703Hz in experiment 5, it is obvious that the actual change into chatter happens approximately 130mm later.
That the change from one dynamic state of the system to the other is postponed by noise is even more impressive in Figure 7.2 when it is known that the change point was set to $t_0 = 160mm$.

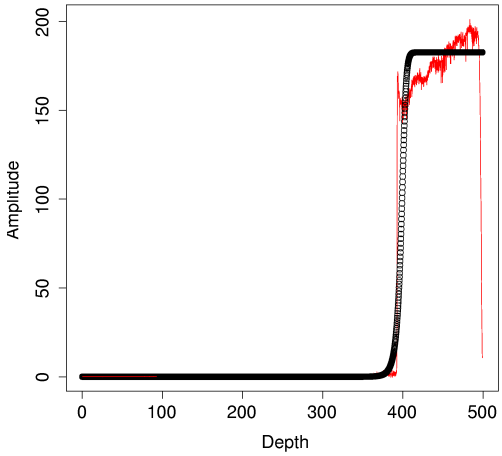

Figure 7.2: Comparison of a simulated amplitude (black) to a real amplitude (red)

Furthermore, Figure 7.2 demonstrates that the behaviour of the simulated data is not far from the real data, and that the logistic function would fit the data perfectly if the data were generated by the mechanism described by Formula (7.9).

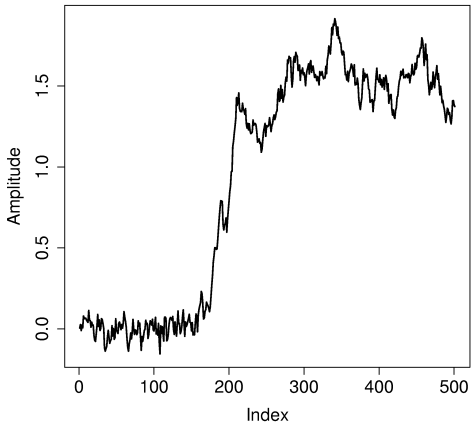

Figure 7.3: Outcome of a simulation using the estimated parameters from Section 6.2.1 for the function $h(t)$ from Formula (7.8.

However, the estimated parameters from the descriptive model found in Chapter 6 do not lead to similar data as can be seen from Figure 7.3 where the set of estimated parameters for the same series as in Figure 7.2 was used. One run of the simulation is plotted which used the calculated function $h(t)$ from Formula (7.8). The simulated data set does not reach the maximum of nearly 300 but only reaches 2.

7.4 Conclusions for further Modelling

In this chapter it was proved that there exists a deterministic solution to the stochastic differential equation proposed by Schöner and Hüsken that links the descriptive model (6.1) from Chapter 6 to this equation. But the results of the last simulation make it clear that estimating parameters of the stochastic differential equation is not possible using this simple semi-parametric approach. In particular, the critical point of change from stable behaviour to chatter cannot be modelled by this description because the parameter m_1 gives the turning point of logistic function and not the time point when the dynamic state changes from stable to instable. This change happens clearly before the amplitude rises to its maximum. The fact that the noise postpones the change into chatter vibration makes it possible to intervene before the chatter vibration fully develops, thus making this a very useful result. Further modelling should therefore be focused on detecting this change point and on how a true change into chatter may be avoided.

8 Résumé

8.1 Conclusions for Experimental Designs and Time Series

The overview on experimental designs and time series in Chapter 3 made it clear that there are many approaches to deal with problems where the observations from the experiments are correlated. There are also optimal experimental designs when the time series model can be specified up to a small number of parameters. And finally there are also D-optimal designs of trajectories for the identification of linear and nonlinear dynamic systems. All these methods were not applicable to the problem of the first experiments on the BTA deep-hole drilling process because no specific model for the on-line measurements was available.
In the literature a possible solution was found in the form of the space-filling or exploratory designs described in Section 3.6. These designs allow you to plan a sensible number of experiments which span the range of possible values of controllable variables as well as possible. Because the number of experiments is controlled by the experimenter it is also possible to allow for a number of repetitions of the complete design. This is absolutely necessary when a dynamic problem is suspected. If no repetitions are carried out when a dynamic phenomenon is under investigation then it could happen that the dynamic nature may go unobserved. This is underlined by the variety of behaviours observed at the centre point of the central-composite design in our experiments (cf. Figures 1.8, 1.9 and 2.6) which showed clearly that no simple link between the machine parameters and the dynamic behaviour can be established. An unanswered question is whether and how the methods for the identification of linear dynamic systems, or the optimal factorial designs for continious processes could be employed in developing control strategies for dynamic systems. It may not be possible to identify a nonlinear dynamic system (Leontaritis and Billings, 1987) but nevertheless constructing trajectories with the methods of Zarrop (1979) based on a linearisation of a proposed system may lead to a set of control actions that could be tested for effectiveness.

8.2 Conclusions for Further Developments on Models on Varying Amplitudes

In Chapter 4 it was proved that the periodogram ordinates of a harmonic process with normal white noise or AR(p) disturbances are either χ^2-distributed at the unimportant frequencies or non-central χ^2-distributed at the important frequencies. The

most important outcome was that this knowledge of the distribution can be used to estimate the variance σ^2 of the error process from the periodogram by means of a robust estimator. On the one hand this estimate can be used to determine relevant frequencies and on the other hand to construct an estimator for the amplitude at the relevant frequencies. The estimator for the amplitude included the application of the square root to the periodogram ordinate which is one possible transformation when the behaviour of a non-central χ^2 random variable is approximated by a normally distributed variable (Johnson et al., 1994).
In Section 4.3 it was shown that the Fourier-transform is not only linear for time stationary functions but also for time varying functions. This makes it possible to use the estimates of the amplitudes on sections of a harmonic process constructed from the periodogram ordinates to estimate the functional form of the development of the amplitudes of relevant frequencies over time.
In Chapter 5 the theoretical results were investigated with regards to their practical application. To this end the methods developed in Chapter 4 were applied to a wide variety of data situations. The first simulation in Section 5.2 only considered a time stationary influence on the amplitudes by a number of variables $\vec{x}$. In general the variance of the errors was slightly overestimated by the method while the amplitudes were underestimated. The overestimation of the variance was traced to a higher influence of leakage than expected. A very positive result was found for the normal approximation because the normality assumption for the parameters in the linear models could not be rejected 94% of the cases. This was a surprisingly positive result considering that the normality approximation is dependent on the degrees of freedom for the non-central χ^2-distribution and the absolute value of its non-centrality parameter.
In Section 5.3 the effect of time varying amplitudes was tested. The first interesting result was that the normality approximation for the periodogram ordinates functioned very well with less than 5% rejections on a 95%-niveau of the Shapiro-Wilk test for normality. The second very positive result was that not just a linear time trend of the amplitudes could be found by the method but also a nonlinear trend could be fitted, and resembled the 'true' function of the amplitude. A serious drawback was the general underestimation of the amplitudes. The method for estimating of the variance of the error process turned out to be much more accurate on the data with time varying amplitudes. This could have been due to the larger number of observations. In some cases it underestimated the variance slightly which could have been caused by the fact that the time varying nature of the amplitude does have a small effect on all periodogram ordinates.
In general the estimates based on the periodogram ordinates underestimated the amplitudes in our simulations which was also suggested by the theoretical investigation of, at least, the time varying amplitudes. A possible solution to this problem could be an exponentially weighted mean on the periodogram ordinates in a small neighbourhood of the relevant frequencies, centred at the relevant frequencies with the highest amplitudes. Such a procedure may not only improve the accuracy of the estimate but also the goodness of the normality approximation by adding degrees of freedom

in the χ^2-distribution.
Further open questions on the topic include the effect of overlapping sections to determine the periodogram data on harmonic processes with varying amplitudes. This would be of interest if the time series that can be collected within an experiment are rather short compared to the number of suspected relevant frequencies. Otherwise it may happen that quite long time series of the harmonic process are recorded. Then it is possible to leave gaps in the spectrogram data and thereby ensure a conditional independence from one time point to the next. Another theoretically challenging question is the effect of error processes with long memory. The question of optimal experimental designs for the discussed models also remains open. The principles of experimental designs for repeated measurements with normal errors can be viewed as prototypes for these models because the normal approximation is obviously valid in most cases, even if the signal-to-noise ratio is small.

8.3 Conclusions for the Investigation of the BTA Deep-Hole Drilling Process

Using the central-composite design to investigate the quality measures and, at the same time, to measure on-line variables for the investigation of the dynamic behaviour proved appropriate because the repetitions at the centre point showed the diversity of possible behaviour of the process. Additionally the experimental design made it possible to distinguish between special and common behaviour. This led us to realise that however different the drilling torque of a certain experiment may look the dominating frequencies were the same for all sets of machine parameters.
The results on the quality measures roughness and roundness showed that the process cannot be optimised by simply using a certain set of machine parameters: when the damper cannot be used the result is a very slow process which can be economically questionable. Even worse a certain amount of chatter vibrations was also observed close to the optimal values found by the surface respond method applied. So no easy way to avoid chatter vibrations without using the damper was found. The use of the damper made it possible to avoid chatter vibrations. To achieve this however it had to be applied at exactly one of the positions where theory suggested effectiveness. Since such positioning may not be possible under all circumstances (e.g. if a very long workpiece is to be machined) it is of great interest to find a way to avoid chatter vibrations by controlling the parameters feed, cutting velocity and flow rate of the cutting fluid.
The spectrograms of the drilling torque suggested the dominance of a few frequencies in the process. This was already shown in the histograms in Section 2.2.2 and the found frequencies proved to be the same as those found by the procedure to detect relevant frequencies (Section 4.2) in Section 6.1. Since the depths at which chatter vibrations became prominent appeared similar we tried to model the developments of the relevant frequencies over the common 'time-axis' depth with the intention of building a general model including the machine parameters. Closer in-

spection revealed however that the developments on the relevant frequencies were too diverse especially for the repetitions at the centre point of the design. Thus only a semi-parametric approach was applied to the individual developments of the relevant frequencies.
When investigating the development of the amplitudes it was suggested that the maximal value of the amplitudes may be linked to the machine parameters. This proved correct and interesting because the maximal amplitudes on different frequency bands indeed turned out to be influenced by different machine parameters. This result was also found for the parameter a describing the maximal value of the basic function from Section 6.2 when $m_1 < m_2$ is true. This result could then be used next to construct control actions especially tuned to different sorts of chatter vibrations.
The individual semi-parametric fits of the basic functions proved much too diverse to establish a common pattern which would have been necessary to construct models across all experiments on the relevant frequencies. One reason for this can be seen in the closeness of the simulation of the stochastic differential equation in Section 7.3 to the data observed. This closeness suggests that the dynamics of the theoretical and practical processes are quite similar. Therefore, the delay of the change in the behaviour by noise known for this kind of stochastic differential equation also applies to the deep-hole drilling process. Thus it can be concluded that the deterministic description implied by the semi-parametric approach is not appropriate in this case. On the other hand this delay provides the opportunity to react to the state of instability before chatter vibrations develop. The parameters in the discrete version of the amplitude equation should therefore be monitored on the relevant frequencies or on appropriate summarising statistics on frequency bands and used as signals when chatter could develop and in the frequency (band) in which chatter might develop.
The signals on the frequencies 234Hz, 249Hz and 2109Hz-2119Hz proved to be good discriminators to distinguish between chatter right after the guiding pads leave the starting bush and no such chatter. This highlights the fact that the very restrictive rule for choosing the relevant frequencies in Section 6.1 did not consider the particularity of the process' start phase so this method has to be applied cautiously. More importantly, it should be noted that this result makes it possible to learn a rule for the cases when chatter vibrations will start right after the end of the start phase of the process. Furthermore, it shows that it is also necessary to monitor the development of the amplitudes in all possible relevant frequencies to distinguish between stable and instable states of the process.

Appendix

A Tables on Fits of Varying Amplitudes

Regressions on Parameters d_1 and d_2

	μ	f^2	v_c^2	$\dot{V}^2$	f	v_c	$\dot{V}$	$f:v_c$	$f:\dot{V}$	$v_c:\dot{V}$	$f:v_c:\dot{V}$	$R^2_{adj.}$
5	.	X	.	X	X	.	.	.	.	.	.	0.318
195	.	.	.	.	.	.	.	.	.	.	.	#
200	.	.	.	.	.	.	.	.	.	.	.	#
205	.	X	+	.	X	+	.	+	.	.	.	0.468
210	.	X	+	+	X	.	.	.	.	.	.	0.398
215	.	.	.	.	.	.	.	.	.	.	.	#
220	.	.	.	.	.	.	.	.	.	.	.	#
225	.	.	.	X	+	X	+	X	X	+	X	0.53
229	.	.	.	.	+	+	+	+	+	+	+	0.209
234	.	.	.	.	.	.	.	.	.	.	.	#
239	X	.	.	.	+	+	+	+	X	+	+	0.379
244	X	.	.	.	X	X	X	X	X	X	X	0.65
249	.	.	.	.	.	.	.	.	.	.	.	#
254	.	X	.	.	X	+	X	X	X	X	X	0.722
259	.	+	+	+	X	X	X	X	X	X	X	0.744
264	.	.	.	.	.	.	.	.	.	.	.	#
269	.	.	.	.	.	.	.	.	.	.	.	#
469	.	.	.	.	.	.	.	.	.	.	.	#
664	.	X	.	.	X	+	X	X	X	X	X	0.706
669	X	.	.	.	X	.	.	.	.	.	.	0.184
674	.	.	.	X	X	X	X	X	X	X	X	0.858
679	X	.	.	.	+	+	.	+	.	.	.	0.174
684	.	.	.	.	.	.	.	.	.	.	.	#
688	.	.	X	.	X	+	X	.	X	.	.	0.645
693	.	.	X	.	X	.	X	.	X	.	.	0.596
698	.	.	X	+	.	X	.	.	.	.	.	0.419
703	.	.	+	+	X	X	X	X	X	X	X	0.655
708	.	X	.	.	+	+	X	X	X	X	X	0.614
713	.	+	+	+	X	X	+	X	X	X	X	0.685
718	.	.	.	.	.	.	.	.	.	.	.	#
723	.	X	.	X	X	+	X	+	X	X	X	0.932
728	.	.	.	.	.	.	.	.	.	.	.	#
732	.	.	.	.	.	.	.	.	.	.	.	#
737	.	.	.	.	.	.	.	.	.	.	.	#
742	.	+	+	X	X	X	X	X	X	X	X	0.791

Table A.1: Model fits of machine parameters to the parameter d_1 corresponding to the maximal parameter a per frequency, lower frequencies.

	μ	f^2	v_c^2	$\dot{V}^2$	f	v_c	$\dot{V}$	$f:v_c$	$f:\dot{V}$	$v_c:\dot{V}$	$f:v_c:\dot{V}$	$R^2_{adj.}$
1143	.	.	.	.	.	.	.	.	.	.	.	#
1147	.	.	.	.	.	.	.	.	.	.	.	#
1152	.	+	+	+	X	X	+	X	X	+	X	0.637
1157	.	X	.	.	+	+	+	+	+	+	+	0.17
1162	.	X	.	.	X	X	X	X	X	X	X	0.813
1167	.	.	X	.	X	X	+	X	+	+	+	0.864
1172	.	.	.	.	.	.	.	.	.	.	.	#
1177	.	X	+	.	X	.	.	.	.	.	.	0.389
1182	.	.	.	.	.	.	.	.	.	.	.	#
1187	.	.	.	.	.	.	.	.	.	.	.	#
1191	.	.	.	.	.	.	.	.	.	.	.	#
1196	X	+	.	.	X	X	X	X	X	X	X	0.702
1201	.	.	+	.	X	X	X	X	X	X	X	0.691
1206	X	.	X	+	+	X	+	+	+	+	X	0.499
1211	.	+	+	+	X	X	X	X	X	X	X	0.662
1216	.	X	.	.	+	X	+	+	X	X	X	0.551
1221	.	.	.	.	.	.	.	.	.	.	.	#
1641	.	X	+	X	X	.	.	.	.	.	.	0.398
1646	.	X	+	+	X	.	.	.	.	.	.	0.404
1650	.	.	.	.	.	.	.	.	.	.	.	#
2109	.	+	+	X	.	.	X	.	.	.	.	0.35
2114	.	+	X	.	.	X	.	.	.	.	.	0.358
2119	.	.	.	.	.	.	.	.	.	.	.	#

Table A.2: Model fits of machine parameters to the parameter d_1 corresponding to the maximal parameter a per frequency, high frequencies.

	μ	f^2	v_c^2	$\dot{V}^2$	f	v_c	$\dot{V}$	$f:v_c$	$f:\dot{V}$	$v_c:\dot{V}$	$f:v_c:\dot{V}$	$R^2_{adj.}$
5	.	X	+	+	X	X	+	X	X	+	X	0.59
195	.	X	.	.	X	+	+	X	X	+	+	0.611
200	.	X	.	.	+	X	X	.	.	X	.	0.646
205	.	.	.	.	.	.	.	.	.	.	.	#
210	.	X	.	.	X	.	.	.	.	.	.	0.298
215	.	.	.	.	.	.	.	.	.	.	.	#
220	.	.	.	.	.	.	.	.	.	.	.	#
225	.	X	+	.	X	+	X	+	X	+	+	0.763
229	.	.	X	+	+	X	X	+	.	X	.	0.58
234	.	X	X	X	+	+	+	X	X	X	+	0.845
239	.	X	+	.	X	X	X	X	X	X	X	0.782
244	X	.	.	.	+	+	+	+	+	+	+	0.285
249	.	X	+	+	X	.	.	.	.	.	.	0.416
254	.	+	+	+	+	+	X	+	X	+	+	0.494
259	.	.	.	.	.	.	.	.	.	.	.	#
264	.	.	.	.	.	.	.	.	.	.	.	#
269	.	.	.	.	.	.	.	.	.	.	.	#
469	.	.	.	.	.	.	.	.	.	.	.	#
664	X	.	+	.	X	+	+	+	X	.	.	0.37
669	.	.	X	.	.	.	.	.	.	.	.	0.149
674	.	.	.	.	.	.	.	.	.	.	.	#
679	.	.	.	X	X	X	X	X	X	X	X	0.795
684	.	+	+	X	.	.	X	.	.	.	.	0.416
688	.	.	+	.	X	+	X	X	X	X	X	0.536
693	.	.	+	.	X	X	X	X	X	X	X	0.701
698	.	.	X	.	X	X	X	X	X	X	X	0.815
703	X	.	+	+	X	.	.	.	.	.	.	0.23
708	.	X	X	X	.	.	.	.	.	.	.	0.681
713	X	.	.	.	X	+	.	+	.	.	.	0.257
718	X	X	X	.	X	X	X	.	X	+	.	0.621
723	.	.	.	.	.	.	.	.	.	.	.	#
728	X	X	.	.	.	.	.	.	.	.	.	0.208
732	.	.	.	.	.	.	.	.	.	.	.	#
737	.	.	.	.	.	.	.	.	.	.	.	#
742	.	.	+	X	+	+	X	+	+	+	+	0.424

Table A.3: Model fits of machine parameters to the parameter d_2 corresponding to the maximal parameter a per frequency, low frequencies.

	μ	f^2	v_c^2	$\dot{V}^2$	f	v_c	$\dot{V}$	$f:v_c$	$f:\dot{V}$	$v_c:\dot{V}$	$f:v_c:\dot{V}$	$R^2_{adj.}$
1143	.	.	.	.	.	.	.	.	.	.	.	#
1147	.	X	.	.	X	X	+	+	X	+	X	0.58
1152	.	+	.	.	.	+	+	.	.	+	.	0.105
1157	.	X	+	.	X	X	X	+	+	X	X	0.877
1162	.	X	.	.	+	X	+	+	X	+	X	0.566
1167	.	X	+	.	X	.	.	.	.	.	.	0.352
1172	X	.	.	.	X	X	+	X	X	X	X	0.608
1177	.	+	+	+	+	X	+	+	X	+	X	0.504
1182	.	X	.	.	.	X	X	.	.	X	.	0.598
1187	.	+	+	+	X	X	+	X	X	X	X	0.692
1191	.	.	.	.	.	.	.	.	.	.	.	#
1196	.	X	.	.	+	X	.	X	.	.	.	0.324
1201	.	+	.	.	+	X	X	+	+	X	.	0.415
1206	.	+	+	+	X	X	X	X	X	X	X	0.688
1211	.	X	+	+	X	X	.	X	.	.	.	0.653
1216	.	X	.	.	X	X	X	X	X	X	X	0.749
1221	.	.	.	.	.	.	.	.	.	.	.	#
1641	.	.	.	.	.	.	.	.	.	.	.	#
1646	.	X	.	.	+	X	.	X	.	.	.	0.549
1650	X	+	.	.	+	+	+	X	+	.	.	0.354
2109	.	.	.	.	.	.	.	.	.	.	.	#
2114	X	.	.	.	+	+	X	+	+	X	+	0.425
2119	.	+	.	.	+	.	.	.	.	.	.	0.128

Table A.4: Model fits of machine parameters to the parameter d_2 corresponding to the maximal parameter a per frequency, high frequencies.

Numbers of Basic Functions

	1	2	3	4	5	6	7	8	9	10	11	12	13	14	15	16	17	18	19	20	21	21a
5	12	14	7	12	1	10	9	9	5	7	14	15	2	13	2	6	13	4	6	5	6	7
195	16	24	10	3	9	10	12	8	8	6	9	13	9	18	12	9	8	17	22	13	21	16
200	8	12	13	17	5	12	12	11	9	19	11	12	12	26	10	21	13	14	14	16	22	6
205	17	15	6	11	15	5	10	18	15	9	6	14	17	22	9	12	10	19	17	20	17	7
210	19	8	2	6	11	10	7	15	12	9	20	10	16	12	12	16	13	14	18	7	13	10
215	16	10	12	12	3	10	7	14	8	6	24	13	10	13	15	15	19	18	9	11	18	8
220	14	12	15	14	1	8	5	7	5	7	11	9	10	15	10	11	8	12	12	12	12	16
225	15	10	11	7	16	7	10	13	5	7	8	11	9	19	19	11	10	17	14	12	16	5
229	10	13	12	13	19	5	8	11	13	6	16	8	8	21	6	9	8	17	9	15	8	7
234	10	13	15	9	12	8	12	7	4	9	14	16	12	14	5	9	10	14	3	13	10	10
239	17	14	12	12	6	5	19	17	11	7	13	11	13	12	11	13	5	9	9	6	15	6
244	19	20	10	9	6	8	8	13	8	6	12	9	15	11	8	12	8	7	14	11	9	11
249	22	15	15	19	4	9	8	13	7	12	13	12	10	14	9	8	7	11	10	6	8	15
254	9	19	4	5	2	16	21	10	11	18	12	9	8	16	9	12	6	10	10	4	7	10
259	16	17	11	11	5	9	6	17	9	12	19	12	10	17	15	20	8	25	18	4	11	6
264	12	18	8	19	15	9	8	13	2	6	12	13	12	14	16	13	21	19	6	11	25	7
269	12	11	20	11	6	9	8	11	18	11	18	16	17	13	14	21	18	14	16	7	14	12

Table A.5: Number of basis functions per frequency and experiment, low frequencies.

	1	2	3	4	5	6	7	8	9	10	11	12	13	14	15	16	17	18	19	20	21	21a
469	15	14	7	5	3	11	3	16	12	12	13	11	12	19	5	14	8	13	15	10	9	1
664	14	27	12	9	15	8	16	10	15	8	11	13	13	14	9	12	13	10	7	9	11	10
669	13	16	14	11	7	8	14	19	13	7	13	14	9	4	10	14	3	12	16	11	15	20
674	15	11	13	7	16	11	11	15	10	3	13	10	8	13	14	12	8	26	11	12	14	8
679	15	12	13	12	11	3	14	14	11	8	16	12	10	12	14	9	15	19	8	10	6	15
684	11	12	7	11	8	6	8	13	15	9	13	11	13	17	12	11	16	15	9	9	14	19
688	13	13	17	8	10	8	11	8	11	8	15	11	11	13	9	12	13	10	12	8	9	16
693	13	15	12	9	12	11	10	11	16	10	12	7	12	14	8	17	12	13	15	8	8	17
698	15	15	7	10	12	9	9	14	10	13	10	10	11	16	14	21	6	16	14	9	11	10
703	12	15	12	15	11	14	10	15	10	7	13	14	12	18	9	14	11	18	17	12	13	15
708	12	14	9	10	11	9	11	12	13	6	12	9	13	9	10	12	11	12	9	7	11	13
713	16	17	9	15	12	17	10	10	14	12	9	9	16	12	12	11	6	15	7	14	13	14
718	11	17	7	14	17	8	19	6	8	9	7	10	10	12	8	12	10	13	14	10	11	9
723	12	15	12	10	9	10	12	14	15	6	10	18	7	11	8	19	11	17	15	7	14	13
728	17	8	9	10	11	9	7	17	20	10	7	9	13	12	9	8	14	17	13	12	10	19
732	10	12	12	13	10	6	14	13	18	6	13	11	11	16	12	15	21	14	13	12	9	21
737	8	16	17	7	14	11	10	10	13	11	15	11	13	20	3	19	10	13	12	5	8	9
742	16	12	10	12	5	5	11	16	11	9	18	9	10	11	12	17	19	10	15	12	8	15

Table A.6: Number of basis functions per frequency and experiment, middle frequencies.

	1	2	3	4	5	6	7	8	9	10	11	12	13	14	15	16	17	18	19	20	21	21a
1143	14	9	6	11	3	10	2	7	2	4	12	14	10	12	13	10	15	15	9	12	15	9
1147	11	7	22	7	9	8	10	7	16	11	11	5	14	12	4	10	12	9	14	8	22	4
1152	12	9	18	8	12	9	8	8	2	5	12	8	14	14	7	12	16	17	13	11	15	4
1157	9	10	13	9	13	2	8	9	4	15	18	10	12	16	7	14	13	15	11	16	7	9
1162	16	12	10	5	10	12	18	11	14	8	17	8	20	14	12	16	9	11	13	21	13	13
1167	18	14	11	7	10	8	10	11	13	6	13	14	14	11	21	10	10	13	12	9	14	10
1172	12	12	6	7	10	9	9	12	12	9	11	9	13	19	12	11	5	15	10	14	10	11
1177	18	15	12	11	11	14	18	15	20	11	9	11	12	14	12	8	6	14	18	9	9	11
1182	12	17	20	11	3	8	20	5	9	3	11	7	15	3	11	6	2	20	16	10	7	16
1187	10	3	11	6	12	7	9	12	19	8	9	9	20	11	13	8	2	14	13	7	14	13
1191	8	8	15	10	10	13	14	6	17	7	8	12	10	9	20	8	7	12	9	14	11	15
1196	9	4	17	13	17	10	21	4	4	9	11	10	9	11	9	10	12	10	6	11	17	23
1201	10	5	14	7	10	11	6	6	13	11	14	8	17	10	8	3	14	12	16	12	13	16
1206	3	7	11	9	22	12	8	5	17	6	15	12	14	15	16	16	20	12	31	18	16	16
1211	4	6	9	5	11	7	9	3	3	12	18	8	14	14	18	26	10	12	29	21	13	16
1216	13	21	12	9	8	9	8	4	7	13	22	10	16	3	17	6	1	15	12	12	15	6
1221	11	14	12	8	10	8	4	4	8	8	21	7	13	7	13	5	14	6	12	3	13	2
1641	15	11	10	11	6	7	4	9	5	10	9	6	13	15	14	10	11	9	11	9	1	12
1646	20	13	10	16	5	13	18	9	2	15	12	14	13	9	13	7	9	12	18	14	7	8
1650	11	8	17	8	5	14	8	14	11	10	8	7	12	13	11	7	5	15	9	12	13	11
2109	14	9	11	12	8	15	17	12	11	14	11	9	14	10	8	11	12	9	5	16	14	12
2114	8	19	14	12	9	8	13	11	18	8	11	9	11	11	7	11	10	11	19	17	14	9
2119	15	9	12	9	6	10	16	10	17	9	15	10	17	11	8	17	7	16	7	2	12	7

Table A.7: Number of basis functions per frequency and experiment,high frequencies.

B Programs to Fit Varying Amplitudes

In this chapter the functions needed to fit the basic function model from Chapter 6 to the data are described and documented.

B.1 General

A generally useful function is the function successive.integer which determines sequences of integers within a vector and returns them as list or as vector of the corresponding indices of the input vector.

```
"successive.integer" <-
  function(x){
    mat <- matrix(c(1,which(c(1,diff(x))>1),
                    which(c(1,diff(x))>1)-1,length(x)),ncol
                      =2)
    erg <- apply(mat,1,function(y)return(y[1]:y[2]))
    if(is.matrix(erg)){
      if(dim(erg)[2]==1){
        erg <- as.vector(erg)
      }else{
        erg <- as.list(as.data.frame(erg))}}
    return(erg)}
```

B.2 Constructing Start Parameters

jumps

The first prestep to the fitting of the basic function is the detection of the most prominent jumps in the time series of the amplitudes.

```
  # Finding jumps in amplitudes as apriori estimates for
     parameter m_ijk
  jumps <- function(datmat,sect=depth.sect,minfract=minfract.
     jumps){
    d <- dim(datmat)[2]
    # Aggregate data over pieces of length depth.sect
    means.sect <- by(datmat[,-d],as.factor(datmat[,d]%/%sect
       ),function(x)return(apply(x,2,mean)))
```

```
sect.depth <- unique(datmat[,d]%/%sect)*sect
n <- length(sect.depth)
means.sect <- matrix(unlist(means.sect),byrow=TRUE,ncol=d
    -1)
m <- dim(datmat)[2]-1
# Detect the most prominent jumps by calculating
    differences and then
# check against empirical quantiles
diff.sect <- apply(means.sect,2,diff)
largerquantile <- function(x,pr=0.95){
  return(which(x>=quantile(x,probs=pr)))
}
lowerquantile <- function(x,pr=0.05){
  return(which(x<=quantile(x,probs=pr)))
}
# Find large jumps
diff95 <- apply(diff.sect,2,largerquantile,pr=1-minfract)
diff5 <- apply(diff.sect,2,lowerquantile,pr=minfract)
# Find directly successive jumps
red.diff.min <- apply(rbind(diff95,diff5),2,function(x){
  x <- sort(x)
  erg <- lapply(successive.integer(x),function(int)x[int
      ])
return(erg)})
# Combine successive jumps
min.jumps <- list()
for(i in 1:m){ # m number of frequencies
  start <- unlist(lapply(red.diff.min[[i]],min))
  end <- unlist(lapply(red.diff.min[[i]],max))+1
#to compensate for reduced length of diff*
  middle <- unlist(lapply(red.diff.min[[i]],mean))*sect
  jumpheight <- unlist(lapply(red.diff.min[[i]],function(
      x){
    return(sum(diff.sect[x,i]))}))
  ups <- which(jumpheight>0)
  downs <- which(jumpheight<0)
  foll.ups <- successive.integer(ups)
  foll.ups <- foll.ups[unlist(lapply(foll.ups,length))>1]
  foll.downs <- successive.integer(downs)
  foll.downs <- foll.downs[unlist(lapply(foll.downs,
      length))>1]
  # Search for jumps in the same direction to eliminate
      jumps
  # from high variation
```

```
    if(length(foll.ups)>0){
      for(foll in foll.ups){
        for(j in 1:(length(foll)-1)){
          if(length(end[ups[foll[j]]]:start[ups[foll[j
            +1]]])>1){
            print(c(j,i,dim(datmat)[1],jumpheight[foll[j
              ]]))
          if(3*sd(diff.sect[(end[ups[foll[j]]]:start[ups[foll
            [j+1]]])-1,i])>=jumpheight[ups[foll[j]]]){
            jumpheight[ups[foll[j]]] <- NaN
          }}}}
    }
    if(length(foll.downs)>0){
      for(foll in foll.downs){
        for(j in 1:(length(foll)-1)){
          if(length(end[downs[foll[j]]]:start[downs[foll[j
            +1]]])>1){
            print(c(j,i,dim(datmat)[1],jumpheight[downs[
              foll[j]]]))
          if(3*sd(diff.sect[(end[downs[foll[j]]]:start[downs[
            foll[j+1]]])-1,i])>=-jumpheight[downs[foll[j
            ]]]){
            jumpheight[downs[foll[j]]] <- NaN
          }}}}
    }
    start <- start*sect
    end <- end*sect
    min.jumps[[i]] <- data.frame(middle,start,end,
      jumpheight)
    min.jumps[[i]] <- min.jumps[[i]][which(!is.nan(
      jumpheight)),]
    min.jumps[[i]] <- data.frame(min.jumps[[i]],gradient
      <- apply(min.jumps[[i]],1,function(x)return(x[4]/(x
      [3]-x[2]))))
  }
  return(list(min.jumps=min.jumps,large.obs.up=diff95,large
    .down=diff5,sect.depth=sect.depth))
}
```

construct.start.par

The next function uses the previous function to generate the start values for the basic functions.

```
construct.start.par <- function(data,relfreq,depth=NULL,
  sections=NULL,endstart=0,form.asymptote=NULL,ccov=NULL,
```

```
    test.value=0.9,depth.sect=10,max.depth=500,minfract.jumps
    =.05,stepfit=TRUE)
{
  if(!is.null(depth)){data <- add.depth(data,depth)}
                  # adding the depth according to t)he
                     respective experiment
  if(endstart>0){ # Estimating mean amplitudes in starting
     phase
    mu <- lapply(data,function(x){
      d <- dim(x)[2]
      erg <- apply(x[(x[,d]<=endstart),-d],2,mean)
      return(erg)})
    mu <- apply(as.data.frame(mu),1,mean)
    }else{mu <- 0}
  # Finding upper quantiles for the estimation of
  # influences on maximal amplitudes
  maxim.data <- lapply(data,function(x){
        d <- dim(x)[2]
        erg <- apply(x[,-d],2,quantile,probs=test.value)
        return(erg)})
  maxim.data <- t(as.matrix(as.data.frame(maxim.data)))
  if(!is.null(ccov)){ # calculate linear models, if constant
     influences given
    fitlms <- function(y,infl,steps,formel){
      attach(infl)
      if(is.null(formel)){
        var.names <- names(infl)
        dcv <- length(var.names)
        formel <- paste("y~",paste(rep("I(",dcv), var.names,
            rep("^2)",dcv),sep="",collapse="+"),"+",paste(var.
            names,collapse="*"),sep="")
        formel <- formula(formel,data=infl)
      }
      erg <- lm(formel)
      sink("test.txt")
      erg <- step(erg)
      sink()
      unlink("test.txt")
      detach(infl)
      return(erg)}
    ak <- apply(maxim.data,2,fitlms,infl=ccov,steps=stepfit,
       formel=form.asymptote)
  }else{ # no constant influences, asymptotes assumed
     constant
```

```
    ak <- apply(maxim.data,2,mean)
    print("Constants for Asymptote")
  }
  data.jumps <- lapply(data,jumps,sect=depth.sect,minfract=
    minfract.jumps)
  return(list(mu.gen = mu,jumps.data = data.jumps, asymptote.
    lm = ak))
}
```

B.3 Fitting Basic Functions to the Amplitudes

profiling

This function fits the proposed basic function to a single frequency.

```
profiling <- function(ampl.ts,depths,minsucc,epsilon=5,toler=
  c(10^(-3),0.5),numtests=5,numval=10,accept.remains=0.05,
  sect=3,...){
   ntol <- seq(from=toler[1],to=toler[2],length=numtests)
   residuals.func <- 0
   fitted.func <- 0
   failed <- numeric(0)
   base.elements <- list()
   endadded <- FALSE
   y <- ampl.ts
   l <- 2
   i <- 1
   k <- 1
   m <- 1
   stepon <- FALSE
   # Main loop to calculate nonlinear regressions
   while(i+k<=dim(minsucc)[1]){
   # Check if two adjacents parts of the series have
     approximately the same
   # height to avoid several functions for just one step
     if(i+k<dim(minsucc)[1]){
       if(abs(mean(ampl.ts[which((minsucc[i,3]<depths)& (
         depths<minsucc[i+k,2]))]) - mean(ampl.ts[which((
         minsucc[i+k,3]<depths)& (depths<minsucc[i+k
         +1,2]))]))<abs(minsucc[i+k,4])){
       k <- k+1
       stepon <- TRUE
     }
     }
     if(stepon){
```

```
  stepon <- FALSE
}else{
if(l==2){
    # Set observations outside the region of support
       equal to 0
    y[(depths<=ifelse(i==1,-1,minsucc[i,l]-epsilon))|y
       <0] <- 0
    l <- ifelse(minsucc[i+k,4]>0,2,3)
  # Check if this is the last jump down and add 0's to
     give nls a chance
    if((minsucc[i+k,l]+epsilon<=max(depths))&(i+k!=dim(
       minsucc)[1])){
      y[depths>minsucc[i+k,l]] <- 0
    }else{
      diffdepths <- diff(depths)[1]
      depths <- c(depths,((length(depths)+1):(length(
         depths)+50))*diffdepths)
      y <- c(y,rep(0,50))
      endadded <- TRUE
    }
  }else{
    # if second jump down, check if next part needs
       basic function
    y[(depths<=minsucc[i,l]-epsilon)|y<0] <- 0
    l <- ifelse(minsucc[i+k,4]>0,2,3)
    # Check if this is the last jump down
    if(minsucc[i+k,l]+epsilon<=max(depths)){
      y[depths>minsucc[i+k,l]+epsilon] <- 0
    }else{
      diffdepths <- diff(depths)[1]
      depths <- c(depths,((length(depths)+1):(length(
         depths)+50))*diffdepths)
      y <- c(y,rep(0,50))
      endadded <- TRUE}
  }       # end else for jumps down
    j <- 1
    # Initializing startvalues for nonlinear regression
d1startvector <- as.numeric(c(1/abs(minsucc[i,4:5]),10/
   abs(minsucc[i,4:5]),abs(minsucc[i,4:5]),runif(numval
   ,min(as.numeric(c(1/abs(minsucc[i,4:5]),abs(minsucc[
   i,4:5]))))+.00001,max(as.numeric(c(1/abs(minsucc[i
   ,4:5]),abs(minsucc[i,4:5]))))-.00001)))
d2startvector <- as.numeric(c(1/abs(minsucc[i+k
   ,4:5]),10/abs(minsucc[i+k,4:5]),abs(minsucc[i+k
```

```
    ,4:5]),runif(numval,min(as.numeric(c(1/abs(minsucc[i
    +k,4:5]),abs(minsucc[i+k,4:5]))))+.00001,max(as.
    numeric(c(1/abs(minsucc[i+k,4]),abs(minsucc[i+k
    ,4]))))-.00001)))
names(d1startvector) <- NULL
names(d2startvector) <- NULL
gmy <- which(y>mean(y))
startm1 <- min(depths[min(gmy)],minsucc[i,1])
startm2 <- max(depths[max(gmy)],minsucc[i+k,1])
names(startm1) <- NULL
names(startm2) <- NULL
    repeat{
   # Try to calculate nonlinear regression on different
       tolerance levels
      numstart <- 1
      repeat{
        # before changing tolerance levels, test
           different start values
        base.elements[[m]] <-  try(nls(y~ a1/((1 + exp
           ((m1 - depths)/d1)) *(1+ exp((-m2 + depths)/
           d2))),start=c(a1=max(y),m1=startm1,m2=
           startm2,d1=d1startvector[numstart],d2=
           d2startvector[numstart]),control=nls.control
           (tol=ntol[j]),... ))
    # check if successful, if not increase number of
       iterations...
        if(is.character(base.elements[[m]])){
        if(length(grep(base.elements[[m]],pat="
           iterations"))!=0){
          base.elements[[m]] <-  try(nls(y~ a1/((1 +
             exp((m1 - depths)/d1)) *(1+ exp((-m2 +
             depths)/d2))),start=c(a1=max(y),m1=startm1
             ,m2=startm2,d1=d1startvector[numstart],d2=
             d2startvector[numstart]),control=nls.
             control(tol=ntol[j],maxiter=100),... ))}}
        #... or check different start values
        if(is.character(base.elements[[m]])&(numstart<(
           length(d1startvector)))){
          numstart <- numstart+1
        }else{
          break} # if this also does not help...
}# end repeat-loop startvalues
  if(!is.character(base.elements[[m]])){
    intobs <- which(y!=0)
```

```
      intres <- y[intobs]-fitted(base.elements[[m]])[
         intobs]
      if(length(intres)>2){
      if(median(intres)>sd(intres)){
        if(j<numtests){
        j <- j+1
      }else{# if everything did not lead to a success,
         take the insufficient, but mark as failed
        failed <- c(i,length(minsucc[,4]))
        break}
      }else{
      break}
    }else{break}
    }else{ #...change tolerance
      if(j<numtests){
        j <- j+1
      }else{# if everything did not lead to a success,
         give up
        failed <- c(i,length(minsucc[,4]))
        return(list(bases=base.elements,fitted=fitted.
           func,residuals=residuals.func,fails=failed))}
    }
      } # end repeat-loop tolerance levels
      if(endadded){
        newfitted <- fitted(base.elements[[m]])[1:length(
           ampl.ts)]
        depths <- depths[1:length(ampl.ts)]
        endadded <- FALSE
      }else{
        newfitted <- fitted(base.elements[[m]])}
      fitted.func <- fitted.func+newfitted
      residuals.func <- ampl.ts-fitted.func
      base.elements[[m]] <- coef(base.elements[[m]])
      y <- residuals.func
  m <- m+1
  i <- i+k
  k <- 1
}# end else of if(step)
  } # end while-loop minsucc
# control if any greater part >0 not explained
# several times, to make sure, max 3 times, because of
   endless repetition
runde <- 0
repeat{
```

```
  runde <- runde+1
means.sect <- by(residuals.func,as.factor(depths%/%sect),
   mean)
if((!any(means.sect>0))|runde==4){
  break
}else{
  greater.zero <- which(means.sect>0)
  greater.zero <- lapply(successive.integer(greater.zero
     ),function(x)return(which(means.sect>0)[x]))
  maxy <- order(unlist(lapply(greater.zero,function(x)
     return(max(means.sect[x])))),decreasing=TRUE)
  sects <- unique(depths%/%sect)*sect
  mingz <-  unlist(lapply(greater.zero,min))[maxy]
  maxgz <- unlist(lapply(greater.zero,max))[maxy]
  lgz <- unlist(lapply(greater.zero,length))[maxy]
  # Define remaining part of the data
  remains <- which(lgz>length(means.sect)*accept.remains)
  if(length(remains)>0){
    d <- length(base.elements)
    for(i in (d+1):(d+length(remains))){
      y <- rep(0,length(residuals.func))
      selectobs <- which((depths>sects[mingz[[remains[i-d
         ]]]])&(depths<sects[maxgz[[remains[i-d]]]]))
      y[selectobs]<- residuals.func[selectobs]
      # Find jumps in y
      gmy <- which(y>mean(y))
      startm1 <- depths[min(gmy)]
      startm2 <- depths[max(gmy)]
      partdepths <- depths[selectobs]
      if(max(partdepths)>=max(depths)){
        diffdepths <- diff(depths)[1]
        depths <- c(depths,((length(depths)+1):(length(
           depths)+50))*diffdepths)
        y <- c(y,rep(0,50))
        endadded <- TRUE}
      j <- 1
      d1startvector <- c(1/max(abs(y)/epsilon),10/max(abs
         (y)/epsilon),max(abs(y)/epsilon),runif(numval,1/
         max(abs(y)/epsilon)+.00001,max(abs(y)/epsilon
         )-.00001))
      repeat{
     # Try to calculate nonlinear regression on different
         tolerance levels
        numstart <- 1
```

```
      repeat{
        # before changing tolerance levels, test
            different start values
  base.elements[[i]] <-  try(nls(y~ a1/((1 + exp((m1 -
     depths)/d1)) *(1+ exp((-m2 + depths)/d2))),start=c
     (a1=median(y[y>0]),m1=startm1,m2=startm2,d1=
     d1startvector[numstart],d2=d1startvector[numstart
     ]),control=nls.control(tol=ntol[j]),... ))
    # check if successful, if not increase number of
        iterations...
      if(is.character(base.elements[[i]])){
      if(length(grep(base.elements[[i]],pat="
          iterations"))!=0){
        base.elements[[i]] <-  try(nls(y~ a1/((1 +
            exp((m1 - depths)/d1)) *(1+ exp((-m2 +
            depths)/d2))),start=c(a1=median(y[y>0]),m1
            =startm1,m2=startm2,d1=d1startvector[
            numstart],d2=d1startvector[numstart]),
            control=nls.control(tol=ntol[j],maxiter
            =100),... ))}}
                                  #... or check
                                     different start
                                     values
      if(is.character(base.elements[[i]])&(numstart<(
          numval+3))){
        numstart <- numstart+1
      }else{break} # if this also does not help...
}# end repeat-loop startvalues
      if(!is.character(base.elements[[i]])){
        break
      }else{ #...change tolerance
        if(j<numtests){
          j <- j+1
        }else{# if everything did not lead to a success
            , give up
          failed <- c(failed,i,length(minsucc[,4]))
          return(list(bases=base.elements,fitted=fitted
              .func,residuals=residuals.func,fails=
              failed))}
      }
    } # end repeat-loop tolerance levels
    if(endadded){
      newfitted <- fitted(base.elements[[i]])[1:length(
         ampl.ts)]
```

```
            depths <- depths[1:length(ampl.ts)]
            endadded <- FALSE
          }else{
            newfitted <- fitted(base.elements[[i]])}
          fitted.func <- fitted.func+newfitted
          residuals.func <- ampl.ts-fitted.func
          base.elements[[i]] <- coef(base.elements[[i]])
          y <- residuals.func
        } # end for-loop remains
      }else{ # if(length(remains)>0)
        break}
    }# end else for means greater 0
   }# end repeat for remains
    return(list(bases=base.elements,fitted=fitted.func,
       residuals=residuals.func,fails=failed))
  }
```

individual.profiles

This function is just a wrapper to apply the previous function to all amplitudes in all experiments

```
individual.profiles <- function(data,startpar,relfreq=1,pr.
    toler=c(10^(-3),0.5),num.tests=5,...){
  require(nls)
  mu.gen <- startpar$mu.gen
  startpar <- startpar$jumps.data
  profiles <- list()
  fails <- list()
  for(i in 1:length(data)){
    profiles[[i]] <- list()
    fails[[i]]<-list()
    d <- dim(data[[i]])[2]
    depths <- data[[i]][,d]
    for(j in 1:(d-1)){
      profiles[[i]][[j]] <- profiling(data[[i]][,j]-mu.gen[j
         ],depths,startpar[[i]]$min.jumps[[j]],toler=pr.toler
         ,numtests=num.tests,...)
      profiles[[i]][[j]]$fitted <- profiles[[i]][[j]]$fitted+
         mu.gen[j]
      if(length(profiles[[i]][[j]]$fails)!=0) fails[[i]][[j
         ]] <- profiles[[i]][[j]]$fails
      print(c(i,j,profiles[[i]][[j]]$fails))
    } #end for-loop in freqband
  } #end for-loop data
  return(list(profiles=profiles,fails=fails))}
```

C Programs for the Simulations

C.1 General Functions for the Construction of Designed Simulations

The following functions are wrapper functions to execute a simulation for which functions for the construction of the data, the evaluation and a report are given.

build.data
This function needs as input the name of the function which generates the deterministic part of the data, fix.func, the name of the function that generates the random part of the data, rand.func, and a function to assemble the data from the parts constructed in these two steps, concat.func. Additionally it needs an experimental design matrix, plan, the number of parameters for the deterministic part and possibly the number of parameters common to random and deterministic part, e.g. number of observations, etc..

```
build.data <- function(plan,sim.func=list(fix.func="id",rand.
    func="rnorm"),concat.func="+",n.fix.param=1,common=0,n.rep
    ,sim.name="test"){
  if(length(sim.func)==2){
    if(sim.func[[1]]!="id"){ # If fixed is the identy just do
        nothing,
                             # else apply fixed to
                                appropriate parameters
      fix.funct <- eval(parse(text=sim.func[[1]]))
      }
    # define function to generate random part
    rand.funct <- eval(parse(text=sim.func[[2]]))
    # function to add error to fixed
    concat <- eval(parse(text=concat.func))
    K <- dim(plan)[2]
    #
    # No random effects:
    if((K-n.fix.param==0)&(common==0)){return(fix.part)}
    #
    # Concatenating random and fixed part for each
       simaulation experiment
```

```
    #
    for(k in 1:dim(plan)[1]){
      if(sim.func[[1]]!="id"){ fix.part <- fix.funct(as.
         numeric(plan[k,1:n.fix.param]))}
    # Some parameters may effect fixed _and_ random part,
    # e.g. length of time series
    if((K-n.fix.param==0)&(common==1)){
              rand.part <- rand.funct(plan[k,K],N=n.rep)}else
                 {
    if((K-n.fix.param==1)&(common==0)){
      rand.part <- rand.funct(plan[k,K],N=n.rep)
    }else{
      rand.part <- rand.funct(plan[k,(n.fix.param-common+1):K
         ],N=n.rep)
    }}
      exp.data <- list(param=plan[k,],data=concat(fix.part,
         rand.part))
      save(exp.data,file=paste("exp-",k,"-",sim.name,".Robj",
         sep=""))}
#    return(exp.data)
  }else{return(print("Please try to aggregate your fixed part
      or random part \n generation to one function each and
     implement further structure \n by using the
     concatenating function"))
  }
}
```

exec.evaluation

As the name suggests exec.evaluation applies a given evaluation to the data constructed by build.data, and carries out reports on each single experiment, and possibly on results from all experiments.

```
exec.evaluation <- function(first=1,last=0,gen.eval,report.
   func,sim.name="test",gesrepfunc=NULL,...){
  if(last==0){
    files <- system("ls exp-*",intern=TRUE)
    last <- max(as.numeric(unlist(lapply(files,function(txt){
       return(unlist(strsplit(txt,split="-"))[2])}))))
  }
  evaluation<- eval(parse(text=gen.eval))
  report <- eval(parse(text=report.func))
  gesrep <- list()
  for(k in first:last){
      load(file=paste("exp-",k,"-",sim.name,".Robj",sep=""))
      results <- evaluation(exp.data,...)
```

```
      save(results,file=paste("res-",k,"-",sim.name,".Robj",
          sep=""))
      rep <- report(results,file=paste("rep-",k,"-",sim.name
          ,".tex",sep=""),sim.name,k,last)
      save(rep,file=paste("rep-",k,"-",sim.name,".Robj",sep
          =""))
      gesrep[[k]] <- rep
      if(k==1){system(paste("cat rep-",k,"-",sim.name,".tex
          > rep-ges-",sim.name,"tex",sep=""))}else{system(
          paste("cat rep-",k,"-",sim.name,".tex >> rep-ges-",
          sim.name,".tex",sep=""))}
    }
  if(!is.null(gesrepfunc)){
    gesrepfunc <- eval(parse(text=gesrepfunc))
    gesrep <- gesrepfunc(gesrep,gesfile=paste("rep-ges-",sim.
        name,".tex",sep=""))
    save(gesrep,file=paste("res-ges-",sim.name,".Robj",sep
        =""))
  }
  invisible(gesrep)
}
```

transform.var

This function carries out arbitrary transformations defined as character strings for each variable in the experimental design plan.

```
transform.var <- function(plan,transf){
  if(dim(plan)[2]==length(transf)){
    for(i in 1:length(transf)){
      if(transf[i]!="id"){
        x <- plan[,i]
        # Convert character string into function and apply
            to x
        x <- eval(parse(text=transf[i]))
        plan[,i]<-x
      }
    }
    return(plan)
  }else{warning("No transformation executed, if you do not
      want to transform certain variables save id into the
      vector transf at the appropriate place")}
}
```

determine.plan

Again a wrapper function calling functions to construct the experimental design and transform.var to transform the variables as needed. The functions for the construction of the designs are not documented here.

```
determine.plan <- function(plan.type="factorial",var.ints=
    matrix(c(0,0,1,1),ncol=2),var.names=c("x","y"),transf=NULL
    ,des.info=NULL,filename=NULL,coded.file=NULL,nexp=20,...){
  if(is.null(des.info)&&plan.type!="coffee-house"){
  nvar <- dim(var.ints)[1]
  if(length(var.names)!=nvar){return("Please enter a name and
      an interval for each variable")}else{
    des.info<-data.frame(vnames=var.names,rein=rep(1,nvar),
       varmin=var.ints[,1],varmax=var.ints[,2])
  }}else{  nvar <- dim(des.info)[1]}
  if(plan.type=="factorial"){plan <- FFfromInfo(des.info
    ,...) }
  if(plan.type=="plackett-burman"){plan <- PBFromDesignInfo(
    des.info)}
  if(plan.type=="d-optimal"){return(print("Not implemented
    yet"))}
  if(plan.type=="central-composit"){plan <- CCfromInfo(des.
    info,...)}
  if(plan.type=="coffee-house"){
    plan <- coffeehousedesign(varints=var.ints,N=nexp,...)}
  if(!is.null(coded.file)){write.table(plan,file=coded.file,
    quote=FALSE)}
  if(!is.null(transf)){plan <- transform.var(plan,transf)}
  if(!is.null(filename)){write.table(plan,file=filename,quote
    =FALSE)}
  return(invisible(plan))
}
```

deviat.normal

This function measures the distance of the empirical quantiles to the corresponding theoretical quantiles of the normal distribution.

```
deviat.normal<-function(x,type="euclid"){
  qu.normal<-qnorm((1:length(x))/(length(x)+1))
  x <- sort((x-mean(x,na.rm=TRUE))/sd(x,na.rm=TRUE))
  rest <- x-qu.normal
  if(type=="euclid"){
    return(sqrt(sum(rest^2)))
  }
  if(type=="max"){
    return(max(abs(rest)))}
```

```
  if(type=="manhattan"){
    return(sum(abs(rest)))}
}
```

C.2 Functions for the Simulation with Fixed Amplitudes

In this section all functions used to construct the data for the simulation with time stationary influences on the amplitudes and its evaluation are presented.

Deterministic Part of the Data

The deterministic part is generated in this case by two functions. The first, harm.model, constructs from given amplitudes amp, frequencies frequ (or a two-column matrix freqamp), and number of observations a harmonic process. The second, festerteil, calculates the linear relationship of the amplitudes to the influences x and then uses harm.model to construct the set of observations for this experiment.

```
harm.model<-function(amp=15,leng=1024,frequ=127/1024,phase=1,
   freqamp=NULL){
  t<-1:leng
  if(is.null(freqamp)){freqamp <- cbind(frequ,amp)}
  harmfkt<-function(ampfr){
    xt<-ampfr[2]*cos(2*pi*ampfr[1]*t+phase)}
  ht<- apply(freqamp,1,harmfkt) # determine harmonic function
      for all
                                  # frequencies and all t
  if(is.matrix(ht)){ ht <- apply(ht,1,sum)} # add up over
     frequencies
  return(ht)
}
festerteil <- function(param){
  nrelfreq <- param[1]
  fourier <- param[2]
  distfreqs <- param[3]
  rate <- param[4]
  # Constructing the full factorial design for the linear
     model of the time
  # stationary influences
  vers <- as.matrix(expand.grid(list(0:1,0:1,0:1)))
  vers <- vers%*%c(3,4,.001)
  vers <- vers+2
  # Construct the frequencies from the parameters
  if(nrelfreq==1){
    freqs <- (5 + fourier)/rate
  }else{
```

```
    freqs <- (c(5,5+distfreqs*(1:(nrelfreq-1))) + fourier)/
        rate
  }
  # Apply harm.model to the vector of amplitudes vers
  data <- data.frame(lapply(vers,harm.model,leng=rate,frequ=
      freqs,freqamp=NULL))
  colnames(data) <- paste("V",1:8,sep="")
  return(data)
}
```

Calculating and Adding the Random Part

The functions zufallsteil and zusammen simply add normal errors to the data constructed before.

```
zufallsteil <- function(param,N){
  rate <- as.numeric(param[1])
  StoN <- as.numeric(param[2])
  sd <- 2/StoN
  x <- rep(rate,8*N)
  rand <- lapply(x,rnorm,sd=sd)
  rand <- as.data.frame(rand)
  rand <- lapply(1:N,function(k){return(rand[,((k-1)*8+1):(8*
      k)])})
  return(rand)
}
zusammen  <- function(fest,zufaellig){
  zusammen <- lapply(zufaellig,function(x){return(t(x+fest
      ))})
  return(zusammen)
}
```

Evaluation of the Data

The function ampl.lm calculates relevant frequencies if they are not specified by the user and then calculates regressions on the time stationary amplitudes influenced by outer variables x.

```
ampl.lm <- function(data,influence=NULL,freqs=NULL,lser=NULL,
    formula=NULL,stepwise=FALSE,sign.level=.05,...){
  if(is.null(influence)){
    if(is.null(lser)){return("Please specify length of series
        !")}
    influence<-as.data.frame(data[,(lser+1):dim(data)[2]])
    data<-data[,1:lser]
    }
  if(is.null(lser)){lser<-dim(data)[2]}
  if(is.null(freqs)){
```

```
  # Check for significant frequencies and if they are equal
      for all
  # observations
  signampl<- apply(data,1,spectrum,plot=FALSE)
  twosigma <- 1/log(2)*median(unlist(lapply(signampl,
     function(x)return(x$spec))))
  crit.val <- qexp(1-sign.level,rate=1/twosigma)
  signfreqs <- unlist(lapply(signampl,function(x){return(
     which(x$spec>crit.val))}))
  tab.freqs <- table(signfreqs)
  rel.freqs <- as.numeric(rownames(tab.freqs)[which(tab.
     freqs==dim(data)[1])])
  if(length(rel.freqs)==0){return("No frequencies found to
     apply lm model to!")
                           }else{
  rel.amp<-unlist(lapply(signampl,function(x){return(x$spec
     [rel.freqs])}))
  rel.amp <- matrix(rel.amp,nrow=length(rel.freqs))
  rel.freqs <- signampl[[1]]$freq[rel.freqs]
 }
}else{ # If frequencies are given, check to which fourier-
    frequencies they correspond
  real.freqs <- real.signif.freq(len=lser,frequ=freqs)
  # Determine the corresponding amplitudes
  rel.freqs<- real.freqs[,1]
  rel.ampl <- apply(data,1,function(x){return(spectrum(x,
     plot=F)$spec)})
  twosigma <- 1/log(2)*median(as.vector(rel.ampl))
  rel.amp <- rel.ampl[rel.freqs,]
}
rel.amp <- sqrt((rel.amp-twosigma)/lser)
if(is.null(dim(rel.amp))){
      startlms <- NULL
  if(is.vector(influence)){
     startlms <- lm(rel.amp~influence)
    }else{
     startlms <- lm(rel.amp~.,influence)}
  if(stepwise==TRUE){
  upper.formula <- paste(unlist(lapply(names(influence),
     function(x){return(paste("I(",x,"^2)",sep=""))})),
     collapse="+")
  upper.formula <- paste("x~",upper.formula,"+",paste(names
     (influence),collapse="*"),sep="")
  upper.formula <- formula(upper.formula,data=influence)
```

```
    endlms <- step(startlms,scope=upper.formula)
    return(list(linmodels=endlms,diffreltosign=diff.found.rel
        ,rel.freqs=rel.freqs),vareps=twosigma/(2*lser))
    }else{
    return(list(linmodels=startlms,rel.freqs=rel.freqs,vareps
       =twosigma/(2*lser)))
    }
  }else{
  rel.amp<-t(rel.amp)
  if(is.null(formula)){
    startlms <- NULL
    if(is.vector(influence)){
      calclm <- function(x,infl){return(lm(x~infl))}
     }else{
      calclm <- function(x,infl){return(lm(x~.,infl))}
     }
     startlms <- apply(rel.amp,2,calclm,infl=influence)
    }else{
     if(!is.formula(formula)){formula <- as.formula(formula
        )}
     calclm <- function(x,infl){return(lm(formula,infl))}
      startlms <- apply(rel.amp,2,calclm,infl=influence)
    }
    if(stepwise==TRUE){
    upper.formula <- paste(unlist(lapply(names(influence),
      function(x){return(paste("I(",x,"^2)",sep=""))})),
      collapse="+")
    upper.formula <- paste("x~",upper.formula,"+",paste(names
      (influence),collapse="*"),sep="")
    infl <- influence
    upper.formula <- formula(upper.formula,data=infl)
    endlms <- lapply(startlms,step,scope=upper.formula)
    return(list(linmodels=endlms,rel.freqs=rel.freqs,vareps=
      twosigma/(2*lser)))
    }else{
    return(list(linmodels=startlms,rel.freqs=rel.freqs,vareps
       =twosigma/(2*lser)))
    }
  }
}
```

The next function is the evaluation specific for the simulation on stationary amplitudes.

```
auswert <- function(daten,geg.freqs=TRUE){
  param <- daten$param
```

```
daten <- daten$data
vers <- as.data.frame(expand.grid(list(0:1,0:1,0:1)))
if(geg.freqs){
  nrelfreq <- as.numeric(param[1])
  fourier <- as.numeric(param[2])
  distfreqs <- as.numeric(param[3])
  rate <- as.numeric(param[4])
  # Calculate true frequencies
  if(nrelfreq==1){
    freqs <- (5 + fourier)/rate
  }else{
    freqs <- (c(5,5+distfreqs*(1:(nrelfreq-1))) + fourier)/
       rate
  }
  # Calculate the linear models on the amplitudes
  erg1 <- lapply(daten,ampl.lm,freqs=freqs,influence=vers)
  # Extract the estimated variances
  erg4 <- unlist(lapply(erg1,function(ergs)return(
     ergs$vareps))
  # Extracting the residuals and checking for distance to
     normality
  erg2 <- unlist(lapply(erg1,function(ergs){
    llms <- ergs$linmodels
    if((nrelfreq>1)|(fourier!=0)){
    abstnorm <- unlist(lapply(llms,function(lms){
      return(deviat.normal(lms$residuals))}))}else{
        abstnorm <- deviat.normal(llms$residuals)}
    return(abstnorm)}))
  # Extracting coefficients
  erg3 <- as.data.frame(lapply(erg1,function(x){
    models <- x$linmodels
    if((nrelfreq>1)|(fourier!=0)){
    coeffs <- data.frame(lapply(models,function(lms) return
       (lms$coefficients)))
    return(coeffs)}else{
      coeffs <- x$linmodels
      coeffs <- coeffs$coefficients
      return(coeffs)}}))
  if(nrelfreq==1){
    if(fourier!=0){
      K <- dim(erg3)[2]%/%2
      erg3 <- list(unten=t(as.matrix(erg3[,2*(1:K)-1])),
         oben=t(as.matrix(erg3[,2*(1:K)])))
    }else{
```

```
      erg3 <- t(as.matrix(erg3))
    }
  }else{
    if(fourier==0){
      erg <- lapply(1:nrelfreq,function(k){return(t(as.
          matrix(erg3[,(1:dim(erg3)[2])%%nrelfreq==(k
          -1)])))})
      erg3 <- erg
    }else{
      unten <- erg3[,(1:dim(erg3)[2])%%2 == 0]
      oben <-  erg3[,(1:dim(erg3)[2])%%2 == 1]
      unten <- lapply(1:nrelfreq,function(k){return(t(as.
          matrix(unten[,(1:dim(unten)[2])%%nrelfreq==(k
          -1)])))})
      oben <- lapply(1:nrelfreq,function(k){return(t(as.
          matrix(oben[,(1:dim(oben)[2])%%nrelfreq==(k
          -1)])))})
      erg3 <- list(unten=unten,oben=oben)
    }
  }
  return(list(ampl.lms=erg1,abst.norm=erg2,coeffs=erg3,
      vareps=erg4))
}else{
  erg1 <- lapply(daten,ampl.lm,influence=vers)
  erg4 <- unlist(lapply(erg1,function(ergs)return(
      ergs$vareps)))
  erg2 <- unlist(lapply(erg1,function(ergs){
    llms <- ergs$linmodels
    abstnorm <- unlist(lapply(llms,function(lms){if(attr(
        lms,"class")=="lm"){return(deviat.normal(
        lms$residuals))}else{NaN}}))
    return(abstnorm)}))
  return(list(ampl.lms=erg1,abst.norm=erg2,vareps=erg4))
}
}
```

C.3 Functions for the Simulation with Varying Amplitudes

In this section all functions for the generation of harmonic processes with time varying amplitudes and the corresponding evalution functions are documented.

C.3.1 Generating the Time Series

harm.model.tdep
is the function which constructs a harmonic process from a given set of frequencies and for each frequency a function by which the amplitude varies.

```
harm.model.tdep<-function(gen.leng=1024,frequ=17/256,amp="sin
    (200*t)",freqamp=NULL){
  t<-1:gen.leng
  if(length(amp)==length(frequ)){
    if(is.null(freqamp)){freqamp <- data.frame(frequ,amp)}
    harmfkt<-function(ampfr){
      freq <- as.numeric(ampfr[1])
      # Change text into function
      amp <- eval(parse(text=ampfr[2]))
      xt<-amp*(sin(2*pi*freq*t)+cos(2*pi*freq*t))}
    ht<- apply(freqamp,1,harmfkt) # determine harmonic
       function for all
                                          # frequencies and all
                                             t
    if(is.matrix(ht)){ ht <- apply(ht,1,sum)} # add up over
       frequencies
  }else{
    print("Warning: frequ and amp must have the same length")
    return("Error")
  }
  return(ht)
}
```

fixedvarampl
is the specific function for the simulation on varying amplitudes.

```
fixedvarampmodel <- function(para){
  nrelfreq <- para[1]
  fourier <- para[2]
  distfreqs <- para[3]
  model <- para[4]
  rate <- para[5]
  if(model==1){
  # Constructing the true relevant frequencies
    if(nrelfreq==1){
      freqs <- (5+fourier)/rate
    }else{
      freqs <- (c(5,5+distfreqs*(2:nrelfreq))+fourier)/rate
    }
  # Calculating the harmonic process
```

```
    data <- harm.model.tdep(10*rate,freqs,amp=rep("2+.001*t",
        nrelfreq))
  }else{
  # Constructing the true relevant frequencies
    if(nrelfreq==1){
      freqs <- (5+fourier)/rate
      amplfunc <- paste("2+2/(1+exp((-t+",as.character(5*rate
          ),")/",as.character((rate)),"))",sep="")
    }else{
      freqs <- (c(5,5+distfreqs*(2:nrelfreq))+fourier)/rate
      amplfunc <- paste("2+2/(1+exp((-t+",as.character((2+(1:
          nrelfreq))*rate),")/",as.character((1/(1:nrelfreq)*
          rate)),"))",sep="")
    }
  # Calculating the harmonic process
    data <- harm.model.tdep(10*rate,freqs,amplfunc)
  }
  return(data)
}
```

errprocess

returns either a normal white noise process or an AR(1) process with autocorrlation $\rho = 0.3$. add.error is the concatenating function in this simulation.

```
errprocess <- function(para,N){
  para <- as.numeric(para)
  rate <- para[1]
  StoN <- para[2]
  AR <- para[3]
  n <- 10*rate
  data <- matrix(rnorm(as.numeric(N*n),0,as.numeric(2/StoN)),
      ncol=N)
  if(AR!=1){
    data <- 0.3*rbind(rep(0,N),data[-1,])+data
  }
  return(data)
}

add.error <- function(fixed,err){
 return(fixed+err)
}
```

C.3.2 Evaluation of the Data

varampl.eval
is the function which calculates the regressions linear or nonlinear on the varying amplitudes.

```
varampl.eval <- function(data){
  # Subroutine to be applied to the data
  analysis <- function(ht,para){
    notruefreq <- FALSE
    ht <- matrix(ht,ncol=para[5],byrow=TRUE)
    # Calculate the spectra on the parts of the time series
    specs <- apply(ht,1,function(X)return(spectrum(X,plot=
       FALSE)$spec)
    # Determine relevant frequencies for white noise ...
    sigmahat <- 1/log(2)*median(specs)
    crit.val <- qexp(.95,1/sigmahat)
    rel.freqs <-specs>crit.val
    rel.freqs <- apply(rel.freqs,1,sum)
    rel.freqs <- which(rel.freqs>5)
    rel.freqs.ar <- NULL
    # ... and AR(1) disturbances
    if(para[7]==1){
      crit.val <- qgamma(.95,shape=2,scale=sigmahat)
      rel.freqs.ar <-specs>crit.val
      rel.freqs.ar <- apply(rel.freqs.ar,1,sum)
      rel.freqs.ar <- which(rel.freqs.ar > 5)
    }
    # Transform the data
    specs <- sqrt(specs-sigmahat)/para[5])
    # Calculate true frequencies to check found relevant
       against true
    if(para[1]==1){
       if(para[2]==0) truefreqs <- 5 else truefreqs <- 5:6
    }else{
      if(para[2]==0) truefreqs <- c(5,5+para[3]*(2:para[1]))
         else truefreqs <- c(5:6,sort(c(5+para[3]*(2:para
         [1]),6+para[3]*(2:para[1]))))
    }
    if(all(truefreqs %in% rel.freqs)){
      if((para[1]==1)&(para[2]==0)) relampl <- as.vector(
         specs[truefreqs,]) else relampl <- t(specs[truefreqs
         ,])
    }else{
      notruefreq <- TRUE
```

```
  relampl <- t(specs[rel.freqs,])
}
# Two subroutines for the regressions
linfit <- function(y){
  res <- lm(y~c(1:10))
  return(res)
}
nonlinfit <- function(y,rate=para[5]){
  t <- 1:10
  startd <- rnorm(10,2,1)
  i <- 1
  repeat{
    # Avoid fitting problems by trying several start
        parameters
    res <- try(nls(y~b+a/(1+exp((-t+m)/d)),start=c(a=max(
        y)-min(y),b=min(y),m=5,d=startd[i])),silent=TRUE)
    if(is.character(res)&i<=9){
      i <- i+1
    }else{
      break
    }
  }
  return(res)
}
relvec <- FALSE
if(is.vector(relampl)){relvec <- TRUE
}else{
if((dim(relampl)[1]==1)|(dim(relampl)[2]==1)) relvec <-
   TRUE
}
if(para[4]==1){
  if(relvec){
    estvarampl <- linfit(as.numeric(relampl))
  }else{
    estvarampl <- apply(relampl,2,linfit)
  }
}else{
  if(relvec){
    estvarampl <- nonlinfit(as.numeric(relampl))
  }else{
    estvarampl <- apply(relampl,2,nonlinfit)
  }
}
```

```
    return(list(models=estvarampl, relfreqs=rel.freqs/para[5],
        relfreqsar = rel.freqs.ar/para[5], estsigma=sigmahat,
        notruefreq=notruefreq))
  }
  result <- apply(data$data,2,analysis,para=as.numeric(
    data$param))
  return(list(results=result,para=data$param))
}
```

Bibliography

V.P. Astakhov, M.O.M. Osman, and M. Al-Ata. Statistical design of Experiments in Metal Cutting – Part One: Methodology. *Journal of Testing and Evaluation*, 25 (3):322–327, 1997a. 21

V.P. Astakhov, M.O.M. Osman, and M. Al-Ata. Statistical design of Experiments in Metal Cutting – Part Two: Applications. *Journal of Testing and Evaluation*, 25 (3):327–335, 1997b. 21

I.I. Berenblut and G.I. Webb. Experimetal Design in the presence of autocorrelated errors. *Biometrika*, 61(3):427–437, 1974. 42

Peter Bloomfield. *Fourier Analysis of Time Series*. John Wiley & sons, New York, 2 edition, 2000. 49

G.E.P. Box and N.R. Draper. *Empirical Model-Building and Response Surfaces*. Wiley & Sons, New York, 1987. 21, 22, 35

David R. Brillinger. The analysis of time series collected in an experimental design. In *Multivar. Analysis III, Proc. 3rd internat. Symp., Dayton 1972*, pages 241–256, 1973. 37, 48

W.S. Cleveland, E. Grosse, and W.M. Shyu. *Statistical Models in S*, chapter Local regression models. Wadsworth & Brooks/Cole, 1992. 96

Laurie Davies. Bifurcation in the presence of coloured noise. In *Vorlesungen aus dem Fachbereich Mathematik der Universität Essen, Heft 10*, pages 229–232, 1983. 97

Laurie Davies. Bifurcation. Personal communication, February 2003. 94

K.H. Esbensen, M. Halstensen, T. Tonnesen Lied, A. Saudland, J. Svalestuen, S. di Silva, and B. Hope. Acoustic chemometrics — from noise to information. *Cemom. Intell. Lab. Sys.*, 44:61–76, 1998. 44

V. Fedorov and Chr. Nachtsheim. Optimal Designs for Time-Dependent Responses. In C.P. Kitsos and W.G. Müller, editors, *Proceedings of MODA 4*, pages 3–13. Physica Verlag, Heidelberg, 1995. 41

Marek Fisz. *Wahrscheinlichkeitsrechnung und Mathematische Statistik*. VEB Deutscher Verlag der Wissenschaften, 1970. 48

A. R. Gallant, Thomas M. Gerig, and J. W. Evans. Time Series Realizations Obtained According to An Experimental Design. *JASA*, 69:639–645, 1974. 37, 48

U. Gather and V. Schultze. Robust estimation of scale of an exponential distribution. *Statistica Neerlandica*, 53(3):327–341, 1999. 51

Y.B. Gessesse, V.N. Latinovic, and M.O.M. Osman. On the Problem of Spiralling in BTA Deep-Hole Machining. *Journal of Engineering for Industry*, 116:161–165, 1994. 18

J. Herrmann. Kreisformfehler geriebener Bohrungen. *Zeitschrift für wirtschaftliche Fertigung*, 65(3):110–112, 1970. 17

Ross Ihaka and Robert Gentleman. R: A Language for Data Analysis and Graphics. *Journal of Computational and Graphical Statistics*, 5(3):299–314, 1996. 24

M.E. Johnson, L.M. Moore, and D. Ylvisaker. Minimax and maximin distance designs. *J. Stat. Plann. Inference*, 26:131–148, 1990. 45

N.L. Johnson, S. Kotz, and N. Balakrishnan. *Continuous univariate distributions*, volume 1,2. Wiley, 1994. 52, 100

J. Kunert and R.J. Martin. On the optimality of finite Williams II(a) designs. *Ann. Stat.*, 15:1604–1628, 1987. 42

Joachim Kunert. Optimal repeated measurements designs for correlated observations and analysis by weighted least squares. *Biometrika*, 72:375–389, 1985. 42

V.N. Latinovic and M.O.M. Osman. Optimal Design of BTA Deep-Hole Cutting Tools with Staggered Cutters. *International Journal of Production and Research*, 27(1):153–173, 1989. 11

I.J. Leontaritis and S.A. Billings. Experimental design and identifiability for non-linear systems. *International Journal of System Science*, 18(1):189–202, 1987. 42, 43, 45, 99

James K. Lindsey. *Models for repeated measurements*. Clarendon Press, Oxford, 1993. 55

R.J. Martin and J.A. Eccleston. Optimal incomplete block designs for general dependence structures. *J. Stat. Plann. Inference*, 28(1):67–81, 1991. 42

R.J. Martin, J.A. Eccleston, and G. Jones. Some results on multi-level factorial designs with dependent obervations. *J. Stat. Plann. Inference*, 73(1-2):91–111, 1998a. 40

R.J. Martin, G. Jones, and J.A. Eccleston. Some results on two-level factorial designs with dependent observations. *J. Stat. Plann. Inference*, 66(2):363–384, 1998b. 40

M.D. Morris and T.J. Mitchell. Exploratory designs for computational experiments. *J. Stat. Plann. Inference*, 43:381–402, 1995. 45, 46

W. G. Müller. Coffee-House Designs. In A. Atkinson et al., editor, *Optimum Design 2000*, pages 241–248. Kluwer Academic Publishers, 2001a. 45

W. G. Müller. *Collecting Spatial Data*. Physica Verlag, Heidelberg, 2nd edition, 2001b. 44

P. A. Papakyriazis. Optimal Experimental Design in Econometrics: The Time Series Problem (STMA V21 426). *Journal of Econometrics*, 7:351–372, 1978. 38, 41

F. Pfleghar. Verbesserung der Bohrungsqualität beim Arbeiten mit Einlippentiefbohrwerkzeugen. In *Bericht des Instituts für Werkzeugmaschinen der Universität Stuttgart*. Technischer Verlag Günter Grossmann GmbH, Stuttgart Veihingen, 1976. 16

Britta Pouwels, Winfried Theis, and Christian Röver. Implementing a new method for Discriminant Analysis when Group Covariance Matrices are nearly singular. In Martin Schader, Wolfgang Gaul, and Maurizio Vichi, editors, *Between Data Science And Applied Data Analysis*, pages 92–99. Gesellschaft für Klassifikation, Springer, 2002. 91

David A. Ratkowsky. *Handbook of Nonlinear Regression Models*. Marcel Dekker, New York, 1990. 68

K. Sakuma, K. Taguchi, and A. Katsuki. Self-Guiding Action of Deep-Hole-Drilling Tools. *Annals of the CIRP*, 30:311–315, 1981. 16, 17

T.J. Santner, B.J. Williams, and W.I. Notz. *The Design and Analysis of Computer Experiments*. Springer, 2003. 56, 57

I.W. Saunders. Algorithm for sampling times on a continuous process. *Austral. J. Statist.*, 36(2):245–251, 1994. 40

I.W. Saunders and I.A. Eccleston. Experimental Design for continuous Processes. *Austral. J. Statist.*, 34(1):77–89, 1992. 39, 40

I.W. Saunders, J.A. Eccleston, and R.J. Martin. An algorithm for the design of 2^p factorial experiments on continuous processes. *Aust. J. Stat.*, 37(3):353–365, 1995. 40

S.S. Shapiro, M.B. Wilk, and M.J. Chen. A comparative study of various tests for normality. *Journal of the American Statistical Association*, 63:1343–1372, 1968. 60

R. Stockert. *Beitrag zur optimalen Auslegung von Tiefbohrwerkzeugen*. Dissertation, Universität Dortmund, 1978. 18

Taylor Hobson Ltd. *The Layman's Guide to Roundness*. URL http://www.taylor-hobson.com/faqround.asp?headingID=1. 13

T. P. Thai. *Beitrag zur Untersuchung der selbsterregten Schwingungen von Tiefbohrwerkzeugen*. PhD thesis, Universität Dortmund, 1983. 15

W.N. Venables and B.D. Ripley. *Modern Applied Statistics with S*. Springer, 4^{th} edition, 2002. 91

C. Weihs and J. Jessenberger. *Statistische Methoden zur Qualitätssicherung und -optimierung*. Wiley-VCH, 1999. 24

K. Weinert, O. Webber, M. Hüsken, J. Mehnen, and W. Theis. Analysis and Prediction of Dynamic Disturbances of the BTA Deep Hole Drilling Process. In R. Teti, editor, *Proceedings of the* 3^{rd} *CIRP International Seminar on Intelligent Computation in Manufacturing Engineering*, 2002. 94

G. Wittwer. On the Distribution of the Periodogram for Stationary Random Sequences. *statistics*, 17(2):201–219, 1986. 49

M. Zarrop. *Optimal experiment design for dynamic system identification*. Springer, New York, 1979. 41, 99